1-1-2007

Performance characteristics of different mineral filler in asphalt concrete mixtures

Calvin Fong
Ryerson University

PERFORMANCE CHARACTERISTICS OF DIFFERNET MINERAL FILLER IN ASPHALT CONCRETE MIXTURES

By: Calvin Fong
Master of Applied Science, 2007

Civil Engineering
Ryerson University

ABSTRACT

With the increase of traffic load in Canada, asphalt mixtures are required to sustain heavier loads and withstand the harsh Canadian winter. This requires careful design and material selection. This study evaluates the performance of different types of mineral filler in asphalt pavements. Five 19mm Superpave mixes were tested with four types of mineral filler namely fly ash (Class C and Class F), Blast Furnace Slag, and General Use Portland cement along with a control mix with limestone dust. The results showed that, Class C fly ash generated the most economical mix by reducing 0.3% asphalt content of total mix. The indirect tensile strength (ITS) and tensile strength ratio (TSR) test results were used to evaluate the effects of different fillers for water susceptibility. Both types of fly ashes have excellent results on Tensile Strength Ratio (TSR) which increase resistance to water susceptibility. These mixes have a very positive effect on stripping resistance. Improvements in binder properties were shown after short and long term aging which was attributable to the reduction of oxidation and aging effect. Binder with fly ash has the best rutting and fatigue resistance out of all tested binder samples.

Acknowledgements

I would like to express my deepest appreciation to Dr. Shehata for his guidance and assistance in the preparation of this thesis. His great advice and support has lead me to succeed in both of my undergraduate and graduate studies. I could not have it done without his help.

Also, I want to say thank you to Dominic Valle and Nidal Jaalouk for helping me in the lab, which made possible to complete my thesis.

Lastly, I would like to take this opportunity to thank my parents, wife and daughter for their love and support during my long years at university.

TABLE OF CONTENT

LIST OF FIGURES

LIST OF TABLES

CHAPTER 1
INTRODUCTION

1.1 General

Highway material researchers have been investigating the use of by-product materials as mineral filler in asphaltic concrete mixtures to replace the traditional asphalt mixes with bag house dust and hydrated lime. Higher quality and more economical materials are required to reduce the production cost and promote higher performance in our pavement structures.

Even though industrial by-products are common ingredients used in concrete mixes, limited studies have been conducted in flexible pavements. In this study, by-product materials, namely fly ash and Blast Furnace slag, were used in hot mix asphalt as mineral filler to investigate the compatibility of these mixes with acceptable properties. GU Portland Cement was also introduced and evaluated as another type of filler material in hot mix asphalt. The intention of this thesis is to report the characteristics, performance, properties, and comparison of each mineral filler materials used under the Superpave mix design methodology by the Asphalt Institute, as well as the short and long term aging rheological behaviour of the asphalt binder.

1.2 Objective

Hot mix asphalt is extremely sensitive to moisture damage. In fact, the main cause of pavement failure is the presence of water, since it results in loss of cohesiveness between the binder and aggregates. Typically, therefore, a proven anti-stripping material, such as hydrated lime, is added to prevent stripping of the binder. In this investigation, different types of anti-stripping additives (fly ash, Blast Furnace Slag and Portland cement) were investigated as filler (passing No. 200 sieve) in asphalt mixes. Other key objectives of this research are list as follows:

1. Determine the anti-stripping characteristics of different mineral fillers.
2. Determine the performance characteristics and properties of each type of mineral filler under the Superpave mix design method.
3. Determine Marshall stability and flow characteristics for each mix, in order to study the properties of mixes with different fillers. Using the traditional asphalt method of mix design which is still being used in some regions and municipalities in Canada.
4. Study the effect of each mineral filler replacement (Fly Ash (Class-C, Class-F), Blast Furnace Slag, Portland cement) on indirect tensile strength (ITS) and tensile strength ratio (TSR) under dry and wet conditions in asphalt concrete mixtures..
5. Determine the short and long term aging characteristics of the filler/binder mastic with Performance Graded Asphalt Cement (PGAC) testing.

1.3 Thesis Outline

Chapter 1 covers a brief introduction of the different types of mineral fillers in flexible pavements. Additionally, the chapter summarized the objectives of this thesis.

Chapter 2 presented the relevant literature review in the order listed as follow:

- Determined the general asphalt binder behavior and mastic properties of asphalt binder with different types of mineral fillers.
- Mechanism of asphalt age hardening due oxidation and characterization of the asphalt aging effect with different types of mineral fillers.
- Classification of different flexible pavement failures and prevention methods.
- Addressed the advantages of mineral filler in asphalt mixes and features to be considered.

Chapter 3 presented the laboratory experiment program in the order listed below:

- Description of the experimental program with different types of mineral filler under the Superpave protocol.
- Explanation of the Superpave mix design method and all testing requirements including sample preparation.
- Summarized the characteristics and properties of all materials (all aggregates and asphalt binder) carried out in this experiment.

Chapter 4 presents a comprehensive experimental results and discussions of each mixture. The chapter also reported the volumetric properties and performance of each mix in

addition to discussion of viscous and elastic behavior of the asphalt binder in different temperature range.

Chapter 5 presented the conclusions of this thesis.

Chapter 6 presented the recommendations for future work.

CHAPTER 2

LITERATURE REVIEW

2.1 Chemical Composition of Asphalt Binder

Asphalt is a by-product of refined crude petroleum, which is a form of organic matter developed over million of years. The general chemical composition of asphalt has 90 to 95 percent by weight of hydrocarbon. The remaining component contains small portions of Nitrogen, Sulfur, Oxygen and Nickel (Asphalt Institute, 1995).

2.2 Molecular Structure of Asphalt Binder

Asphalt is a highly associated molecular agglomerate with asphaltenes, resins, and light oil (Little, 2005). There are three basic types of molecular structure found in asphalt binder, including aliphatics, cyclics, and aromatics. The molecular structure of each is illustrated in Figures 1 to 3 (Asphalt Institute, 1995). The physical and chemical behaviour of the asphalt binder depends on different combination of these molecular structures. The bonds holding the molecules together are relatively weak and can be easily broken by external heat sources, thereby explaining the viscoelastic properties of the binder. When the binder cools off, these weak links reform and regroup itself back to its original state. However, these chemical structures may not necessarily reform back to the same structural format as before heating (Asphalt Institute, 1995).

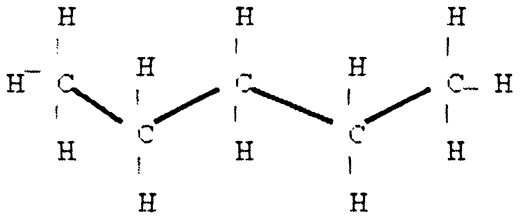

Figure 1 Types of Asphalt Molecules - Aliphatic (Asphalt Institute, 1995)

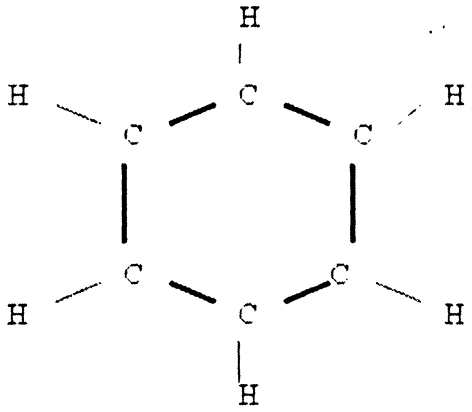

Figure 2 Types of Asphalt Molecules - Aromatic (Asphalt Institute, 1995)

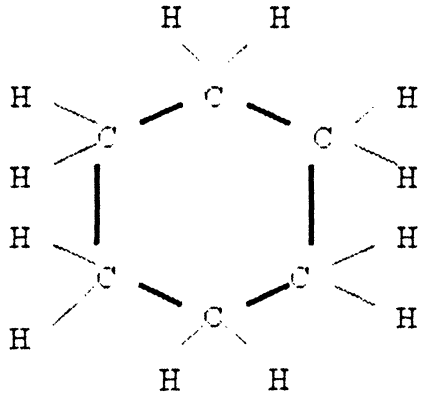

Figure 3 Types of Asphalt Molecules – Cyclic (Asphalt Institute, 1995)

In Branthaver's (1993) research, he classified these molecules into either polar or non-polar. The polar molecules form a network, providing the elastic behaviour of the asphalt. The non-polar molecules form around the network and provide the viscous properties of asphalt. Both polar and non-polar molecules are mixed homogenously in

the asphalt. It is important to have a balance between the polar and non-polar molecules in order to maintain a good balance of the asphalt's vicoelastic properties to satisfied in both hot and cold climates, which is necessary for good pavement performance.

2.3 Asphalt Binder Behaviour

2.3.1 General

In the Superpave binder specification, the rotational viscosity is measured at 135°C at a recommended rate of 20 rpm. This shear rate was selected because most un-modified asphalts show Newtonian behaviour (viscosity independent of shear rate) at this rate, and it simulates the shear rates during the pumping and handling operations in refineries and asphalt plants (Anderson et al. 1994).

2.3.2 Newtonian Flow Characteristic of Asphalt Binder

The Newtonian flow characteristic of asphalt is represented by the ratio of shear stress (τ) to shear strain ($d\gamma/dt$) rate with a constant slope known as viscosity (□), as illustrated in Figure 4. Liquid with a Newtonian flow characteristic provides better workability in asphalt. It ensures that the asphalt will be at its liquid state, and accordingly the viscosity and other rheological properties of fluid still apply. A non-Newtonian asphalt means the ratio between the shear stress and shear rate varies, as shown in Figure 5. The viscosity decreases as the shear strain increases. Too much polymer in asphalt changes its viscous behavior to Non-Newtonian liquids, which is not favourable in asphalt production, as it leàd to the asphalt being too mastic to handle.

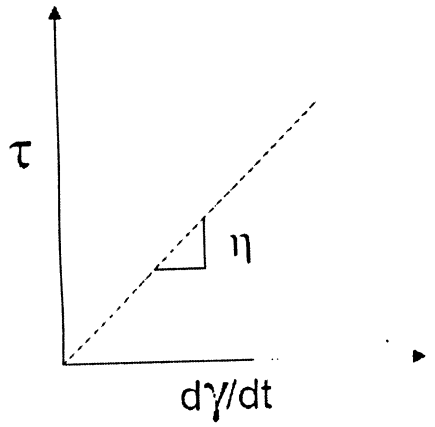

Figure 4 Newtonian Flow Characteristic of Asphalt Binder

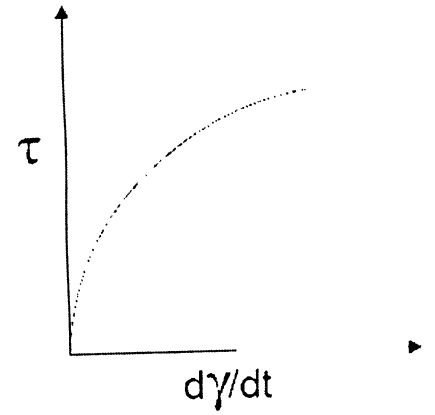

Figure 5 Non-Newtonian Flow Characteristic of Asphalt Binder

Asphalt with low asphaltene content tends to behave like Newtonian fluid at high temperature, as the asphaltene content does not significantly interact in the asphalt structure itself. As the asphaltene content increases, the asphalt changes to non-Newtonian flow characteristics. The change of flow characteristic is caused by the interaction between the micro-structure within the asphalt matrix, creating a resistance to flow. The increase of the interaction of the micro-structure can be induced by lowering the temperature.

According to Anderson's (1994) study, the author describes that un-modified asphalt does not behave with as much variation in between the shear stress and shear rate ratio as shown in Figure 5. Most un-modified asphalt should act like Newtonian liquid at lower temperature, and when tested at higher temperatures (at mixing temperature), the asphalt is essentially Newtonian. The linear viscosity line in Figure 4 is determined by a rheological analysis where the asphalt binder acts as a Newtonian fluid. Determining the Newtonian properties will satisfy the performance binder test required under in Superpave testing procedures. It is important to maintain a dust proportion ratio of 0.8 to 1.2 while designing for asphalt mixes, as according to the Superpave specification.

2.3.3 Non-Newtonian Asphalt Binder

The current original asphalt cement viscosity test under the Superpave protocol is not applicable for non-Newtonian materials. A linear relationship must obtain in order to characterize the asphalt binder. It is difficult to characterize non-Newtonian asphalt since it provides different viscosities at different stress levels. The consistency of a non-Newtonian fluid varies even when the temperature and static pressure are constant. The variation in consistancy can also be affected by the applied shear stress' duration.

2.4 Asphalt Binder and Mineral Filler Mastics Properties

Mastic properties of asphalt generally define the hot mix performance. To understand the relationship between the asphalt binder and hot mix asphalt properties, it is necessary to understand the effects of different filler types and the content in asphalt mastic (asphalt-filler composite) that serves as the binder in hot mix asphalt, as illustrated in

Figure 6. According to Dukatz and Anderson's (1980) study, when the particle size of the fillers are thicker than the binder film, the filler particles contribute to the interlocking of the aggregate. When the filler's particle size is smaller than the thickness of the binder film, the filler particles are suspended in the asphalt binder and become mastic.

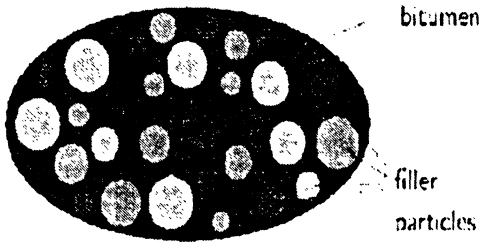

Figure 6 The Micromechanical Model for Asphalt-filler Composite (Anderson, 1980)

Dukatz and Anderson (1980) also studied how the characteristics of different filler correlates to the performance of the mastic behaviour in hot mix asphalt . Some of their findings are concluded, as follows:

- Different mineral fillers generate different stiffening effects to the added asphalt binder. These stiffening effects are varied based on the fineness of the filler particles and the physico-chemical interactions to the binder.
- The compaction of the mixtures are affected by the stiffening effects caused by the amount and type of mineral filler added.
- The creep stiffness of the binder (long term, non-recoverable measure) is affected by the stiffening effect of the mineral filler in the asphalt/filler matrix.

Two mineral fillers (quartz and calcite) were used in Anderson's (1992) study. For each

asphalt-filler mastic, a constant of 0.5 (by volume) filler to asphalt ratio was used. The ratio was chosen to represent the typical ratio used in dense-grade hot mix asphalt. The findings of Anderson's research are summarized, as follows:

- The additional filler prolonged the relaxation times (it takes longer time for asphalt binder to go back to its original form) thereby stiffening the asphalt sample.
- The use of mineral filler did not significantly affect the rate of oxidation or physical hardening (explained in section 2.5).
- The asphalt filler samples act as "leathery-like" material under low temperature, and the mastic effect enhanced the strain characteristic of the asphalt cement.

In Jiang et al (1996) research, it was discussed that mineral filler increases the viscosity and decreases the shear index of asphalt binder. However, lower frequency or higher temperature can decrease the viscosity of the asphalt binder. All of the effects are more distinct with an increase of the Filler/Asphalt (F/A) ratio. Another interesting observation was noted where that mineral fillers with small particle size, lower bulk density and higher compressibility were found to be more effective in asphalt binder.

Gubler et al (1999) focused his study on the aging mechanism of the asphalt binder. It is interesting to note that filler might "age" the binder by promoting oxidation or polymerization, and thereby cause hardening of the asphalt binder. At the same time, filler might retard the aging process by obstructing oxygen diffusion into the binder, due to the fact that the filler fraction is completely impermeable to oxygen.

2.5 Asphalt Oxidation and Aging

2.5.1 Mechanism

Like other organic materials, asphalt binders are influenced by oxidation and heat after a period of time known as age hardening. Age hardening can cause the asphalt binder to stiffen and increase its viscosity (Huang, 2007). Such effects can be explained by having too much polar material presented in asphalt binder, which leads to thermal cracking, brittleness, and fatigue cracking in the pavement structure. The main causes of asphalt age hardening are summarized as follows (Huang, 2007):

- Rapid loss of light oil components during high temperature aging.
- Changes in composition by reacting with atmospheric oxygen.
- Molecular restructuring that causes stiffening and hardening.

Branthaver (1993) studied the rheological properties of asphalt binder associated with different mineral fillers and found positive results in rheological properties. Kallas and Puzinausakas (1961) indicated that asphalt binder associated with different mineral filler types can generate different stiffening effects in system.

Branthaver (1993) also explained that when aging proceeds, the molecular weight and quantity of the non-polar molecules are reduced over time, as they are converted into polar carbonyl groups. These polar molecules attract other polar molecules from the system and combined into much stronger polar molecules that are more susceptible to cracking. It should be noted that asphalt binder with too many non-polar molecules can also cause rutting and moisture damage. Therefore, it is important to keep a balance

level of polar and non-polar molecules after aging. As indicated by the results of Huang's (2007) study, the stiffness effect can reduce asphalt age hardening when mineral filler is added.

2.5.3 Characterization of Aging Effect with Different Types of Mineral Filler

In Huang and Zeng's (2006) study, two different types of mineral fillers were mixed with two different grades of asphalt binder: Asphalt A with 20% asphaltene content and Asphalt B with low asphaltene content of 7%. Both aged and un-aged rheological properties were investigated and the conclusions are as follows:

- When additional filler was added to the asphalt binder, a reduction of stiffness after long-term aging was observed.
- Similar stiffening effects were observed with different types of mineral filler before aging. However, adding fillers to Asphalt A (20% asphaltene content) decreased stiffness aging (after long-term aging) more than adding the same fillers to Asphalt B (7% asphaltene content).
- Increasing the filler content in the asphalt binder did not change the shear susceptibility of the binder samples regarding long-term age hardening by oxidation and heat.

2.6 Mineral Filler act as an "Extender" in Hot Mixes

The intention of an asphalt extender is to replace portions of the asphalt binder and act as a lubricant of the aggregate structure with less compaction effort. Sufficient amount of mineral filler content could lead to the filler serving as an "extender", which successfully

reduces the effective asphalt content and makes the asphalt mix become more mastic.

In Suheibani's (1986) study, three types of fly ash with different particle sizes were used to replace part of the asphalt content in hot mix asphalt. It was found that fly ash particles sized between 1 μm to 44 μm behave best as an "extender," as fly ash in these size ranges had the least effect on viscosity and air void content. Coarse fly ashes will add more air void content in the mix, which means more asphalt, is needed to satisfy volume metric properties. Fly ash particles sized greater than 44 μm will act as fine aggregates instead of filler thus lead to mixes that are more mastic with higher viscosity and air voids.

Tons et al. (1983) proved that Class F fly ash is an excellent "extender" in asphalt mixes. Asphalt cement content was reduced by increasing different fly ashes content. Different tests were performed on specimens to determine rutting, fatigue life analysis and resistance to moisture damage. It was found that adding fly ash lead to significant improvements on the test results, with the increase of fly ash content causing a reduction of voids in mineral aggregate (VMA) and air void content.

2.7 Mix Design of Asphalt Mixtures

The main objective of the Superpave mix design is to optimize the mixture's asphalt content while satisfying properties with respect to strength, durability, flexibility, fatigue, low temperature cracking, rutting resistance, and workability. The optimized mineral filler content would be incorporated into the Superpave mix design methodology to

satisfy all design criteria under the AASHOT protocol.

2.7.1 Approaches to Proper Mix Design

Compatible filler selection is the key factor to successful mixes. Asphalt mixtures are normally created via the traditional Marshall design method or the Superpave design method, which is used to optimize mineral filler and asphalt content and other important volumetric properties.

This section reviews the Superpave method of mix design with different types of mineral filler. Two key features in the Superpave mix design system include using the Superpave gyratory compactor (SGC) and more sophisticated performance testing. The mix design process involves aggregate gradation adjustments to accommodate the required asphalt and desired air void content. Each test and design step provides direct relationships to field performance. The Superpave Level 1 mix design involves material selection and satisfying volumetric design criteria. The aggregate selection is based on physical properties such as percent crushed particles, flat elongated particles, and sand equivalent (clay content), and the fine aggregate angularity test. A binder test is conducted to measure the binder's physical properties at a specified temperature range. More comprehensive testing and results, such as indirect tensile strength (ITS) and tensile strength ratio (TSR), are then undertaken to predict a more reliable field performance by simulating field conditions in a controlled laboratory environment. Figure 7 summarizes the mix design procedure in a flow chart presentation.

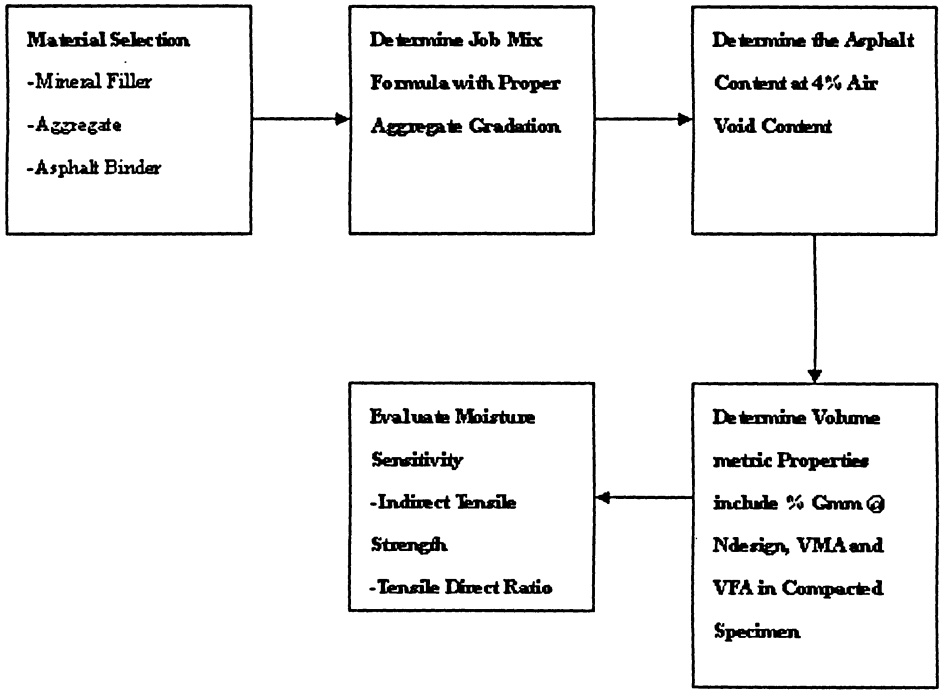

Figure 7 Mix Design Procedures

2.8 Pavement Failure

With the increase of daily traffic volumes, unexpected pavement failures have occurred rapidly in the past years, which cost millions of dollars each year to fix. The use of mineral filler materials in hot mix asphalt serve as an environmental friendly and economical solution. However, there are many questions and uncertainties still unsolved. Before having a closer review on the mineral filler mixes, it is important to further understand the cause of various pavement failures and the various studies pursued by different authors.

2.9 Permanent Deformation (Rutting)

2.9.1 Mechanism

The main objective of this section is to have a better understanding of the various causes

of rutting and recommendations to overcome such failures. Permanent deformation in pavement structures occur when small amounts of unrecoverable deformation accumulated under periodic loading. Each time a heavy truck passes though, it will cause deformation on the asphalt layer and form wheel path rutting over time. This wheel path rutting is an indication of weak shear strength mixture to resist repetitive heavy loading. Such rutting may occurred at the surface layer or both surface and base layer. Rutting deformations are usually found in road intersections that exist in both cold and hot weather conditions. Campen and Nebraska (1981) found that although there are significant rutting at the intersection, there is no sign of rutting in the same pavement along the road away from the intersection. This is could be explained by hot mix asphalt exhibiting low stiffness under slow moving traffic, along with warmer climates. It seems logical that pavements in warmer temperatures are more prone to oxidation, which results in further decrease of stiffness.

The investigation by Campen et al (1981) in Omaha, Nebraska established that most of the rutting and shoving occurred where heavy traffic channeled near the bus stops. The samples taken illustrated that the VMA were lower than normal in conventional mixes, caused by the low dense gradation and making the surface wearing course with very low rut resistance.

Lingle (1986) observed that asphalt mixtures with higher asphalt contents showed a greater loss in stability. When the density of the asphalt mixture approached the maximum theoretical density, the mixture rapidly lost stability and started rutting, since it

could no longer consolidate.

A recent study has demonstrated that mineral filler with sufficient hydrated lime content has a significant positive effect on asphalt binder (Little, 2001). It was found to generally increase the stiffness of the asphalt binder and significanty improve the rheological properties (Little, 2001).

2.9.2 Improve Rutting at Mix Design Stage

To help eliminate the potential rutting deformation problem occurring in hot mix asphalt during the conventional mix design process, Lingle's (1986) study found the following points:

- Lower asphalt content: Mixes with lower asphalt content was proven to have greater rut performance in hot climate conditions. While higher asphalt content mixes were more flexible for fatigue and durability improvements, asphalt mixtures with higher asphalt content were more prone to rutting deformations. Therefore a compromise level of asphalt content is required.

- Coarser gradation: The larger sized materials used meant that course aggregate gradation had greater stability and strength.

- Higher value in fine aggregate angularity: Asphalt mixtures that are easily compacted most likely can rut easily under traffic loads. Fine aggregates

contribute approximately 45-55% of the mixture weight, and are the primary factor affecting the asphalt workability. Mixtures with low workability were often found to have a higher rut resistance, caused by the angularity of crushed fine aggregates. Angular and rough texture properties of fine aggregates have much more particle-particle contact than rounded aggregates which are prone to shearing forces subjected to the pavement matrix.

- High Viscosity Asphalt Binder: Asphalt binder with high viscosity at 60 °C tends to have a more plastic flow which provides better bonding to the aggregate skeleton.

2.9.2.1 Improve Rutting with VMA and Air Void Properties

Research was conducted on the relationship between Voids in Mineral Aggregate (VMA) and air void in terms of rutting performance. According to Barksdale, in normal conventional hot mix asphalt, the asphalt binder between aggregates is squeezed out to the available air spaces. Mixes with low voids in mineral aggregate (VMA) and low air voids has no available space for the asphalt binder, which it acts as lubricant and offsets the pavement skeleton. Wearing course mixtures with a minimum VMA value of 16% and air void of 3 to 4% are ideal for rutting resistance. It is not recommended to increase the VMA by lowering the asphalt content since the amount of asphalt has a direct contribution on durability and raveling issues of the pavement structure itself. The VMA value can be increased by the suggested method as follows:

- Create sufficient air voids from the maximum density gradation line.
- Use angular fine aggregates.

2.9.3 Improve Rutting with Mineral Filler

The best way to prevent rutting is to develop an elastic solid mixture with a stiffer asphalt binder and utilize rut resistance mineral aggregates in asphalt mixes. The stiffer asphalt binder will act as a "rubber band" and allow the mix to return to its original shape rather than deforming. The mineral aggregate will increase the internal shear strength of the compacted mixture by increasing the friction necessary to provide better particle to particle contact.

A laboratory study was conducted by Huang (2006) to investigate the effects of different filler materials subjected under the wheel path rutting test. The results indicated that the rut depth increased slightly for mixtures with 5% filler replacement compared to those with 2% filler replacement. However, significant improvements on rut depth are observed on mixtures with higher filler content at 10% (Huang, 2006). The stiffening effect is based on the amount of filler content added to the asphalt binder. By adding 10% filler content, the performance grade (PG) of the asphalt binder may increase by one full grade to provide greater rutting resistance.

2.9.4 Evaluate Rutting with Rheological Property (G*/Sin (δ))

A parameter G*/Sin (δ) is conducted to evaluate the rut resistance by the Strategic Highway Research Program (SHRP) on binder. The complex shear modulus (G*) and phase angle (δ) are determined to analyze the viscous (non-recoverable) and elastic (recoverable) behaviour of the asphalt samples. The value of "G*" is the measure of the total resistance to deformation of the asphalt binder, subjected to repetitive shear stress.

The value of "δ" determines the viscous and elastic behaviour of the material. The value of "G*/sin δ" is used to determine the permanent deformation at test temperature. An increase of this parameter is observed with hydrated lime added into the asphalt binder. A shown in Figure 8, the lime increases the viscosity (stiffness) in both types of asphalt binder (AAD with up to 20% asphaltene content and AAM with up to 4% asphaltene content) with an increase of G*/Sin(δ). The stiffening effect caused reduction of rutting potential during pavement life (Little, 1996).

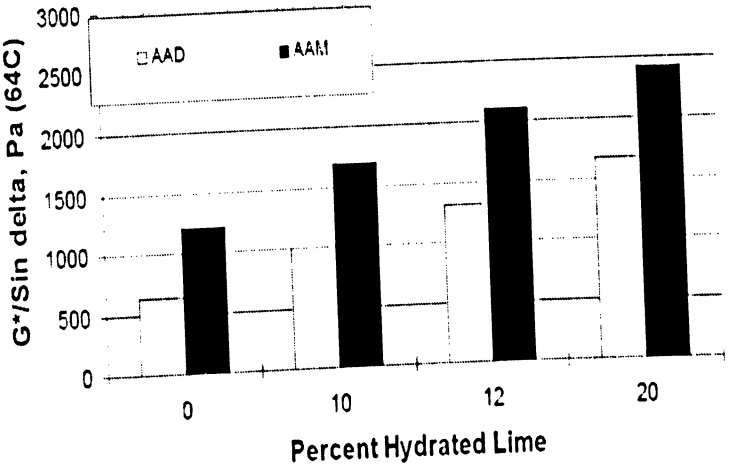

Figure 8 Effect of the Addition of Hydrated Lime on Asphalt Binder Rheology (Little, 1996)

2.10 Fatigue Cracking

2.10.1 Mechanism

Fatigue cracking is usually found at the bottom of the asphalt layer, and is caused by rapid high deflection cycles. The high deflection causes the bottom of the asphalt layer to be subjected to an enormous level of tensile stress. An advanced state of fatigue cracking is presented when many transverse cracks are connected with longitudinal cracks covering large areas (known as "alligator cracking"). Such form of pavement distress eventually will lead to future pot holes. Pavement engineers expect to see such

failure at the end of the pavement designed life cycle. If these failures occur at earlier stages of the pavement life cycles, then it is likely that repeated heavy traffic loads are the reasons for such failures.

2.10.2 Fatigue Characteristic Study with Different Design Methods

A fatigue characteristic study was conducted with the use of Superpave and Hveem method by Hartman and Gilchrist (2001). Fatigue cracking generally begins at the bottom of the asphalt layer, due to binder aging. The cracks are reflected to the surface asphalt layer over time. A detailed study was conducted using a flexural beam fatigue test with both strain-controlled modes loading to evaluate the general fatigue behaviour. The effect of long-term oven aging on the fatigue performance was also evaluated to determine its characteristics near the end of the pavement life cycle under controlled laboratory conditions. Laboratory compacted field mixtures sampled behind the pavers were carried out from three different sites with both Hveem and Superpave method. The Hveem samples acted as a baseline reference in this scenario. Different field samples from each contract were sampled to evaluate the fatigue characteristics as follows:

- Beam specimens were prepared for both aged and un-aged asphalt binder, and prepared in accordance with ASTM D3202 to test for fatigue resistance under the strain-controlled mode loading.
- The long-term aged samples were prepared according to AASHTO PP2-01 with 20 hours at 85 ^{o}C in the aging oven. The samples were prepared to simulate the

long-term aging effect after 20 years.

- Fatigue characteristics of the Superpave and Hveem mixtures (both aged and un-aged) were determined using the fatigue relationship by SHRP.
- Different strain levels of each mixture were compared for aged and un-aged binder.

In conclusion, the fatigue resistance results obtained from the three contracts were very inconsistent, and proved that different design methods did not generate an impact on fatigue resistance. A clear correlation cannot be made between the initial flexural stiffness and type of asphalt binder (modified and unmodified binder) used. Some of the mixtures experienced a reduction of fatigue performance caused by aging, while others did not.

However, it is noted that samples with high asphalt content generated a better result on fatigue resistance at 22 °C. Samples conducted by Superpave mixtures have a higher asphalt content and film thickness than Hveem mixtures, and out-performed the Hycem mixtures in fatigue resistance. The same results applied to samples carried out by Hveem method having higher asphalt content and film thickness than Superpave mixtures.

A note should be made on film thickness where gradation and asphalt content have a direct influence. Mixtures with higher film thickness most likely had a courser gradation with higher asphalt content, which is a good characteristic of fatigue resistance. Therefore, engineers should achieve a minimum VMA value of 16 at the design stage.

2.10.3 Control Fatigue Cracking by Mix Design

Fatigue cracking can be reduced at the mix design stage. Research conducted by the Asphalt Institute (Asphalt Institute, Manual Series No. 22), and showed that as the pavement air void increases at the design stage, the pavement fatigue resistance reduces dramatically. Another cause associated with fatigue cracking of the pavement structure is low asphalt content. Pavement with low asphalt content have a higher tendency of fatigue cracking (Asphalt Institute, Manual Series No. 22).

2.10.4 Reduced Fatigue Cracking through Appropriate Pavement Design

The thickness and strength of the pavement structure has great impact on fatigue cracking. Pavement structure with significant thickness and strength with supported subgrade can prevent load-associated cracks. A well designed pavement will provide better support and will not bend as much under loading as compared to thin or poorly supported pavements (Asphalt Institute).

2.10.5 Reduce Fatigue Cracking by Asphalt Binder Selection

Fatigue cracking can be eliminated at the asphalt binder selection stage. Hot mix Asphalt must have enough tensile strength resistance to overcome the applied tensile stress. A stiffer asphalt binder has a greater tendency to be resilient under repetitive loading. A pavement containing asphalt that has aged and hardened will mostly likely have low fatigue resistance. It is important to use a modified binder that provides flexible and elastic characteristics (Asphalt Institute).

2.10.6 Reduce Fatigue Cracking by Mineral Filler

In Didier and Little's research in 1999, they found that active mineral filler, such as lime, improve the stiffness of the asphalt binder. The additional lime filler is chemically active with the polar molecules and will remove undesirable components in the pavement matrix. The active particles are distributed throughout the mix and give more resistannce to fatigue cracking. These particles are more able to intercept and deflect micro-cracks, preventing them from turning into more severe pavement distress.

2.11 Low Temperature Cracking

2.11.1 General

Low temperature cracking is caused by extreme weather conditions. Such pavement distress occurs when the asphalt layer shrinks under cold climates. Tensile stress is developed when the asphalt shrinks, resulting in a tensile stresses exceeding the tensile strength of the aged asphalt layer after periodic low temperature cycle(s). Hardening of asphalt binders is mainly caused by oxidization aging over time (Huang, 2007). Mixes that have higher air void content are also prone to low temperature cracking. It is important to meet all volumetric properties to minimize such pavement failure.

2.11.2 Other Causes of Low Temperature Cracking

There are other types of low temperature cracking presented by Nahass's (1990) paper, namely:

- Crack formations occur on sub-grade when subjected to freezing and shrinking.

These cracks can reflect to the pavement surface.

- Freezing and shrinking on the sub-base and base level caused cracking that reflected to the pavement surface.

2.11.3 Creep Stiffness (S)

In Lackner's paper (2005), the author studied the effect of filler on low-temperature creep stiffness of asphalt mastic. A bending beam rheometer (BBR) was used in an experiment to characterize the effects of different filler types on the content asphalt mastic-scale interface (Bitumen-filler composite). The creep stiffness (S) value is used to determine the stress relaxation capacity in flexible pavements in low temperature conditions. According to the AASHTO TP-1 specifications, the creep stiffness should not exceed 300 Mpa, since asphalt samples with a higher value are usually too stiff to provide any flexibility for pavement structures. An optimum (not low, not so high) creep value is required to avoid thermal shrinkage cracking under cold winter temperatures. Lackner (2005) suggested that the results of the experiment showed that *only the volume fraction of the filler* has an effect on creep properties, and that the shape of the filler particles does not significantly influence creep stiffness.

2.11.4 m-value

The m-value obtained from the BBR was used to determine the stress relaxation rate of the bitumen-filler matrix at particular time and temperature. It measures the rate of the creep stiffness (S) changes in logarithm as a function of time at specific temperature and *loading time. The m-value is a very important parameter* of asphalt behaviours at low

temperatures because it is believed that when a pavement structure is subjected to low-temperatures, the asphalt binder relaxes internal stresses more slowly, creating internal stress much faster than a binder with a higher m-value (higher stress relaxation rate). Asphalt with a lower stress relaxation rate and thus lower m-value will have internal stress exceeding the tensile strength of the asphalt binder, and cause cracking (Gallagher, Bahia, 1996).

2.11.5 Use of Mineral Filler to Minimize Low Temperature Cracking

Kumar and Goetz (1997) explained that the hardening effect by aging increases the stiffness and modulus of the asphalt cement. However, the stiffening effect lowers the strain and causes cracking. Therefore, it is necessary to control the strain corresponding to hardness of the asphalt at a desirable level. There are two ways to reduce low temperature cracking, namely by lowering the viscosity and hardening the asphalt cement. To overcome the hardening effect by aging, a soft and durable asphalt binder should be used for low temperature susceptibility (King, 1993). The results of Huang's (2007) study show that mineral filler reduces oxidation and aging to maintain the pavement flexibility, which is favourable to low temperature cracking. In addition, Petersen (1987) recommended that a less chemically active filler, such as lime, will not cause the asphalt binder to become more brittle at low temperatures. The performance grade of the asphalt cement may be increased respective to the filler content; however, the low temperature grading will remain unaffected.

Both researchers Hills and Brien (1966) found that an increase of binder content has little

influence on low temperature cracking. The additional binder increases the coefficient of thermal expansion and decreases the stiffness of the asphalt mixture. A field inspection studied was later conducted in Manitoba. Three different penetration graded asphalt binders were selected in this experiment, and the stiffness modulus was calculated respectively. The breaking stress and strains were determined under low temperature conditions. Based on the results obtained, Hills and Brien predicted the failure temperature with actual results from the actual pavement structure. The predicted temperatures were consistently lower than the actual fracture temperatures obtained in the field. However, other researchers, such as Aschenbrener, concluded that asphalt plays an important role in low temperature cracking and the use of polymer-modified asphalt has dramatic impact on thermal cracking, due to the flexibility of the polymer-modified asphalt structure.

2.12 Moisture Sensitivity Damage (Stripping)

2.12.1 Mechanism

Moisture sensitivity and stripping are closely related to each other. Stripping of the asphalt essentially is caused by over-exposure to moisture over a period of time. The moisture weakens the asphalt's cohesive strength, which is the primarily contributor to asphalt and aggregate bonding reduction at the pavement matrix (Little & Epps, 2001). Based on the difference in thermal expansion of aggregate and asphalt cements, the asphalt/aggregate bond is weakening by thermal contraction and expansion in time. The thermal contraction may also initiate internal cracks, which permits water to penetrate to the asphalt/aggregate interface (El, 1991). The asphalt pavement may experience loss of

strength due to the presence of moisture absorbed into the pavement matrix and cause stripping. The moisture susceptibility is influenced by (Little & Epps, 2001):

- Properties of the aggregate.
- Properties of the asphalt binder.
- Characteristics of the mixture.
- Climate.
- Traffic volume.

2.12.2 Aggregate Selection

It is usually the aggregate properties that dominate the water susceptibility properties in hot mix asphalt (Little, 2001). Detailed examinations of the aggregate properties are required. Polished aggregate and aggregates that are known to stripping should be avoided.

2.12.3 Asphalt Binder Selection

If an aggregate-related water susceptibility problem cannot be overcome, an unmodified asphalt binder with superior anti-stripping properties may be applied.

2.12.4 Traffic Volume Related to Stripping

Pavement with high traffic volume is subjected to more premature distress than similar pavements with lower traffic volume (Little, 2001). A pavement structure with higher compacted air void content is more likely to experience stripping than pavements with lower air void content (Little, 2001). (may want to explain why..I'm assuming ilt is due

to the increased space that water can slip into.

2.12.5 Mineral Filler Improves Aggregate-Asphalt Bonding

A laboratory study conducted by Chan, (1996) and the author proved that fly ash as a mineral filler is highly beneficial in terms of strength and stripping resistance. The improvements on stripping resistance increased significantly with the increase of fly ash content (Chan, 1996). In additional, Sankaran and Rao (1973) conducted research based on 2% fly ash filler content, and found that mixes with 2% fly ash and 5% asphalt obtained the highest stability, and retained strength after immersion.

Petersen (1987) concluded that hydrated lime is a superior anti-stripping agent in HMA. It reacts with the aggregates in the system to strengthen the aggregates-asphalt bonding. At the same time, lime reacts with the highly polar molecules (water-soluble soaps) at the asphalt binder that promotes stripping. When lime reacts with these molecules, they have a tendency to form insoluble salt that is not favourable to water attraction.

The physical-chemical mechanisms of stripping are not fully understood. Detachment, pore water pressure, and asphalt-aggregate properties have been proposed to define the cause of water susceptibility problems. More detailed study is needed to fully understand the basic mechanism of this problem. However, traditional lime material is a proven anti-stripping agent (Little, 2001).

Other potential stripping agents, such as Portland cement, have been tested. Figure 9

shows the TSR results with different anti-strip additives (Epps, 1992), where hydrated lime performed the best with highest retained strength. Mixtures with hydrated lime have been proven to improve resistance to moisture damage.

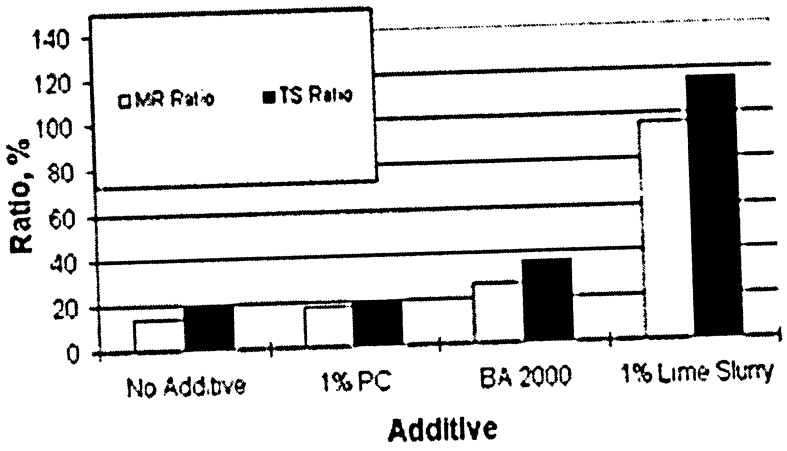

Figure 9 Effect of Various Additives on Retained Strength with 6% Asphalt Cement (Epps, 1992)

2.13 Type of Mineral Fillers

Filler material is produced at the production stage by crushing and screening of the material passing the number 200 sieve (less than 75 μm). Mineral filler that is finer than the thickness of asphalt film will make the asphalt binder more mastic. Many researchers have proved that sufficient amount of mineral filler replacement will enhance pavement performance by stiffening the asphalt binder. Laboratory studies have been shown that mineral filler in asphalt mixtures could achieve similar properties of hot mix asphalt with hydrated lime. It is believed that the gradation, particle shape, size and texture of the mineral filler have influences on hot mix performances. Four different types of mineral filler are discussed in this section:

- Hydrated Lime.

- Fly Ash.
- Blast Furnace Slag.
- Portland Cement.

2.14 Hydrated Lime

2.14.1 General

Hydrated lime is a traditional and popular material used in the asphalt industry with many associated benefits. Many studies have been conducted to evaluate the performance of the asphalt binder with the use of hydrated lime. It is important to understand why hydrated lime is so effective in hot mix asphalt. Highway material researchers have been investigating the use of by-product materials as filler in asphaltic concrete mixtures to replace the traditional asphalt mixes with hydrated lime in order to reduce production costs.

2.14.2 Asphalt Binder Behaviour with Hydrated Lime

Petersen's (1987) paper concluded that the chemical reaction between the calcium oxide (CaO) found in hydrated lime and the polar molecules in the asphalt mix reduce the oxidation and aging of the asphalt binder. When the calcium hydroxide reacts with the polar molecules, the asphalt binder is inactive with the environment. The pavement structure remains flexible for longer service life than without lime. The flexibility given by hydrated lime will reduce the chance of fatigue and low temperature.

2.14.3 Low Temperature Cracking

An extensive review and additional research was conducted by Johannson (1998) on lime in asphalt binder at low temperatures. Some of Johannson's findings are listed as follows:

- Adding 20% hydrated lime (by weight of asphalt) has significant increase in creep stiffness. However, the physical hardening of the binder did not increase. This is considered as a positive effect at low temperatures since it reduces fracture potentials (Little, 2001).
- Lime fillers do not impact the binder's relaxation rate at low temperatures while increasing its low temperature stiffness and fracture toughness (Lesueur et al. 1998).
- The age-hardening effect associated with hydrated lime is found more at high temperature than at low temperature conditions.

2.14.4 Moisture Susceptibility

Laboratory and field tests have been conducted, and proved that the use of hydrated lime in hot mixes has significant reduction in moisture susceptibility, improved asphalt-aggregate bonding, and improved water-induced damage resistance (Little, 2001).

2.14.5 Field Study

A field study was conducted by Jones (1997) that concluded that while the viscosity of the asphalt binder was reduced compared to a "No Additive" mix, the hardening effect stabilized with hydrated lime after eight years of aging time, as illustrated in Figure 10. Similar research was carried out at Western Research Institute and found that the

hardening effect of the asphalt could be reduced by adding hydrated lime (Petersen et al., (1987). A minimum of one percent of hydrated lime is needed to achieve reduction of age hardening.

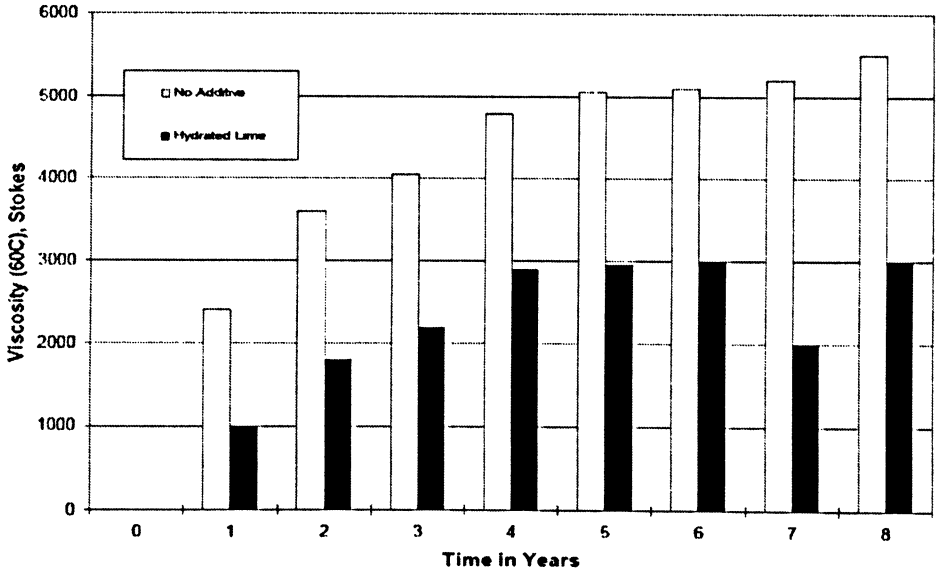

Figure 10 Effect of Hydrated Lime on the Hardening of Asphalt Binder (Jones, 1997)

2.15 Fly Ash

Fly ash was found to have positive effects on hot mix asphalt as a mineral filler. Fly ash is a glassy, amorphous structured material created after the combustion process of coal at a power plant. It is commonly used in asphalt mixes as an anti-stripping additive, as well as an asphalt extender due to its particles' fineness (Suheibani 1986). The performance properties of fly ash in asphaltic concrete mixtures vary by the amount of lime present. Two classified Fly ashes under the ASTM standards were chosen for examination in this study, and they are classified based on their chemical composition, fineness and calcium content: Class C with high lime content and Class F with low lime content. Fly ashes with low calcium content may not have significant improvements in its physical

performance of the asphalt specimens. However, fly ashes with high calcium content shows significant improvements in retain strength and asphalt stripping under laboratory conditions.

2.15.1 Fly Ash in Asphalt Mixtures

Fly ash has been used as mineral filler in hot mix asphalt mixtures. Mixtures with 5% (by weight of aggregate) fly ash has compatible mix design properties with mixtures containing hydrated lime and lime stone dust (Huang, 2006). It has been shown to have comparable physical properties to limestone dust with good void filling and water resistance characteristics, which make it an excellent anti-stripping agent (Zimmer, 1970).

A study on fly ash as mineral filler was conducted at the North Dakota State University, and the results were compared with mixes containing hydrated lime and crusher dust. Mixes with fly ash has higher retained stability and provided excellent anti-stripping characteristics (Carpenter, 1952).

2.15.2 Stripping Properties with Fly Ash

Further confirmation of the stripping properties of fly ash occurred during Rosener's study in 1982, where two types of fly ash (Class C and Class F) were utilized in hot mix asphalt mixtures. All mixes with fly ash showed significant improvement on retained stability and immersion Marshall stability results. A similar study was conducted by Galloway (1980), which concluded that the use of fly ashes as mineral filler retards the rate of age hardening in asphalt binder. At the same time, it was found fly ashes with high lime content indicated excellent anti-stripping results with polish-susceptible

aggregates. Low calcium content fly ash may not be a significant influence of pavement performance. Fly ash with high calcium content believes to be influential in pavement performance, especially to prevent asphalt stripping.

2.15.3 Workability of Hot Mix with Fly Ash

A detailed laboratory study was conducted by Galloway (1980) to prove that the predominantly spherical shape and particle size of fly ash particles lead to significant improvement on compaction of hot mix asphalt. Mixes with fly ash had a greater workability index compared to conventional hot mix. Galloway (1980) suggested that mixes with fly ash required less energy at the mixing and compaction stages, by allowing temperatures reductions to as low as 110°C and 85°C respectively without affecting the pavement performance and properties.

2.16 Blast Furnace Slag Filler

2.16.1 General

Granulated Blast Furnace Slag (GBFS) is an active material commonly used as a supplementary cementitious material in concrete applications. It is a glassy material with a particle shape, size and texture dependent on the chemical composition and purification process. Variability during the purification process can directly lead to low consistency in its physical properties, such as angularity, fineness, absorption, and specific gravity. Therefore, the performance and properties of a hot mix asphalt containing Blast Furnace Slag is affected by the variability of the Blast Furnace Slag. It should be noted that un-combusted particles in the Blast Furnace Slag may lead to future stripping problems during the pavement life.

Blast Furnace Slag is a very common material found in Ontario. However, limited research has been conducted for its use in hot-mix asphalt applications.

2.17 Portland Cement

Portland cement (PC) is a combination of hydraulic calcium silicates is widely used in asphalt mixes. The performance and properties of the PC are controlled during the manufacturing stage with appropriate proportions of calcium, silica, alumina, and iron components (Portland Cement Association, 2002). Studies have proven that PC greatly contributes to anti-stripping of pavement. Asphalt mixes with PC filler significantly improves the Marshall properties, including stabilities and flow (Aljassar, 2004). Ramzi and Amer (2002) reported that all mix design properties (air void, Marshall stability, flow, Voids Mineral Aggregate, and Voids Filled with Asphalt) meets the minimum specifications for both surface and base course. Also, Ramzi and Amer (2002) suggested that the optimum percentage of PC should not exceed 5% by weight of the aggregate. Any percentage higher would produce an uneconomical mix with higher required asphalt content.

2.17.1 Cement-Coated Aggregates Improves Stripping Property

The application of PC to hot mix asphalt leads to aggregate particles being coated with a hydrated cement film when the asphalt is applied, as illustrated in Figure 11 (Bayomy, 1992). The Portland cement film adheres to the aggregate surface with appropriate time for hydration, and provides a rough textured surface on the aggregate particle. This

improves the stripping property and reduces pavement distress caused by increases in particle internal friction. It also increases the bonding between the asphalt binder and aggregate.

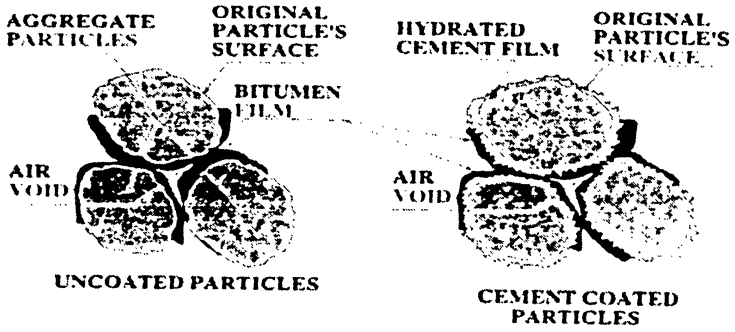

Figure 11 Cement Coated Aggregate Concept (Bayomy, 1992)

2.17.2 Marshall Properties with Portland Cement

Al-Suhaibani (1992) has conducted a research study to evaluate the use of Portland cement as an alternative to traditional lime stone filler in hot mix asphalt. It was found that the Marshall and mechanical properties, including Marshall stability, specific gravity, and indirect tensile strength, increase as the cement dust content increases. The flow values, air void and VMA decrease as the cement dust content increases. These are great advantages which would lead to many positive results increasing the service life of the pavement structure.

2.17.3 Effect on VMA

There is no significant difference in VMA value at 3% Portland cement filler content as a partial replacement of limestone dust. However, there is significant reduction of VMA when Portland cement content is greater than 5.5%. It is clear that all actual VMA values are lower than design value. The low VMA results in less available space for the

asphalt to have a sufficient coating and durability (Al-Suhaibani, 1992).

2.17.4 Effect on Marshall Stability

In Aljassar and Metwali 's research, it was concluded that PC content greater than 5% resulted in reduction of Marshall stability and an increase in the retained strength. Therefore, 5% cement content should be the optimum filler content in HMA, as shown in Figure 12.

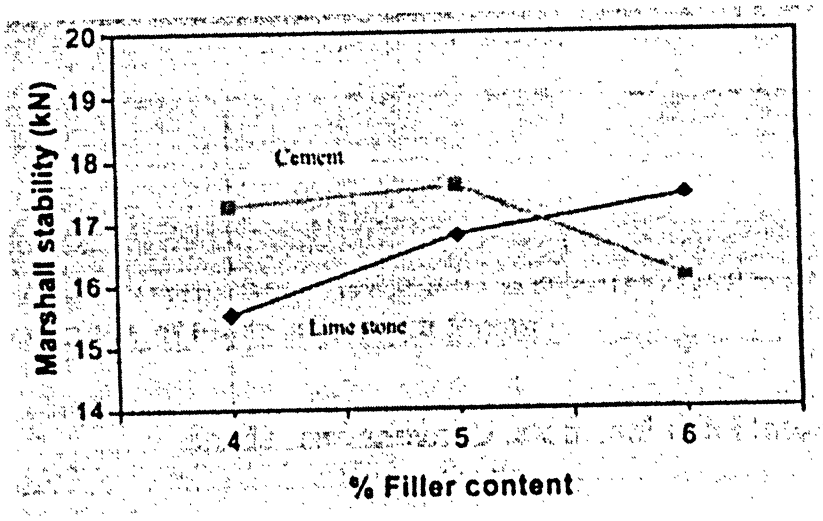

Figure 12 Marshall Stability as a Function of Filler Content (Aljassar and Metwali, 2004)

2.17.5 Effect on Retained Strength

The use of hydrated lime is a known filler material decreases moisture susceptibility. Portland cement was also found to improve anti-stripping properties in hot mix asphalt as a filler material (Ramswamy et al., 1983). A detailed study was conducted by Aljassar and Metwali (2004) on the effectiveness of Portland cement on the retained strength of asphalt concrete. In their study, it was found that the index of retained strength values almost double when cement was used as filler when compared to limestone filler (as shown in Figure 13). An increase of retained strength was also observed as the cement

filler content increases, respectively. However, at 6% limestone filler content, the retained strength has a tendency to drop to the value previously found at 4%. In this study, a 5% content for limestone fillers and 6% for Portland cement fillers were found to be the optimum filler content for these mixes.

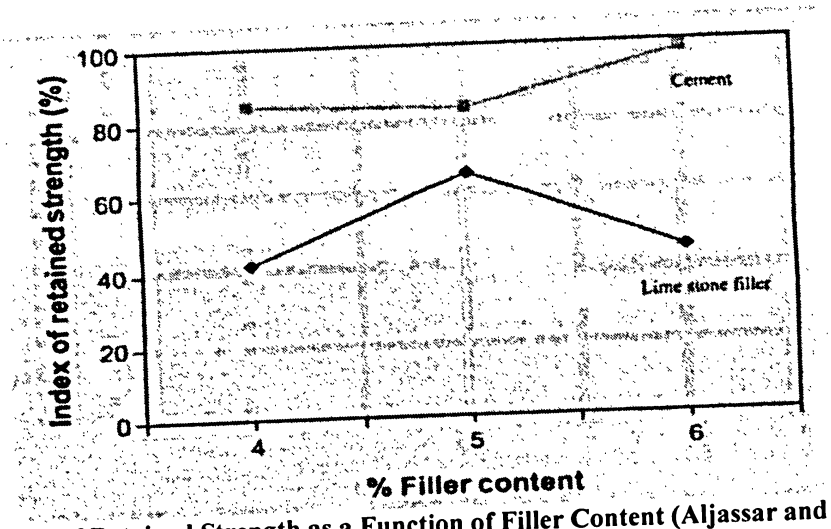

Figure 13 Index of Retained Strength as a Function of Filler Content (Aljassar and Metwali , 2004)

2.18 Mineral Filler Mixes Vs. Conventional Mixes

Reusing mineral filler in asphalt mixes is a worldwide trend. Mineral fillers were originally added to reduce air voids in HMA mixtures. However, fillers were also found to extend the asphalt binder, stiffen the asphalt binder, or both (NCHRP). The binder modification occurs by adding the filler to the asphalt concrete matrix.

Asphalt mixes with additional mineral filler generally have greater performance, especially in Indirect Tensile Strength (ITS) value and improvements on the bonding of aggregate-asphalt binder in the pavement matrix. Kandhal and Parker (1999) concluded the influences of HMA properties with mineral filler were as follows:

1. Depending on the particle size of the filler, it can act as an extender of the asphalt binder. All asphalt extender usually causes flushing and rutting in many cases. Reduction of asphalt cement content is a common practice to prevent pavement bleeding.
2. Certain fillers make HMA mixtures susceptible to moisture damage. The stripping of HMA mixes is closely related to the properties of the filler-asphalt combination.
3. Certain fillers have significant effects on the asphalt binder. The stiffening effect of the asphalt binder caused in association with the filler can seriously affect pavement performance.

2.19 Advantages of Filler in Asphalt Mixes

Mineral filler plays an important role in the performance of hot asphalt mixes. In general, an asphalt mix with mineral filler has the following advantages:

1. A substantial amount of limestone dust could be replaced by mineral filler to make it an economically feasible alternative (Khatri, 1993).
2. Mineral filler mixes provide essentially equal or better performance compared to conventional hot mix asphalt concrete (Khatri, 1993).
3. The same equipment that is used for mixing, placing and compacting with a conventional hot mix is applicable to an asphalt mix with mineral filler.
4. Mineral filler with high lime (CaO) content has significant improvements on indirect tensile strength and tensile strength ratio.
5. A successful mix with mineral filler will enhance asphalt and aggregate

bonding, which provides high stripping resistance.

6. Certain mineral fillers act as asphalt extenders that reduce the amount content necessary for optimum asphalt content, thereby generating an economical mix.
7. Mixes with mineral fillers containing hydrated lime tend to have higher retained strength and Marshall stability when compared to normal conventional mixes (Ahmad, 2004).
8. Mineral filler replacement mixes can be produced with available materials and Superpave equipment.
9. Mixtures with 5% filler replacement meet all Marshall design properties, including stability, flow, VMA, and VFA.
10. With all filler types containing high lime (CaO) content, the asphalt penetration generally decreased as the filler content increased (Ramzi, 2001).
11. With all filler types containing high lime (CaO) content, the ductility decreased as the filler content increased (Ramzi, 2001).
12. No environmental hazards are expected as a result of using mineral filler as fine replacement (Khatri, 1993).
13. Filler stiffens the asphalt binder to prevent rutting and fatigue cracking (Little, 2001).
14. Mineral filler improves short and long-term aging by altering oxidation kinetics (Little, 2001). Increasing the filler content in the asphalt binder does not change the shear susceptibility of binder samples regarding long-term aging hardening by oxidation and heat (Huang and Zeng, 2006).

2.20 Features to be Considered for Filler Mixes

Features to be considered for mineral replacement mixes include:

1. Substitution of 5% filler replacement is the optimum value used in asphalt mixes. Mixes with more than 5% filler would require more asphalt binder in the mixture, which generates an uneconomical mixes (Ramzi, 2001).
2. A mastic mix may be presented when filler replacement is greater than 5%.
3. Mixes with mineral filler are usually tender and difficult to compact under hot weather conditions.
4. Mineral filler materials are typically dusty materials, which may generate more dust during the production stage.
5. Mixes with mineral filler, such as slag, might cause rougher surfaces in a full depth pavement system (Khatri, 1993).
6. Optimum asphalt content and volumetric properties vary due to the percentage of different types mineral filler.
7. Mineral fillers with rough particle textures increase the stiffening of the mixture and became more mastic.

CHAPTER 3

LABORATORY EXPERIMENT

3.1 Description of Experimental Program

Five 19 mm Superpave mixes were selected in this study, and are classified as binder course in overall pavement structure. The main scope of this study was to determine the potential use of different filler materials in flexible pavements. Based on the results of Ramzi's 2001 study, a maximum filler material content of 5% (by weight of aggregate has significant improvement on Indirect Tensile Strength and Tensile Strength Ratio properties. Mixes with more than 5% filler would require more asphalt binder in the mixture, which is uneconomical to produce. The mix design was optimized with 4% dust passing the No. 200 sieve (0.075 mm) based on volumetric properties. Therefore, 4% dust was replaced with 4% mineral fillers of total weight of aggregate. Five 19 mm Superpave mixes were conducted, as follows:

1 Control Mix A: 4% limestone dust (Control Mix)

2 Filler Replacement Mix B: 4% fly ash (Class C) filler (high calcium oxide)

3 Filler Replacement Mix C: 4% fly ash (Class F) filler (low calcium oxide)

4 Filler Replacement Mix D: 4%Blast Furnace Slag filler

5 Filler Replacement Mix E: 4% Portland cement filler

3.2 Properties of Materials

All aggregates, including the two coarse and one fine aggregate, were selected from Dufferin Aggregates. House dust was used as a filler to achieve the volumetric properties of the control samples. These materials were selected to satisfy the Superpave design system based on the climate condition (temperature range based on binder grade PG58-28) and design traffic volume (traffic category D with design ESALs between 10 to 30 million). The properties of the materials are described next.

3.2.1 Coarse Aggregate

Two crushed limestone coarse aggregates with nominal size of 12.5 mm and 19 mm from Dufferin Aggregates were selected in this study. Both coarse aggregates were washed over the No. 200 sieve (passing 0.075 mm) to have a better control of the dust content and eliminate any possible anti-stripping additive pre-applied to the aggregate at the stockpile. The grain size analysis was carried out, followinged by the ASSHTO LS702 and LS 602 protocols. Both results are summarized in Tables 1 and 2, while the graphical results are illustrated in Figure 14 and 15.

Table 1 Gradation Test Results for 19mm Coarse Aggregate

Sieve Sizes (mm)	Percent Passing (%)
25.4	100
19	82.1
12.5	26.2
9.5	9.8
4.75	0.7
2.36	0.5
1.18	0.1
0.6	0.1
0.3	0.1
0.15	0.1
0.075	0

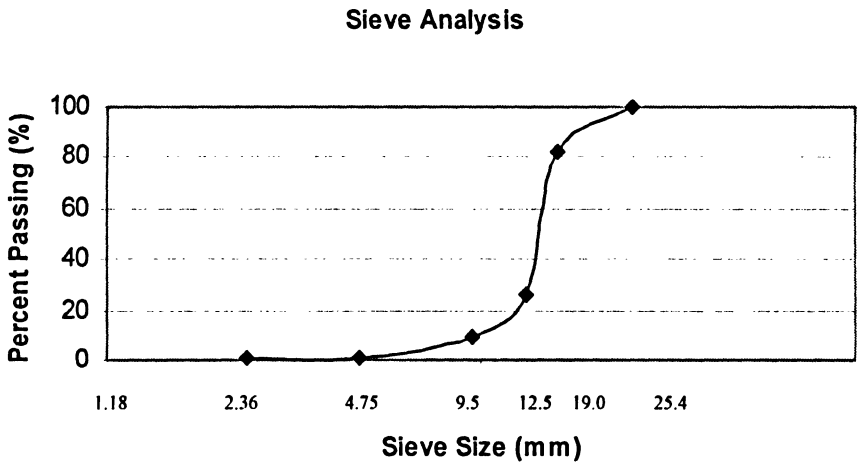

Figure 14 Gradation Test Results for 19mm Coarse Aggregate

Table 2 Gradation Test Results for 12.5mm Coarse Aggregate

Sieve Sizes (mm)	Percent Passing (%)
25.4	100
19	99.1
12.5	92.1
9.5	59.7
4.75	6.3
2.36	1.6
1.18	1.6
0.6	1.3
0.3	1
0.15	1
0.075	0

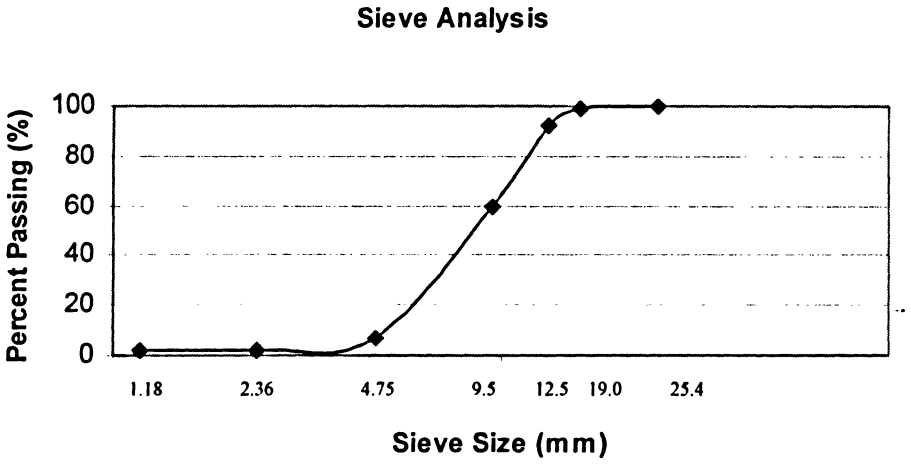

Figure 15 Gradation Test Results for 12.5mm Coarse Aggregate

3.2.2 Fine Aggregate

The fine aggregate used in this study was crushed trap rock screening manufactured from Dufferin Aggregate. The fine aggregate was washed over the No. 200 sieve (passing 0.075 mm) to have a better control of the dust content and eliminate any possible anti-stripping additive pre-applied on the aggregate at the stockpile. The results are summarized in Table 3, while the graphical results for the fine aggregate is illustrated in Figure 16.

Table 3 Gradation Test Results for Fine Aggregate

Sieve Sizes (mm)	Percent Passing (%)
4.75	100
2.36	94
1.18	66.6
0.6	43.2
0.3	22.5
0.15	10.5
0.075	0

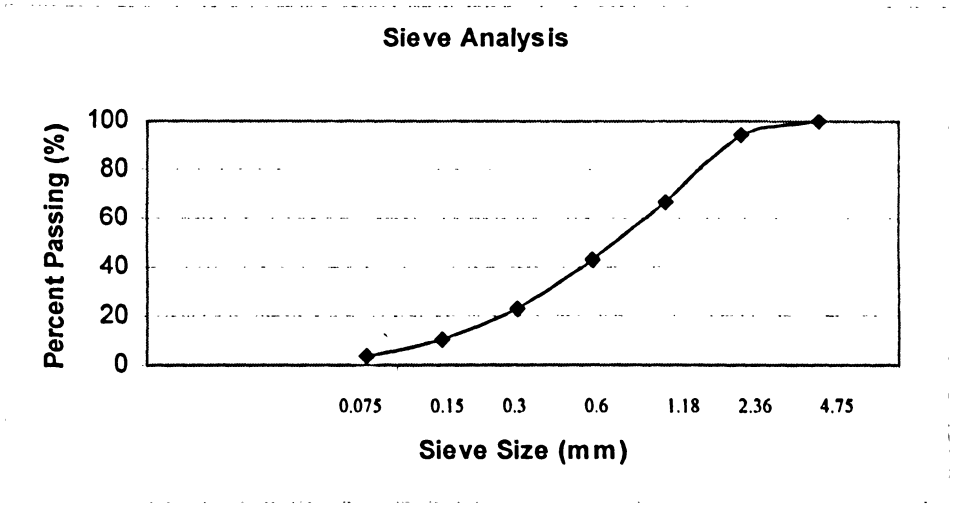

Figure 16 Gradation Test Results for Fine Aggregate

3.2.3 House Dust

In this study, 4% limestone dust (passing 0.075 mm sieve) from Dufferin Aggregates was used to assist achieving volumetric properties and lead to better control samples.

3.2.4 Consensus Properties

The Superpave design guidelines were conducted to determine the consensus properties of the aggregates. These properties have to achieve minimum criteria to satisfy critical climate conditions and high traffic volume requirements. These properties are:

1. Coarse aggregate angularity (% Crushed Particles).
2. Fine aggregate angularity.
3. Flat and elongated particles.
4. Clay content (Sand Equivalent).

3.2.5 Coarse Aggregate Angularity (% Crushed Particles)

The coarse aggregate anularity (% crushed particles) test determines coarse aggregate angularity for design traffic volume (category D) followed under OPSS LS-607. This property is important for aggregate internal friction and rutting resistance of asphalt mixes. It is defined as percentage by mass of aggregates larger than 4.75 mm with one or more fractured faces. The coarse aggregate angularity results for 19 mm and 12.5 mm stone are summarized in Tables 4 and 5.

Table 4 Coarse Aggregate Angularity Test Results for 19mm Aggregate

Fraction	Mass of Crushed (g)	Total Mass of Particles (g)
19.0mm - 16.0mm	243.4	243.4
16.0mm - 12.5mm	423.4	428.8
12.5mm - 9.5mm	328.3	332.8
9.5mm - 6.7mm	219.8	223.1
6.7mm - 4.75mm	116.3	123.9
Total Particles	1331.2	1352
% crushed particles	98.50%	

Table 5 Coarse Aggregate Angularity Test Results for 12.5mm Aggregate

Fraction	Mass of Crushed (g)	Total Mass of Particles (g)
19.0mm - 16.0mm	14.4	14.4
16.0mm - 12.5mm	14.6	14.6
12.5mm - 9.5mm	103.6	108.2
9.5mm - 6.7mm	549.3	559.9
6.7mm – 4.75mm	915.6	922.3
Total Particles	1597.5	1605
% crushed particles	99.50%	

3.2.6 Fine Aggregate Angularity

The angularity of fine aggregate is determined by measuring the uncompacted voids over washed and dried aggregates passing the 2.36 mm sieve, as according to the AASHTO TP33 protocol. The uncompacted void value provides an indication of the fine aggregate angularity. The sample was prepared and proportioned under the method "A" procedure. The prepared sample was placed at the funnel and free fell to the cylinder at a given height. The sample was scraped off the cylinder and leveled with a spatula. The uncompacted void value was calculated with Equation 1 and the test result is presented in Table 6.

$$\text{Uncompacted Void} = \frac{V - W/G_{sb}}{V} \times 100\%$$

Equation 1

W = Mass of fine aggregate

V = Volume of cylinder

G_{sb} = Bulk specific gravity of fine aggregate

Table 6 Fine Aggregate Angularity Test Results for Fine Aggregate

Description	
Volume of the cylinder (ml)	99.9
Tare weight of cylinder (g)	186.1
Weight of sample + cylinder (g)	328.4
Weight of sample (g)	142.3
Bulk specific gravity	2.905
Uncompacted voids, (min 45)	51

3.2.7 Flat and Elongated Particles

Coarse aggregate particles that have a maximum to minimum dimension ratio greater than five are considered not suitable for Superpave mixes, since flat and elongated coarse aggregates are undesirable in asphalt mixes. These undesirable aggregates have a greater tendency to fracture under traffic and during the construction stage. The maximum limit for than base layer is less then 10% as per ASTM 4791. The flat and elongated particle result for 19.0 mm and 12.5 mm aggregate are summarized in Tables 7 and 8.

Table 7 Flat and Elongated Particles Test Results for 19mm Aggregate

Fraction	Flat & Elongated Particles by Mass (g)	Total Mass of Particles (g)	Flat & Elongated (%)
19.0mm - 16.0mm	0	243.4	0
16.0mm - 12.5mm	8.2	428.8	1.9
12.5mm - 9.5mm	9.5	332.8	2.9
9.5mm - 6.7mm	7.8	223.1	3.5
6.7mm - 4.75mm	4.2	123.9	3.4
Total	29.7	1352	2.2

Table 8 Flat and Elongated Particles Test Results for 12.5mm Aggregate

Fraction	Flat & Elongated Particles by Mass (g)	Total Mass of Particles (g)	Flat & Elongated (%)
19.0mm - 16.0mm	0	14.4	0.0
16.0mm - 12.5mm	0	14.6	0.0
12.5mm - 9.5mm	4.1	108.2	3.8
9.5mm - 6.7mm	9.4	559.9	1.7
6.7mm - 4.75mm	9.8	922.3	1.1
Total	0	14.4	0.0

3.2.8 Clay Content (Sand Equivalent)

The sand equivalent test measures the percentage of sand particles over clay in fine aggregates finer than 4.75 mm. The flocculating solution is mixed with the material in a graduated cylinder. The sand equivalent ratio is then determined by measuring sand to clay height readings, and expressed in percentages. The minimum value should be 50% as per AASHTO T176. The sand equivalent test results of the control mix are expressed in Table 9.

Table 9 Clay Content Test Results of the Control Mix

Parameter	Sample No.1	Sample No. 2
Sand Reading	5.3	5.1
Clay Reading	7.1	6.9
Sand Equivalent (%)	75	74
Average	75	

3.2.9 Filler Material

Four types of filler materials, including fly ash (Class C), fly ash (Class F),Blast Furnace Slag and Portland cement, were selected in this study. Chemical analysis of each was carried out on a dry, ignited basis using the Bruker S4 X-ray fluorescence spectrometer, according to the ASTM D4326 protocol. The fineness test was followed under the ASTM C311 and C430 test procedure. The chemical compositions, fineness and specific gravity for each filler material are presented in Table 10.

Table 10 Chemical Composition of Mineral Filler

	Fly Ash (Class C)	Fly Ash (Class F)	Slag	Portland Cement
Fineness, % Passing	88.85%	72.57%	94.30%	88.04%
Specific Gravity	2.79	2.43	2.91	3.12
Silicon Dioxide, SiO2	32.42%	61.99%	36.90%	20.93%
Aluminum Oxide, Al2O3	16.92%	21.02%	7.82%	5.48%
Iron Oxide, Fe2O3	5.80%	9.28%	0.68%	2.42%
Sulfur Trioxide, SO3	2.11%	0.38%	0.45%	4.16%
Calcium Oxide, CaO	31.81%	2.99%	39.90%	61.44%
Sodium Oxide, Na2O	1.62%	0.39%	0.76%	0.20%
Magnesium Oxide, MgO	5.81%	0.98%	11.20%	2.84%
Potassium Oxide, K2O	0.57%	1.12%	0.52%	1.11%
Phosphorus Pentoxide, P2O5	1.18%	0.06%	322ppm	0.12%

3.2.10 Asphalt Cement

The physical properties and performance of the asphalt binder can be altered by an asphalt modifier to meet specific climate conditions and traffic volumes at a specified zoned area. In this experiment, virgin binder graded PG58-28, manufactured by McAsphalt Industries Limited, Ontario, was selected in all mixes without any asphalt modifications. Five different asphalt contents of 3.5, 4.0%, 4.5%, 5.0% and 5.5% were selected for each trial blend to determine the optimum asphalt content for each mix and other volumetric properties. The compaction and mixing temperature of this asphalt was pre-determined at 138°C and 150°C, respectively.

3.3 Mix Design Method

The Superpave mix design method developed by the Strategic Highway Research Program (SHRP) was followed to establish the optimum asphalt content with design blended aggregate gradation. Two aggregate types (limestone course aggregate and trap rock fine aggregate) with PG 58-28 virgin asphalt binder were used in this experiment.

The straight red line in Figure 17 represent the maximum density line (zero percent air void) and trial blend closer to the line means it has less air void compared to the trail blend farther away from the line. Two trial blends were conducted: Trial 1 (Coarse blend away from the maximum density line) and Trial 2 (Fine Blend closer to the maximum density line), and their volumemetric properties were evaluated. The designed gradations complied with the OPSS 310, Superpave 19 mm specification, except for the air void contents, which were at 4.5% and 3.0% for Trial 1 and Trial 2.

Based on the air void content of each trail blend, the job mix formula was adjusted by linear interpolation to comply with 4% air void. The gradation is illustrated in Figure 17 with design limits. The job mix formula gradation was blended with 10% CA1, 43% CA2, 43% FA1, and 4% house dust.

Figure 17 Job Mix Formula for Superpave 19mm Mix

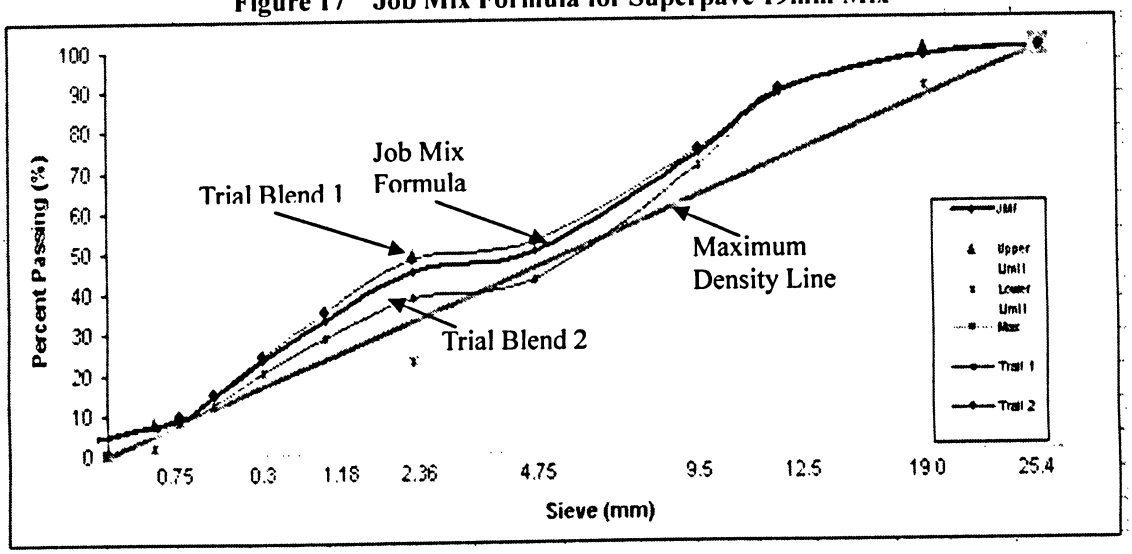

Sieve (mm)	25.4	19	12.5	9.5	4.75	2.36	1.18	0.6	0.3	0.15	0.075
Upper Limit	100	100				49					8
Lower Limit		90				23					2
JMF	100.0	97.8	89.2	73.7	49.8	45.2	33.3	23.1	14.1	9.0	4.0
Trail 1	100.0	97.8	88.7	70.8	43.2	38.7	28.8	20.2	12.6	8.3	4.0
Trail 2	100.0	97.9	89.5	74.9	52.6	47.9	35.3	24.4	14.8	9.2	4.0

3.3.1 Volumetric properties

The volumetric properties of the compacted specimens, such as maximum specific gravity (Gmm), bulk specific gravity of compacted specimen (Gmb), air voids (Va), voids in the mineral aggregate (VMA), and voids filled with asphalt (VFA), are used to calculate the optimum binder content. This information helps determine the optimum asphalt content and desired air voids at 4% for each mix. The calculations for

volumetric properties are listed in Equations 2 to 5, as follows:

For Percent Air Voids in Compacted Mixture

$$Va = \frac{(Gmm - Gmb)}{Gmm}$$

Equation 2

Va = air voids in compacted mixture

Gmm = maximum specific gravity of loose mixture

Gmb = bulk specific gravity of compacted mixture

For Percent Voids in Mineral Aggregate

$$VMA = \frac{(Gmb \times Ps)}{Gsb}$$

Equation 3

VMA = voids in mineral aggregate (%)

Gmb = bulk specific gravity of compacted mixture

Ps = aggregate content, percent by total mass

Gsb = bulk specific gravity of total aggregate

For Percent Voids Filled with Asphalt

$$VFA = \frac{(VMA - Va)}{VMA}$$

Equation 4

VFA = voids filled with asphalt (%)

VMA = voids in mineral aggregate

Va = air voids in compacted mixture

For Bulk Specific Gravity of Aggregate

$$Gsb = \frac{(P1 + P2 + \ldots\ldots Pn)}{\frac{P1}{G1} + \frac{P2}{G2} + \ldots\ldots \frac{Pn}{Gn}}$$

Equation 5

Gsb = bulk specific gravity of aggregate

Pn = individual percentages by mass of aggregate

Gn = individual bulk specific gravities of aggregate

3.3.2 Sample Preparation

In this study, a total of 25, 19 mm Superpave mixtures were conducted. Each mixture (4 mineral filler mixtures and 1 control mixture) was tried at 3.5, 4.0, 4.5, 5.0 and 5.5% asphalt content. Each briquette weight (include weight of asphalt binder) was prepared at approximately 4950g. A set of three briquettes were carried out for each trial.

Another set of two samples were prepared for theoretical maximum density testing, with approximately 2600g (including weight of asphalt binder) for each trail.

The aggregates were heated overnight at a mixing temperature of 150°C. The asphalt binder was heated in the oven until it reached the mixing temperature, prior to mixing at 150°C. After blending the aggregate and asphalt, each specimen was placed in the oven at compaction temperature of 138°C for two hours for absorption and short term aging, prior to compaction with the use of Superpave Gyratory Compactor (SGC).

3.3.3 Required Number of Gyrations

The design ESALs are the anticipated traffic levels based on over a 20 year period of time. The traffic category D was selected with design ESALs between 10 to 30 million,

which is commonly used for all major highways in Canada. The compaction parameters are summarized in Table 11.

Table 11 Compaction Parameters

Traffic category	Compaction Parameters		
	$N_{initial}$	N_{design}	N_{max}
D	8	100	160

3.3.4 Moisture Sensitivity Procedure

Moisture sensitivity and stripping (AASHTO T-283) test results were performed on all mixtures at a designed aggregate skeleton. Six specimens were gyrated to 7 ± 0.5 percent air voids and then divided into two subsets of threes. A set of three dry samples were sealed in plastic bags to prevent moisture exposure and placed in a control water bath at 25 ± 1°C before a tensile strength test. Another set of three wet specimens were placed in water and subjected to vacuum until each specimen reached between 70 to 80% degree of saturation under the ASSHTO protocol. The degree saturation of the surface dry specimens was calculated by Method A of AASHTO T-166. After the saturation process, the conditioned specimens were then placed in a freeze cycle for 24 ± 1 hr and subsequently left in a warm water bath at 60°C for 24 hrs. The conditioned samples were then placed in water bath at 25 ± 1°C for 3 hours for re-condition prior to strength test. All specimens were then tested for maximum load and the tensile strength, as determined by using Equation 6.

$$S = \frac{2000P}{\Pi\, t\, D}$$

Equation 6

S = tensile strength (kPa)

P = maximum load, (Newton)

t = specimen thickness, (mm)

D = specimen diameter (mm)

The Tensile Strength Ratio (TSR) was determined by using Equation 7.

$$TSR = \frac{S_2}{S_1}$$

Equation 7

S_1 = average tensile strength of the dry subset, (kPa)

S_2 = average tensile strength of the conditioned subset, (kPa)

3.3.5 Marshall Stability and Flow Test

Each specimen was heated to the compaction temperature of 140°C, as determined in Section 3.5.1. The specimens were compacted with a Marshall hammer with 75 blows on each side and excluded at room temperature, after being placed in a 60°C water bath prior to load testing. The maximum loads obtained were recorded at its peak value and the flow values were recorded in 0.25 mm increments.

3.4 Effects of Different Binder on Asphalt Cement

Four asphalt binder specimens were prepared with the addition of 2% filler (by total weight of asphalt), along with a virgin control specimen. Original binder graded 58-28 was mixed homogeneously by a stirring rod for approximately two minutes at mixing temperature of 150°C with each filler prior to testing. The performance grade (PG) cement was classified and provided precise determinations of failure points at critical

temperatures under the AASHTO M320 and ASTM protocols. Seven tests were conducted on each mixture. The required tests and practices for PG classification are listed as follows:

1. Original Dynamic Shear at 2 temperatures (AASHTO TP5)
2. Rolling Thin Film Oven (AASHTO T240)
3. RTFO Dynamic Shear with 2 temperatures (AASHTO T240)
4. Pressure Age Vessel (PAV) (AASHTO PP1)
5. PAV Dynamic Shear at 2 temperatures (AASHTO TP5)
6. Bending Beam Rheometer (BBR) (AASHTO TP1) at 2 temperatures

3.4.1 Dynamic Shear Test (Original, after RTFO and after PAV)

Two important asphalt behaviours of loading time and temperature are measured by the Bohlin dynamic shear rheometer (DSR). The DSR test operates with two parallel plates with a fixed bottom plate and an oscillating plate on top. Asphalt samples are placed in between the plates with specified gapping space. The Bohlin DSR machine was performed at a frequency of 10 radians per second, which is equivalent to 1.59 Hz (cycles per second) in all temperature ranges.

Two main results of complex shear modulus (G*) and phase angle (δ) was determined to analyze the viscous (non-recoverable) and elastic (recoverable) behaviour of the asphalt samples. The value of "G*" is the measure of the total resistance to deformation of the asphalt binder subjected to repetitive shear stress. The value of "δ" determines the viscous and elastic behaviour of the material. The rheological properties of the asphalt

binder are dependent on the aging time duration. Increasing the aging time, respectively increases the complex modulus (G*) and decreases the phase angle. Similar effects are found in association with temperature, since the complex modulus increases as temperature decreases, and the phase angle decreases as the temperature decreases (Huang, 2007).

For the original and after RTFO asphalt DSR tests, the gap spacing between the plates was set at 1000 microns plus extra 50 microns. The pre-mixed asphalt samples was placed between the 25 mm diameter oscillating and fixed plate. The asphalt specimen was trimmed to the same size as the oscillating plate and the gap spacing was then reduced to 1000 microns. Two (2) testing temperatures were selected at 58°C and 64°C according to the Superpave specification and the results obtained were used to determine the performance grade of each specimen. The main results of complex shear modulus (G*) and phase angle (δ) were obtained automatically by rheometer software.

The value of "G*" divided by sine "δ" (G*/sin δ) was used to evaluate the permanent deformation at the test temperature. The permanent deformation limits greater than 1.00 kPa for original binder and 2.20 kPa for RTFO binder were used during the data analysis stage.

3.4.2 Rolling Thin Film Oven Test (RTFO)

The purpose of Rolling Thin Film Oven (RTFO) process is to condition asphalt samples under a short term aging environment at 163°C. 35 grams of samples were poured into RTFO bottles and placed in a bottle carriage in the oven for 85 minutes. This procedure

simulates the mixing stage at the asphalt plant. The samples were then poured into a single container after the RTFO process for the pressure aging vessel test.

3.4.3 Pressure Aging Vessel (PAV)

The pressure aging vessel (PAV) simulates the long-term aging conditions under high pressure and temperature for 20 hours. The pressure vessel is pre-set to operate at 2070 kPa and 100°C, as according to AASHTO PP1 specifications. 50 grams of samples (after the RTFO process) was poured onto a plate and placed on a sampling rack. The samples were then placed in the PAV machine and aging begins.

3.4.4 Intermediate Temperature Dynamic Shear Evaluation

Similar apparatus was setup for the dynamic shear evaluation after the pressure aging. An 8 mm diameter oscillating and base plate was changed prior to the test. The gapping space for PAV dynamic sheer rheometer specimen was set to 2000 micron plus extra 50 microns. Two different intermediate test temperatures were selected at 19°C and 22°C, as according to the Superpave guideline.

The "G*" multiply by sine "δ" (G*sin δ) value was used to evaluate fatigue cracking properties after the pressure aging step. The test result governs when the test limit is less than 5000 kPa at test temperature. Asphalt samples with test results greater then 5000 kPa have a greater tendency of fatigue cracking.

3.4.5 Bending Beam Rheometer (BBR)

The bending beam rheometer (BBR) was developed to target the asphalt performance at low temperatures where asphalt acts like an elastic solid. It measures the creep value under a constant creep load at a specific temperature by applying a constant load at the center of the asphalt beam. This creep load simulates the thermal stresses developed in a pavement at low temperature. The creep stiffness is the resistance of the asphalt binder to creep loading. The creep stiffness (s) and creep rate (m) are calculated automatically by the BBR software from the center deflection of the asphalt beam.

The asphalt specimens were prepared with a rectangular aluminum mould. The specimens were trimmed evenly after a 45 minute cooling period. The specimens were then released from the mould and placed in the BBR test bath and conditioned for 60 minutes. Measurements were then obtained automatically by the computer software. The creep stiffness should not exceed 300 MPa according to the AASHTO TP-1 specifications. The equation for calculating creep stiffness S(t) is listed in Equation 8.

$$S(t) = \frac{PL^3}{4bh^3\,\delta(t)}$$

Equation 8

S(t) = creep stiffness (MPa)

P = applied constant load (N)

L = distance between beam supports, (102mm)

b = beam width at 12.5mm

h = beam thickness at 6.25mm

$\delta(t)$ = deflection (mm)

The m-value is the slope of the creep stiffness S(t) vs. log loading time. The specification calls for minimum of 0.300 at 60 seconds. The greater the m-value, the more quickly that the asphalt binder tends to relaxes internal stress to prevent cracking.

CHAPTER 4

EXPERIMENTAL RESULTS AND DISCUSSIONS

4.1 Superpave Characteristics and Properties

Five Superpave 19 mm mixes were designed as previously described. Their performance characteristics and properties are summarized and discussed in this section. Four percent mineral filler passing the No. 200 (0.075 mm) sieve were used in the 4 mixes with the same aggregate skeleton. Different optimum asphalt contents were determined for each type of filler, which was required to achieve 4% ± 0.1 air voids and other volumetric properties at N_{design} compaction level (100 gyrations), as summarized in Table 12.

Table 12 Volumetric Properties at Ndesign

	Control	Fly Ash (Class C)	Fly Ash (Class F)	Slag	Portland Cement
Asphalt Content(%)	4.3	4.0	4.0	4.3	4.5
Bulk Relative Density (BRD) at N_{design}	2.487	2.495	2.489	2.498	2.497
Maximum Density (MRD)	2.587	2.601	2.591	2.602	2.599
Air Void (%)	3.9	4.1	3.9	4	3.9

4.1.1 Discussion

Fly ash acts as an excellent "asphalt extender" according to Suheihani (1986) and Tons's (1983) findings. There is 0.3% reduction in asphalt content in both types of fly ash from the control mix, which act as an excellent asphalt reducer with desirable volume metric

properties. Although all specimens were conducted with similar filler particle sizes, as shown in Table 10., There is no indication of asphalt content reduction in mixes containing Blast Furnace Slag and Portland cement filler. Instead, mixes with Portland cement filler shows 0.2% increments in asphalt content. This is indicative that not only the particle size of the filler contributes to the reduction of asphalt content, but also that the particle shape strong influences a filler's ability to act as an "extender". Fly ash is the only filler with a spherical particle shape in this study, which provides better flow characteristics. More detail studies should follow.

4.2 Volumemetric Properties for Superpave 19mm Control Mix with 4% Limestone

Superpave 19 mm mix with 10% CA1, 43% CA2, 43% FA1, and 4% limestone dust were prepared, and five trials with asphalt content ranging from 3.5% to 5.0% were carried out. The detailed worksheets for each trial are presented in Appendix 1. The test results are summarized in Table 13 and Figure 18.

The design asphalt content was established at 4.0% air void, while 4.3% asphalt content was optimized for the control mix. All mixture properties were verified at 4.3% asphalt content. The test results are summarized in Table 14. The detailed worksheet at the optimum asphalt content is found in Appendix 2, while the mix properties worksheets are presented in Appendix 3.

Table 13 Test Results for Superpave 19mm with Limestone Dust (Control Mix)

Parameters	Results				
AC Content (%)	3.5	4.0	4.5	5.0	5.5
Gmb @ Ndesign	2.479	2.484	2.493	2.498	2.5
Gmm	2.599	2.593	2.585	2.573	2.566
% Gmm @ Ndesign	95.4	95.8	96.4	97.1	97.4
Air Voids (%) @ Ndesign	4.6	4.2	3.6	2.9	2.6
VMA (%)	13.7	14	14.1	14.4	14.8
VFA (%)	66.4	70	74.8	79.8	82.6
Gsb, bulk specific gravity	2.773				

Table 14 Test Results for Superpave 19mm with Limestone Dust at Optimum Asphalt Content

Mix Properties	Criteria	Selected Results
AC Content (%)	-	4.3
Gmb @ Ndesign	-	2.487
Gmm	-	2.587
% Gmm @ N_{design} = 100		96.1
% Gmm @ N_{ini} = 8	less than 89	88.2
% Gmm @ N_{max} = 160	less than 98	97.1
Air Voids (%) @ Ndesign	4%	3.9
VMA (%)	13.0 min	14.2
VFA (%)	65-75	72.7
Dust Proportion	0.6 - 1.2	0.94

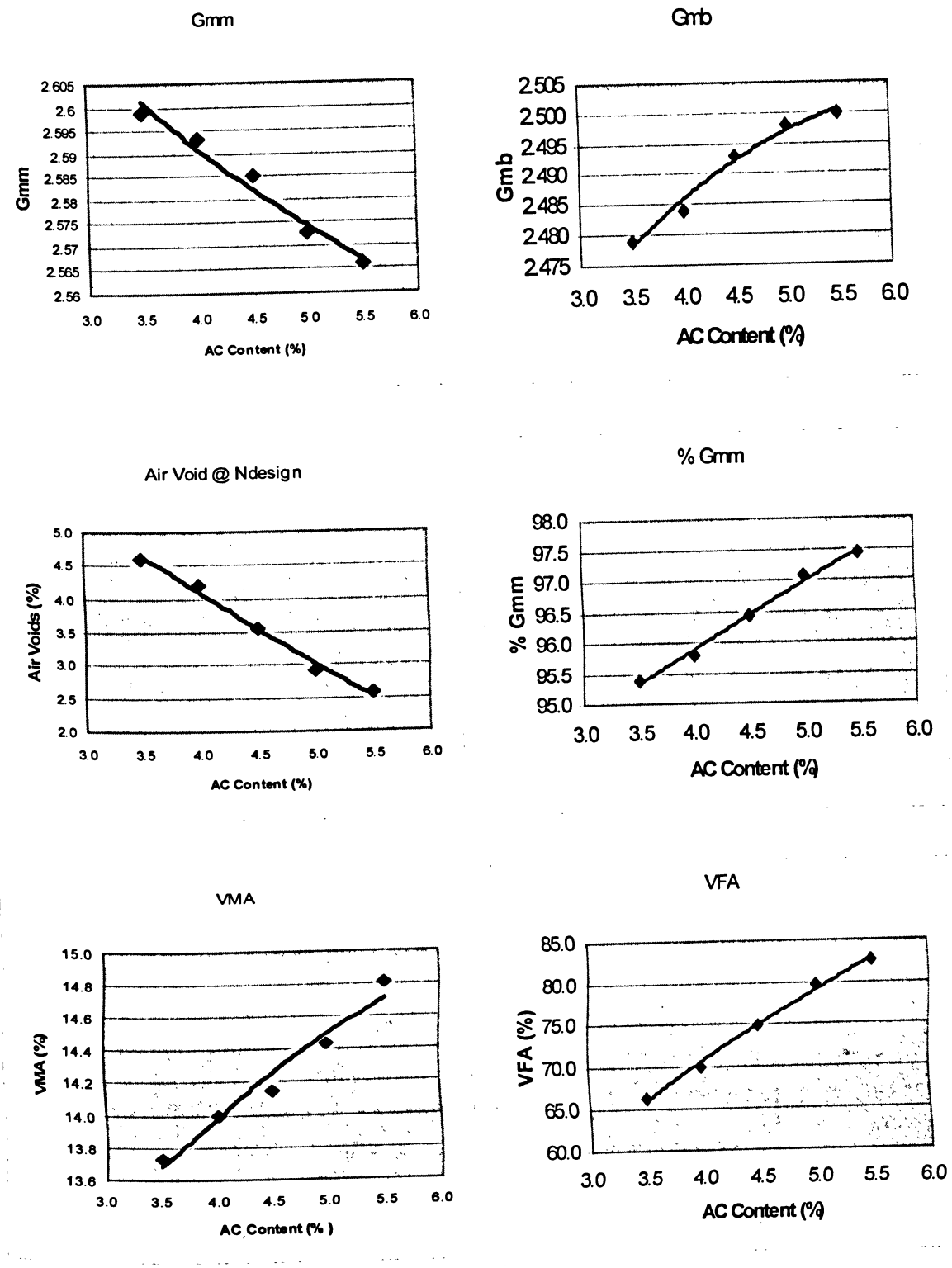

Figure 18 Mix Properties Curve for Superpave 19mm with Limestone Dust

4.3 Volume Metric Properties for Superpave 19mm Mix with 4% Fly Ash (Class C)

Five trials with asphalt content ranging from 3.5% to 5.0% were carried out as previously described. The detailed worksheets for each trial are presented in Appendix 1. The test results are summarized in Table 15 and Figure 19.

Four percent asphalt content was optimized for this mix. All the test results at the optimum asphalt content are summarized in Table 16, and all detailed worksheets are presented in Appendices 2 and 3.

Table 15 Test Results for Superpave 19mm with Fly Ash (Class C)

Parameters	Results				
AC Content (%)	3.5	4.0	4.5	5.0	5.5
Gmb @ Ndesign	2.485	2.495	2.508	2.512	2.519
Gmm	2.609	2.601	2.592	2.587	2.574
% Gmm @ Ndesign	95.2	95.9	96.8	97.1	97.9
Air Voids (%) @ Ndesign	4.8	4.1	3.2	2.9	2.1
VMA (%)	13.6	13.7	13.7	14	14.2
VFA (%)	65.1	70.3	76.4	79.3	85
Gsb, bulk specific gravity for the total aggregate	2.776				

Table 16 Test Results for Superpave 19mm with Fly Ash (Class C) at Optimum Asphalt Content

Mix Properties	Criteria	Selected Results
AC Content (%)	-	4
Gmb @ Ndesign	-	2.495
Gmm	-	2.601
% Gmm @ N_{design} = 100	-	95.9
% Gmm @ N_{ini} = 8	less than 89	88.9
% Gmm @ N_{max} = 160	less than 98	97.2
Air Voids (%) @ Ndesign	4%	4.1
VMA (%)	13.0 min	13.7
VFA (%)	65-75	70.3
Dust Proportion	0.6 - 1.2	1

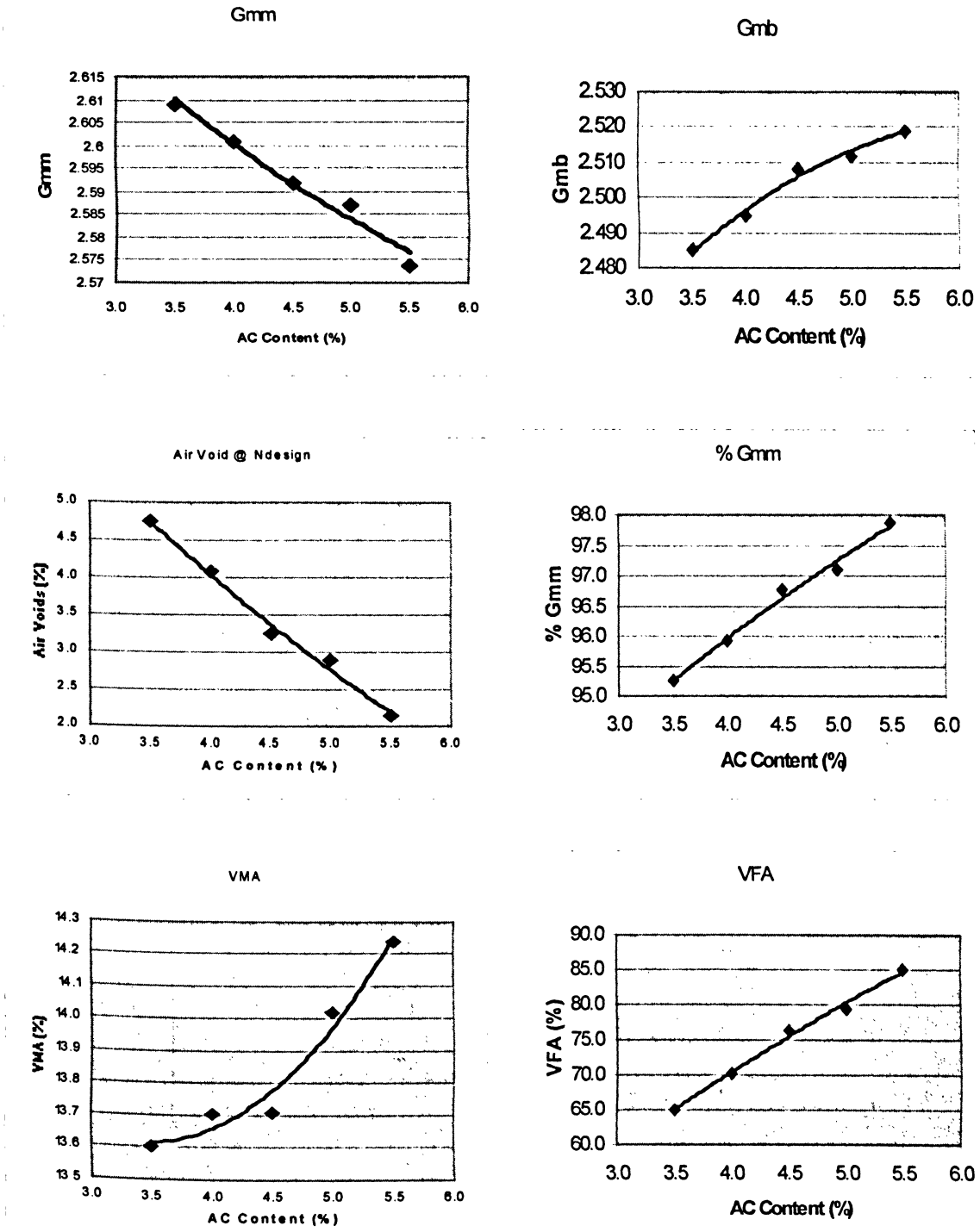

Figure 19 Mix Properties Curve for Superpave 19mm with Fly Ash (Class C)

4.4 Volume Metric Properties for Superpave 19mm Mix with 4% Fly Ash (Class F)

Five trials with asphalt content ranging from 3.5% to 5.0% were carried out as previously discussed. The test results are summarized in Tables 17 and 18, and in Figure 20. All detailed worksheets used to optimize the asphalt content are presented in Appendices 1 to 3.

Table 17 Test Results for Superpave 19mm with Fly Ash (Class F)

Parameters	Results				
AC Content (%)	3.5	4.0	4.5	5.0	5.5
Gmb @ N_{design}	2.474	2.489	2.508	2.515	2.518
Gmm	2.605	2.591	2.583	2.576	2.575
% Gmm @ N_{design}	95	96.1	97.1	97.6	97.8
Air Voids (%) @ N_{design}	5	3.9	2.9	2.4	2.2
VMA (%)	13.7	13.7	13.5	13.7	14
VFA (%)	63.4	71.2	78.4	82.7	84.2
Gsb, bulk specific gravity	2.767				

Table 18 Test Results for Superpave 19mm with Fly Ash (Class F) at Optimum Asphalt Content

Mix Properties	Criteria	Selected Results
AC Content (%)	-	4
Gmb @ Ndesign	-	2.489
Gmm	-	2.591
% Gmm @ N_{design} = 100	-	96.1
% Gmm @ N_{ini} = 8	less than 89	88.3
% Gmm @ N_{max} = 160	less than 98	97.4
Air Voids (%) @ Ndesign	4%	3.9
VMA (%)	13.0 min	13.7
VFA (%)	65-75	71.2
Dust Proportion	0.6 - 1.2	1

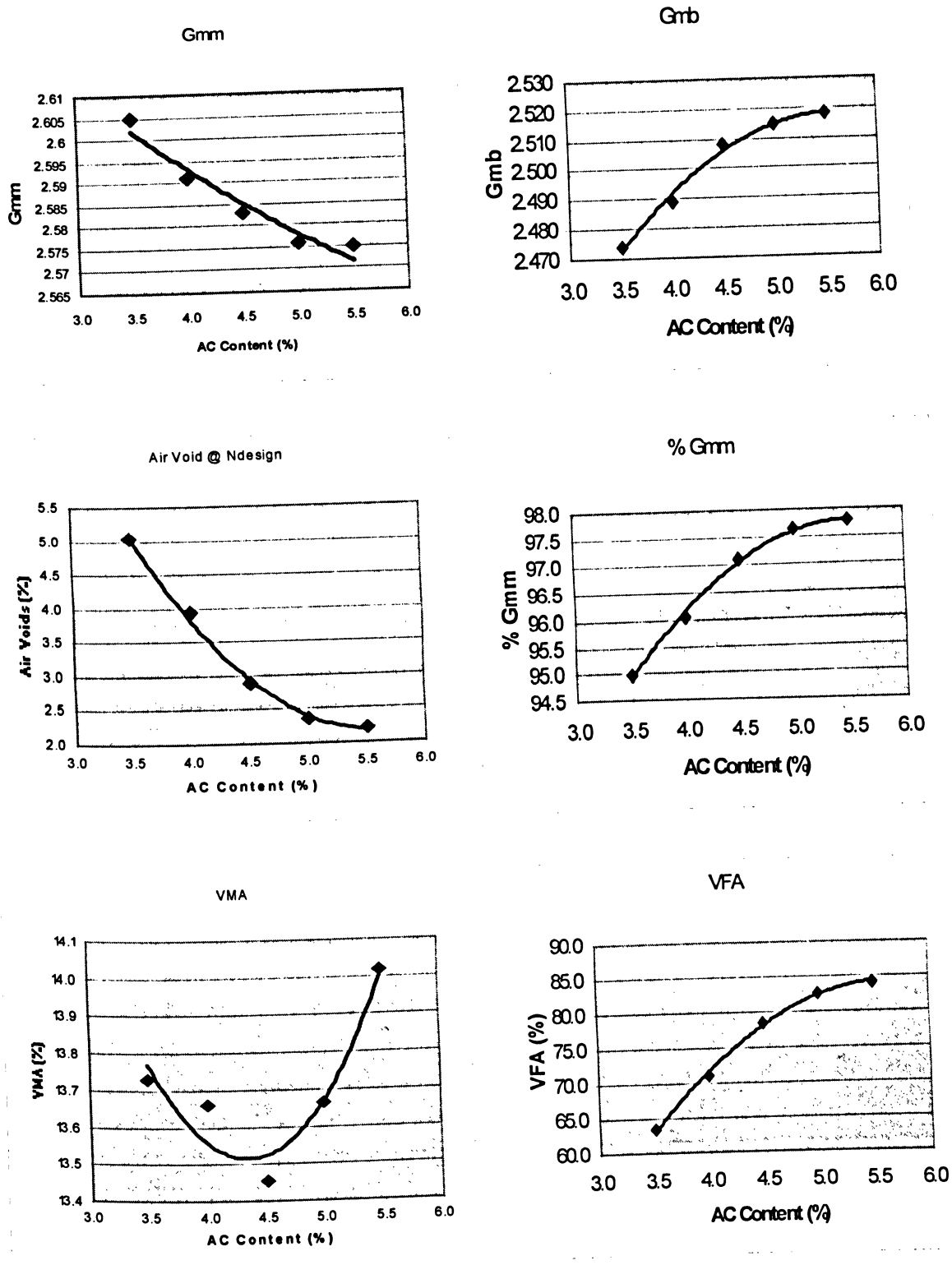

Figure 20 Mix Properties Curve for Superpave 19mm with Fly Ash (Class F)

4.5 Volume Metric Properties for Superpave 19mm Mix with 4% Blast Furnace Slag Filler

Five trials with asphalt content ranging from 3.5% to 5.0% were carried out with slag filler. Tables 19 and 20 and Figure 21 summarize the test results. All detailed worksheets used to optimize the asphalt content are presented in Appendices 1 to 3.

Table 19 Test Results for Superpave 19mm with Slag

Parameters	Results				
AC Content (%)	3.5	4.0	4.5	5.0	5.5
Gmb @ Ndesign	2.487	2.495	2.504	2.512	2.517
Gmm	2.611	2.604	2.597	2.586	2.577
% Gmm @ Ndesign	95.3	95.8	96.4	97.1	97.7
Air Voids (%) @ Ndesign	4.7	4.2	3.6	2.9	2.3
VMA (%)	13.6	13.8	13.9	14.1	14.4
VFA (%)	65.1	69.6	74.3	79.7	83.8
Gsb, bulk specific gravity	2.778				

Table 20 Test Results for Superpave 19mm with Slag at Optimum Asphalt Content

Mix Properties	Criteria	Selected Results
AC Content (%)	-	4.3
Gmb @ Ndesign	-	2.498
Gmm	-	2.602
% Gmm @ N_{design} = 100		96
% Gmm @ N_{ini} = 8	less than 89	87.9
% Gmm @ N_{max} = 160	less than 98	96.9
Air Voids (%) @ Ndesign	4%	4
VMA (%)	13.0 min	13.9
VFA (%)	65-75	71.3
Dust Proportion	0.6 - 1.2	0.98

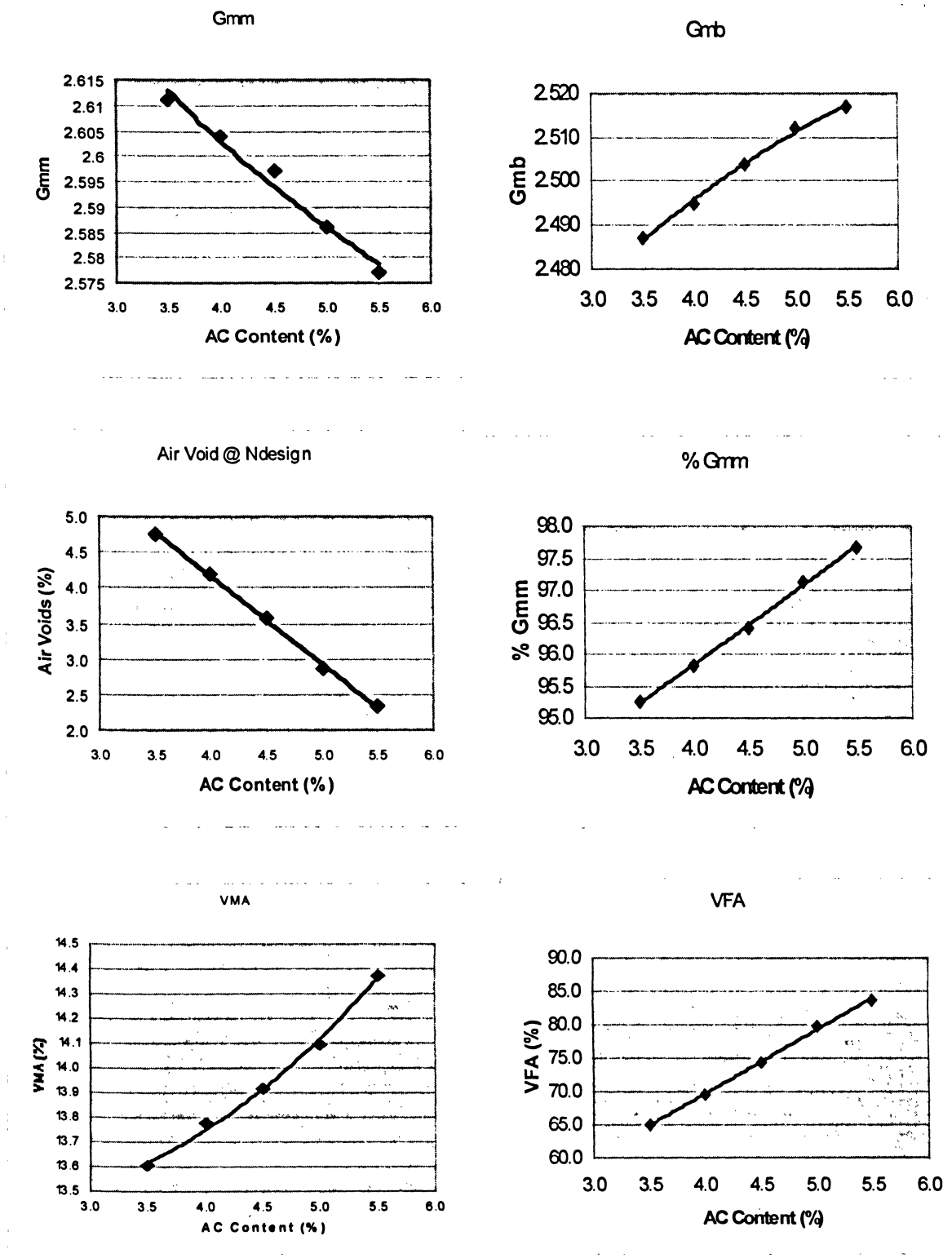

Figure 21 Mix Properties Curve for Superpave 19mm with Blast Furnace Slag

4.6 Volume Metric Properties for Superpave 19mm Mix with 4% Portland Cement Filler

Superpave 19 mm mix with Portland cement filler was conducted with optimized asphalt content. The test results are summarized in Tables 21 and 22, and in Figure 22. All detailed worksheets used to optimize the asphalt content are presented in Appendices 1 to 3.

Table 21 Test Results for Superpave 19mm with Portland Cement Filler

Parameters	Results				
AC Content (%)	3.5	4	4.5	5	5.5
Gmb @ Ndesign	2.459	2.476	2.497	2.503	2.518
Gmm	2.633	2.622	2.599	2.587	2.572
% Gmm @ Ndesign	93.4	94.4	96.1	96.8	97.9
Air Voids (%) @ Ndesign	6.6	5.6	3.9	3.2	2.1
VMA (%)	14.7	14.5	14.3	14.5	14.5
VFA (%)	55	61.7	72.5	77.6	85.5
Gsb, bulk specific gravity	2.781				

Table 22 Test Results for Superpave 19mm with Portland Cement Filler at Optimum Asphalt Content

Mix Properties	Criteria	Selected Results
AC Content (%)	-	4.5
Gmb @ Ndesign	-	2.497
Gmm	-	2.599
% Gmm @ N_{design} = 100		96.1
% Gmm @ N_{ini} = 8	less than 89	87.9
% Gmm @ N_{max} = 160	less than 98	97.2
Air Voids (%) @ Ndesign	4%	3.9
VMA (%)	13.0 min	14.3
VFA (%)	65-75	72.5
Dust Proportion	0.6 - 1.2	0.94

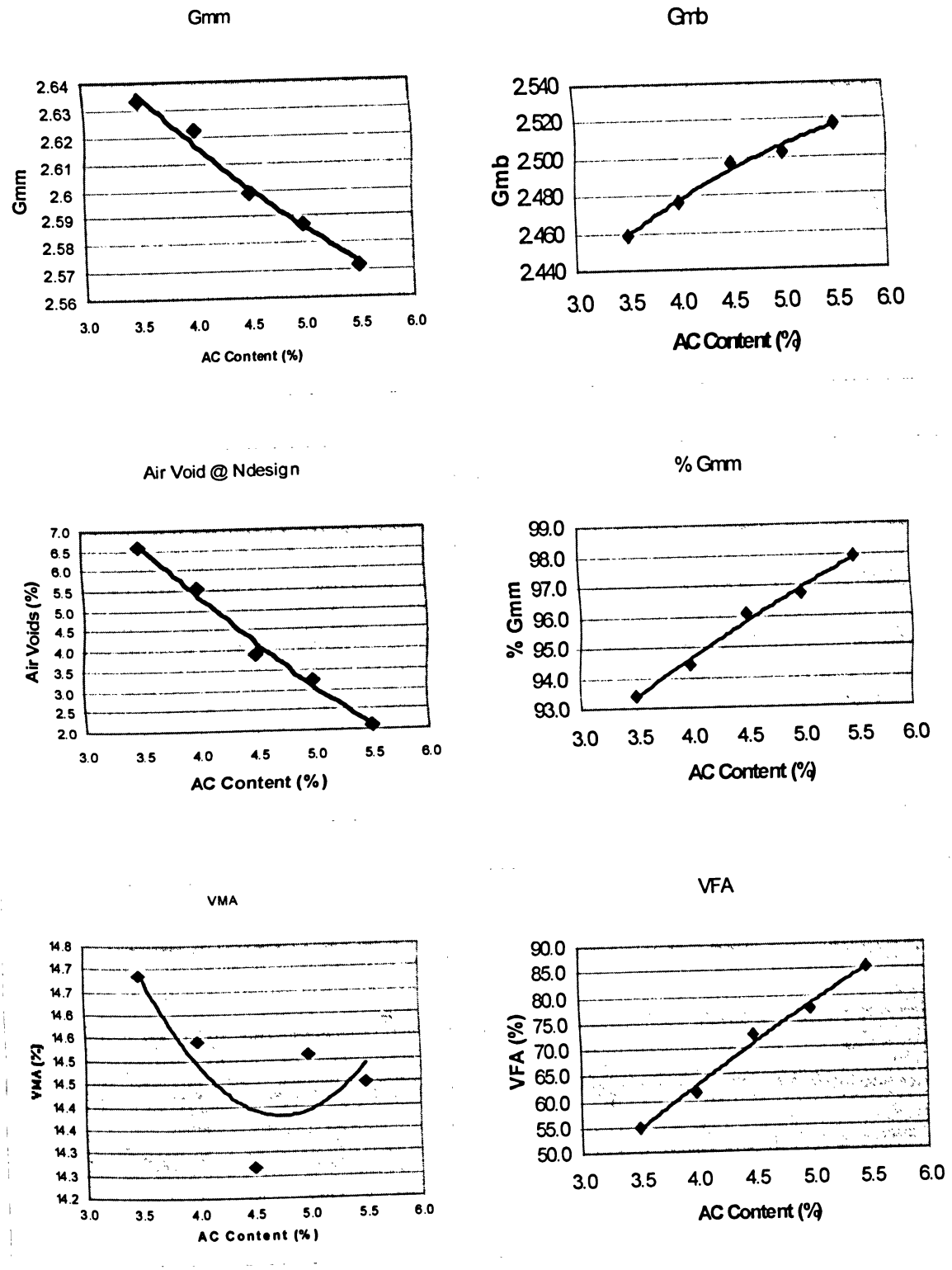

Figure 22 Mix Properties Curve for Superpave 19mm with Portland Cement Filler

4.7 Compaction Characteristics

Each sample was compacted using the design and maximum number of gyrations. The heights of each sample are summarized in Appendix 3. A set of three samples were compacted in N_{design} compaction level (100 gyrations) at selected optimum asphalt content for each mix. Another set of two samples were compacted in N_{max} compaction level (160 gyrations) for each mix. The results are summarized in Table 23.

Table 23 Percent Compaction at NInitial, Ndesign and Nmax

Number of Gyration	Percent Compaction (%)				
	Control	Fly Ash C	Fly Ash F	Slag	Portland Cement
8, Nintial	87.8	88.8	88.6	87.4	87.5
100, Ndesign	95.7	95.8	96	95.4	95.7
160, Nmax	97.2	97.3	97.5	96.9	97.2

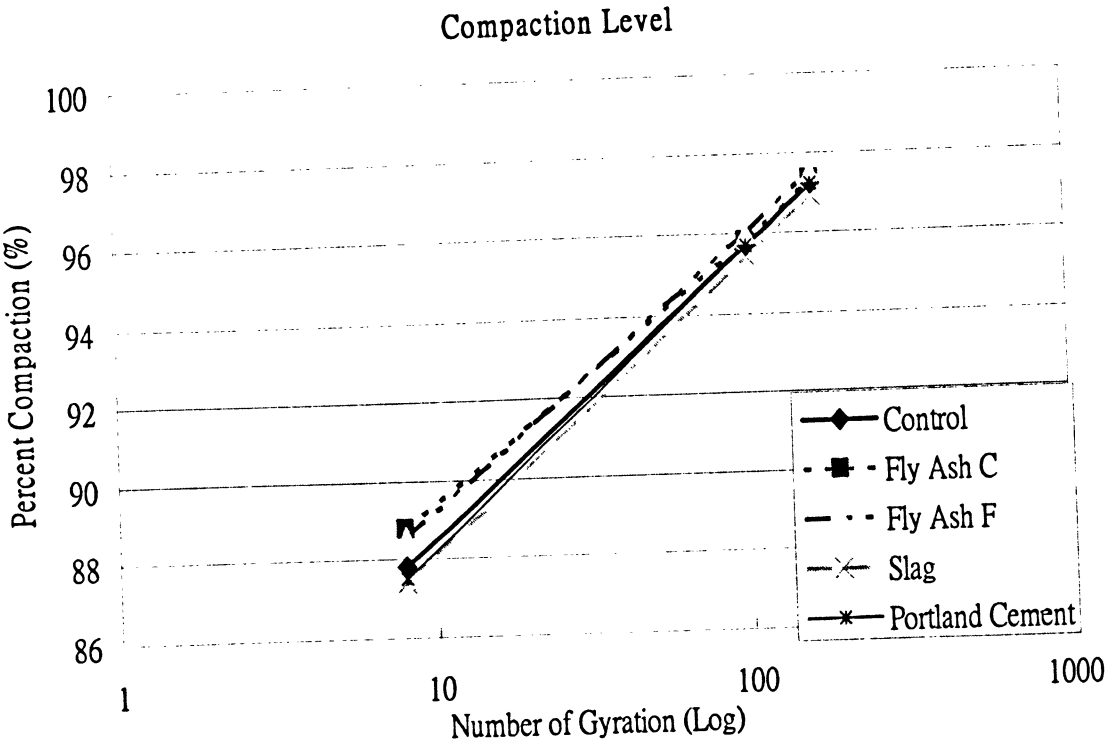

Figure 23 Compaction Characteristics of Each Mixture

4.7.1 Discussion

The compaction characteristics of each mix are illustrated in Figure 23. Figure 23 shows how the density of the asphalt mixture increases with increasing gyrations. It was found that samples containing Class C and F fly ash required less compaction effort at $N_{Initial}$ and N_{design} compared to all other mixtures, since they both specimens obtained the highest percent compaction values. It means less energy is required to achieve air void and compaction effort for these mixes in the field. The results may be influenced by the particle shape and size of the filler. Both types of fly ash is the only filler with a spherical particle shape is this study which provides better flow characteristics and compaction characteristics (Suheihani (1986) and Tons (1983). Mixes with Blast Furnace Slag and Portland cement behaved similar to the control mix in terms of compaction characteristics.

4.7.2 Visual Observation

Specimens containing Portland cement produced very lean (appearing to need more binder) mixes compared to the control mix. Portland cement mixes also seem to be very harsh (seemed to require more effort to mix) during mixing. Both types of fly ash mixes were slightly richer in appearance and were found to be more workable during the mixing stage. Mixes with fly ash enhanced workability that provided better compaction results, as shown in Figure 23. Mixes that are too lean with low binder content are the main contributor to asphalt raveling in the field. Therefore, engineers should pay attention to mixes with slag and Portland cement filler in hot mix asphalt.

4.8 Moisture Sensitivity Test Results

The moisture sensitivity and stripping results were conducted following by the AASHTO T283 method. The effectiveness of the additives and stripping level were determined by TSR values. All five mixes were conditioned and tested under an identical laboratory environment. The ITS and TSR results are illustrated in Figure 24 and 25.

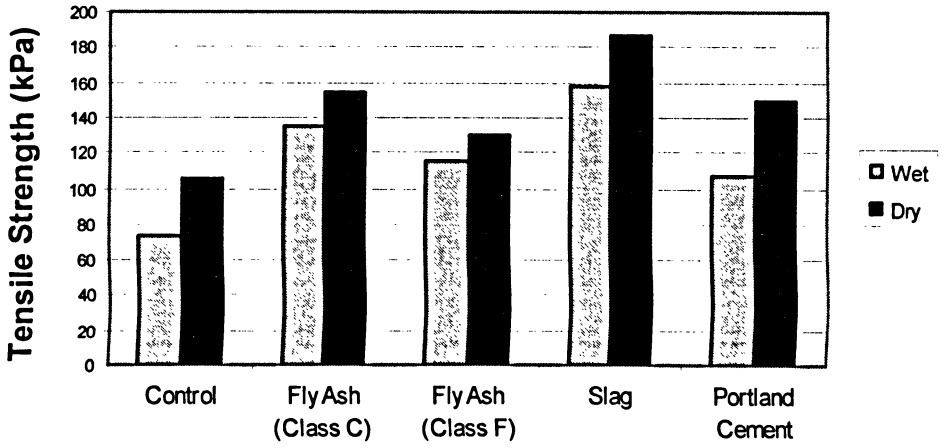

Figure 24 Indirect Tensile Strength Test Results

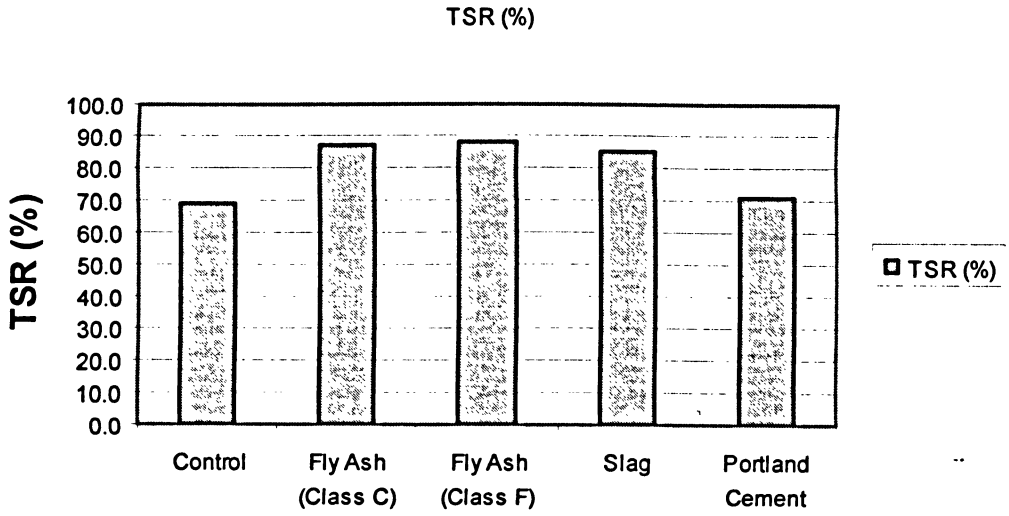

Figure 25 Tensile Strength Ratio Test Results

Figure 24 shows that all mixes have significant improvements on ITS values compared to

the control mix, under both dry and wet conditions. Mixes with Blast Furnace Slag and Portland cement have the best dry ITS results, followed by Class C and Class F fly ash mixes. Similar results were obtained in wet ITS values; however, the Portland cement mix has the lowest ITS values under wet conditions compared to the other filler sources tested. In this investigation, mixes containing slag fillers have highest ITS values than the other fillers.

According to the ASTM T-283, a minimum TSR value of 80% has to be achieved. Figure 25 indicated that the control mix and Portland cement mix did not meet the minimum requirement of 80%. Mixes with fly ash (Class C), fly ash (Class F) and Blast Furnace Slag showed the best TSR results at 87.5%, 88.5% and 84.7%, respectively. In this investigation, mixes with fly ash fillers had the best TSR values, which indicates that fly ash fillers can be expected to provide excellent resistance to stripping. Field tests are recommended to draw confirmed conclusions regarding these findings.

It is explained in Petersen (1987) study, how mineral filler improved the aggregates-asphalt asphalt and aggregate bonding in hot mix. The calcium oxide reacts with the aggregates in the system to strengthen the aggregates-asphalt bonding. At the same time, calcium oxide reacts with the highly polar molecules (asphalthene) in the asphalt binder and it have a tendency to form insoluble salt (non-polar) that is not favourable to water attraction.

4.8.1 Stripping Observation

The degree of stripping of each mix is summarized in Table 24, and the samples are illustrated in Figures 26 to 30. Severe stripping was observed with the control and Portland cement mixes. There is slight indication of stripping in the fly ash (Class C), fly ash (Class F), and Blast Furnace Slag mixes.

Table 24 Degree of Stripping of Each Mix

	Control	Fly Ash (Class C)	Fly Ash (Class F)	Slag	Portland Cement
Rate of Stripping	Severe Stripping	Slight Stripping	Slight Stripping	Slight Stripping	Severe Stripping

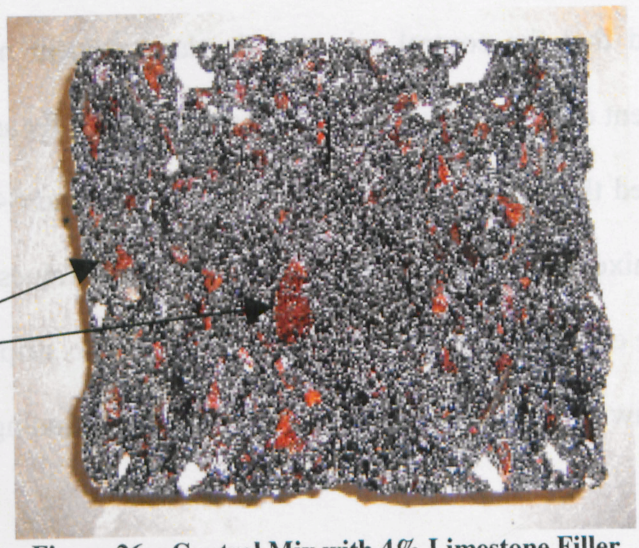

Figure 26 Control Mix with 4% Limestone Filler

Figure 27 Superpave 19mm Mix with 4% Fly Ash (Class C)

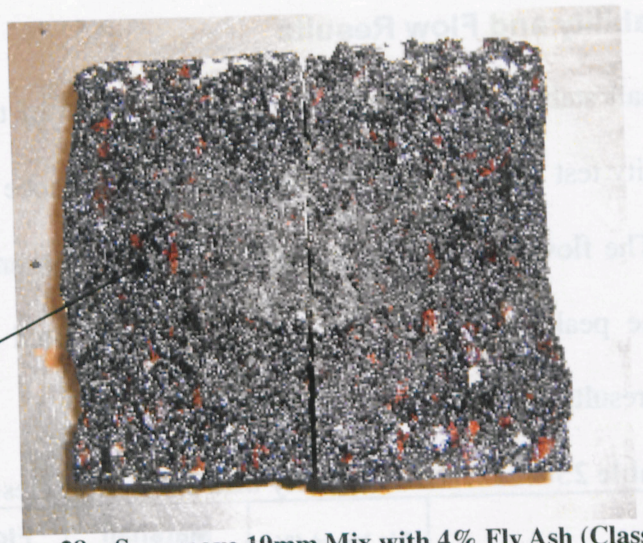

ght Stripping

Figure 28 Superpave 19mm Mix with 4% Fly Ash (Class F)

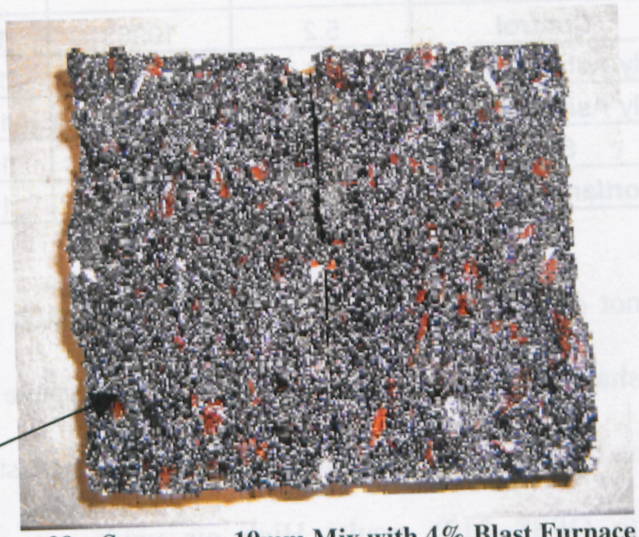

Slight Stripping

Figure 29 Superpave 19mm Mix with 4% Blast Furnace Slag

evere Stripping

Figure 30 Superpave 19mm Mix with 4% Portland Cement

4.9 Marshall Stability and Flow Results

The test for Marshall stability and flow was conducted for all of the Superpave 19 mm mixes. The stability test was performed to measure the resistance to deformation under a constant load. The flow test was performed to determine the amount of deformation occurring under the peak loading. All mixes were compacted as per the Marshall Method. The test results are summarized in Table 25.

Table 25 Marshall Stability and Flow Test Results

	Air Void (%)	Marshall Stability (N)	Flow (0.025)
Control	5.2	10983	12.3
Fly Ash (Class C)	5.1	12933	10.5
Fly Ash (Class F)	5.2	12625	10.8
Slag	5.5	13467	12.7
Portland Cement	5.1	13600	11.3

All specimens did not comply with the 4% air void specification since the compaction energy by the Marshall method its different from the Superpave gyratory compactor. The air void content for all specimens was high with satisfied stability (minimum of 8,000N according to OPSS 312) results High air voids are associated with high permeability, which allows moisture though the hot mix. The moisture causes premature hardening of the asphalt, raveling and possibly asphalt stripping off the aggregates. Even if good stability results are obtained, the excessive air void contents are needed to reduce to the 4% limit, as according to the Superpave specification. The air void can be reduced by adjusting the aggregate gradation closer to the maximum density line.

The job mix formula was adjusted closer to the maximum density line, as illustrated in

Figure 31. The new mixture was then blended with 17% CA1, 37% CA2, 42% FA1, and 4% house dust. The new mixes were compacted with the new optimum asphalt content by the Marshall method, and the test results are summarized in Table 26.

Figure 31 New Adjusted Job Mix Formula for Marshall Method

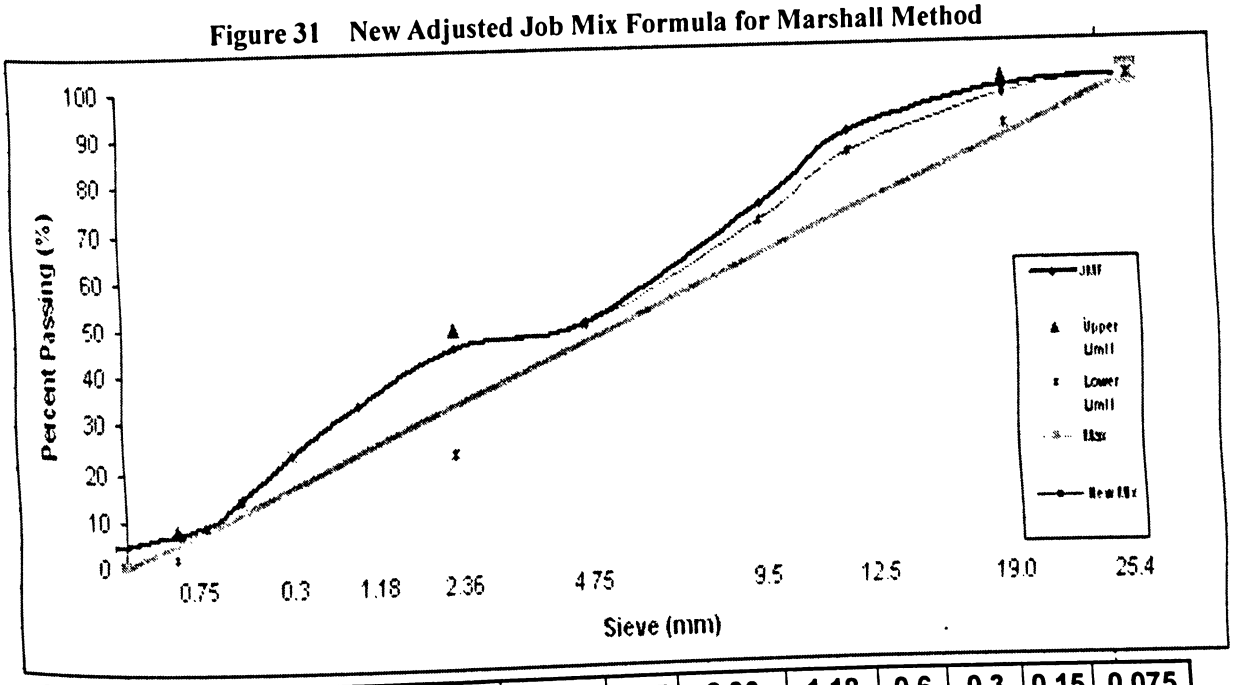

Sieve (mm)	25.4	19	12.5	9.5	4.75	2.36	1.18	0.6	0.3	0.15	0.075
Upper Limit	100	100				49					8
Lower Limit		90				23					2
JMF	100.0	97.8	89.2	73.7	49.8	45.2	33.3	23.1	14.1	9.0	4.0
New Mix	100.0	96.6	84.6	70.2	49.4	45.1	33.2	23.1	14.1	8.9	4.0

There is significant improvement on Marshall stability results in all filler replacement mixes. Portland cement obtained the greatest stability result at 13566N, followed by Blast Furnace Slag with 13467N. The increased stability provides more rutting resistance to the mix. Mixes with too high stability may be too brittle and rigid for pavement service. Mixes with fly ashes achieved better stability at the same binder content as that of the control.

The flow results obtained meet the minimum requirement of eight (0.25 mm). All filler

mixtures have less flow value than control. Mixes that have lower flow values are usually of higher Marshall stability, which correlates with the results obtained. Mixes with high flow values are considered too plastic and have a shorter pavement service life.

Table 26 Marshall Stability and Flow Test Results for New Job Mix Formula

	Asphalt Content (%)	BRD	MRD	Air Void (%)	Marshall Stability (N)	Flow (0.025)
Control	4.5	2.476	2.58	4.0	11530	12.8
Fly Ash (Class C)	4.2	2.48	2.583	4.0	12893	10.9
Fly Ash (Class F)	4.2	2.477	2.579	4.0	12746	11.2
Slag	4.6	2.483	2.585	3.9	13534	12.7
Portland Cement	4.7	2.48	2.581	3.9	13566	12.6

4.9.1 Discussion

After adjusting the job mix formula for the Marshall method for the stability and flow evaluation, it is interesting to note that a finer aggregate skeleton with higher asphalt content were obtained in all mixes compared to the Superpave mixes. This could be explained by the increase in surface area by using finer aggregates. In other words, mixes generated by the Superpave method are usually having a coarser aggregate skeleton to provide a greater stability performance and lower asphalt content to reduce production cost.

4.10 Performance Graded Asphalt Cement (PGAC) Test Results

4.10.1 Viscous and Elastic Behaviour at Original Dynamic Shear

The dynamic shear test was conducted to evaluate the asphalt's performance at its original stage. The dynamic shear results were used to characterize both viscous and elastic behaviour under designed temperature. The obtained test results demonstrate that mineral filler with high calcium content has significant impact on the asphalt binder.

When the calcium oxide reacts with the polar molecules, the asphalt binder is inactive with the environment (Petersen, 1987). The asphalt binder remains elastic for longer time at high temperature. By adding 2% (by weight of asphalt binder) filler, the asphalt binder showed similar viscosity values at 58 °C and 64 °C, as shown in Figures 32 and 33. No significant improvements were founded in viscous behaviour, as represented by G*Sin(δ). However, the elastic property, represented by G*Cos(δ), improved in all filler mixes at 58°C and 64°C, as the filler material tended to enhance the elastic property of the asphalt binder, as illustrated in Figures 32 and 33. In this investigation, the binder with Class C fly ash filler had highest elastic values compared to other filler sources tested at 58°C. The Blast Furnace Slag mix behaves more elastic at 64°C. These two filler mixes have larger elastic components at both temperature ranges, which tends to recover more from traffic loads.

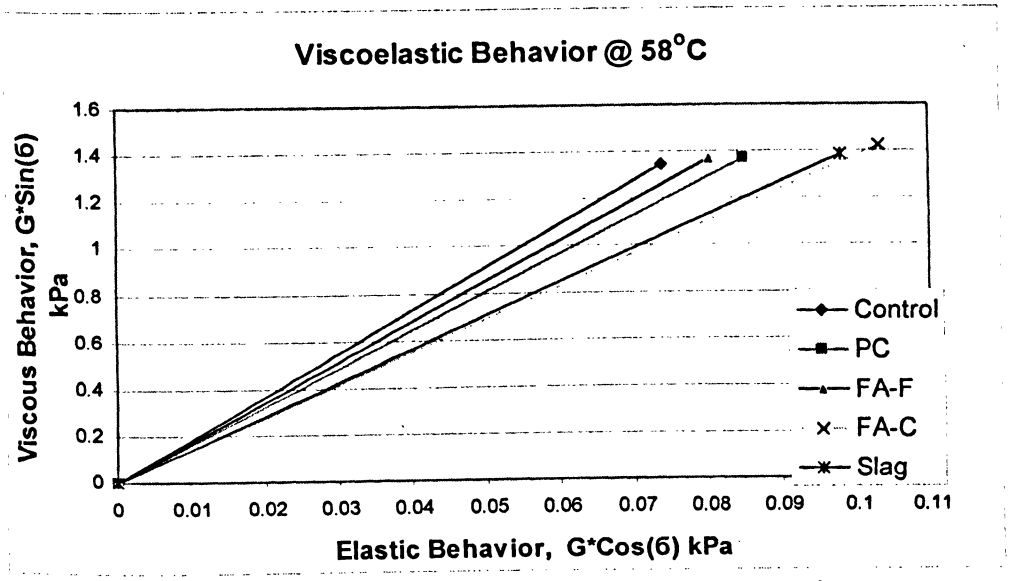

Figure 32 Viscoelastic Behaviour of the Binders at 58°C

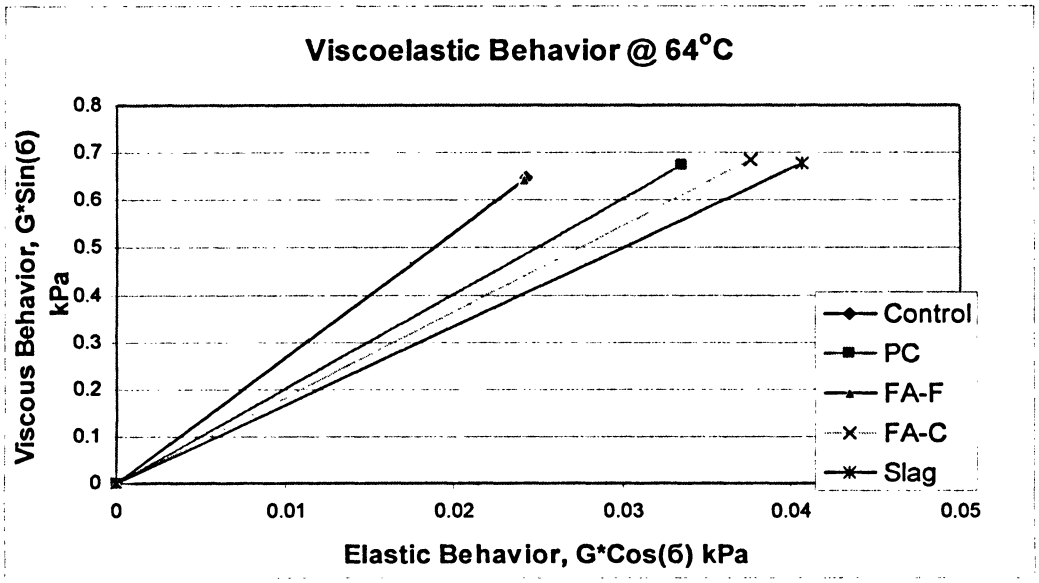

Figure 33 Viscoelastic Behaviour of the Binders at 64°C

4.10.2 Viscoelastic Parameters (G*/Sin (delta))

The viscoelastic parameter is obtained from the rheometer, which measures the complex modulus (G*) and the phase angle (δ). The parameter G*/Sin (δ) is conducted to evaluate the rut resistance by the Strategic Highway Research Program (SHRP). An increase of this parameter is observed with different types of filler added into the asphalt binder. The stiffness of binder respectively increases as the parameter increases. Tables 27 to 31 illustrate that Class C fly ash has the greatest improvement on G*/Sin (δ) value at both temperatures which is a good indication for rut resistance. Asphalt samples containing Class C fly ash filler had highest elastic value (G*Cos (δ)) which provides more elasticity and stiffer asphalt binder. The stiffer asphalt binder will act as a "rubber band" and allow the mix to return to its original shape rather than deforming at high temperatures.

Table 27 Viscoelastic Test Results with Virgin Asphalt Binder (Control)

	Virgin 58-28 (Control)	
	Original	
Temperature (°C)	58 °C	64 °C
G*(kPa)	1.3477	0.6487
delta	86.9	87.9
G*/sin(delta), kPa	1.3497	0.6492
PGAC (°C)	61	

Table 28 Viscoelastic Test Results with Fly Ash (Class C)

	Fly Ash (Class C)	
	Original	
Temperature (°C)	58 °C	64 °C
G*(kPa)	1.4306	0.68552
delta	85.9	86.9
G*/sin(delta), kPa	1.4269	0.68651
PGAC (°C)	61.5	

Table 29 Viscoelastic Test Results with Fly Ash (Class F)

	Fly Ash (Class F)	
	Original	
Temperature (°C)	58 °C	64 °C
G*(kPa)	1.3751	0.64517
delta	86.7	87.9
G*/sin(delta), kPa	1.3774	0.64561
PGAC (°C)	61.1	

Table 30 Viscoelastic Test Results with Blast Furnace Slag

	Slag	
	Original	
Temperature (°C)	58 °C	64 °C
G*(kPa)	1.3925	0.67708
delta	86	86.6
G*/sin(delta), kPa	1.3958	0.67824
PGAC (°C)	61.3	

Table 31 Viscoelastic Test Results with Portland Cement

	Portland Cement	
	Original	
Temperature (°C)	58 °C	64 °C
G*(kPa)	1.3729	0.6758
delta	86.5	87.2
G*/sin(delta), kPa	1.3755	0.6766
PGAC (°C)	61.2	

4.10.3 Viscous and Elastic Behaviour after RTFO (Short Term Aging)

A DSR test was conducted to evaluate the asphalt's performance after the RTFO. No significant change could be found under the viscous behaviour represented by G*Sin (δ). The elastic property, represented by G*Cos(δ), increased slightly at both temperatures of 58 °C and 64 °C after short term aging with the RTFO. The filler binder samples tended to have a slight increment in asphalt binder elasticity, as illustrated in Figures 34 and 35. Such effect may reduce the rutting potential in the field. Both types of fly ash have the best elastic performance at both temperatures after short term aging.

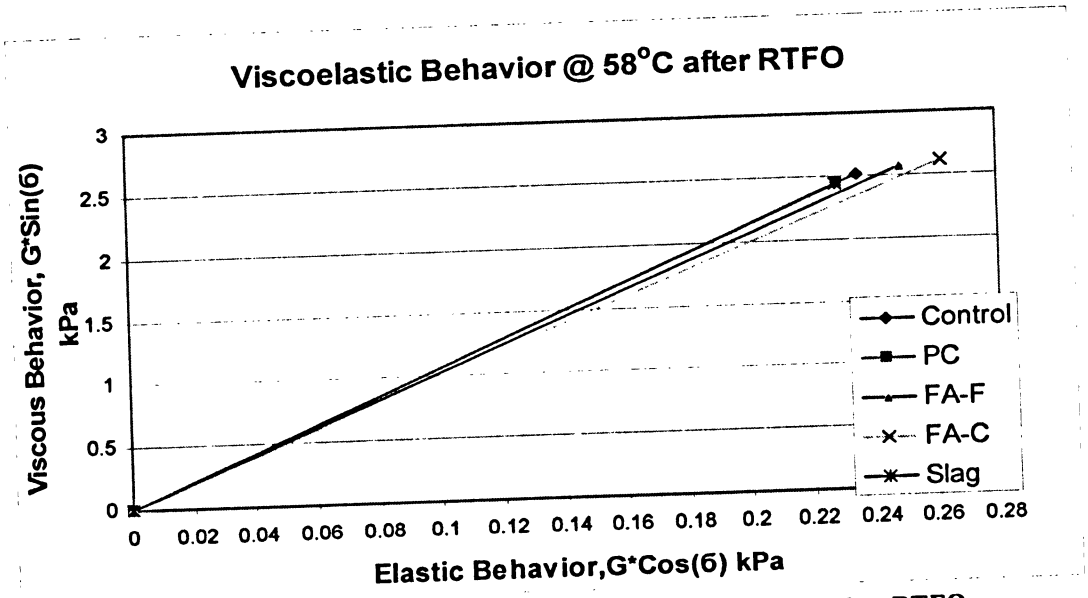

Figure 34 Viscoelastic Behaviour of the Binders at 58oC after RTFO

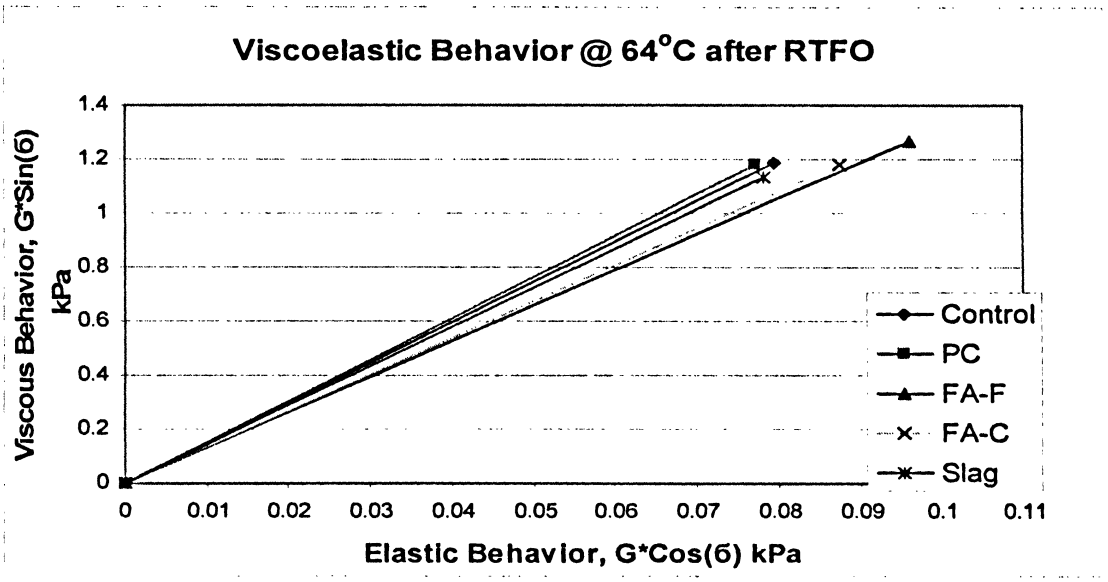

Figure 35 Viscoelastic Behaviour of the Binders at 64°C after RTFO

4.10.4 G*/Sin (delta) after RTFO

The G*/Sin (delta) parameter was conducted at the prescribed at two temperature (58°C and 64°C). A slight increase of this parameter was observed when the Class C fly ash filler was added to the asphalt binder at both temperature settings. Class C Fly ash sample also had the tendency to improve rutting properties. A slight reduction of the G*/Sin (delta) parameter was observed in other mixes, as illustrated in Tables 32 to 36. This reduction was not significant enough to increase the rutting potential after short term aging.

Table 32 Viscoelastic Test Results after RTFO with

	Virgin 58-28 (Control)	
	RTFO	
Temperature (°C)	58 °C	64 °C
G*(kPa)	2.5242	1.1861
delta	84.7	86.2
G*/sin(delta), kPa	2.535	1.1887
PGAC (°C)	60.4	

Table 33 Viscoelastic Test Results after RTFO with Fly Ash (Class C)

	Fly Ash (Class C)	
	RTFO	
Temperature (°C)	58 °C	64 °C
G*(kPa)	2.6211	1.1832
delta	84.3	85.8
G*/sin(delta), kPa	2.6335	1.1892
PGAC (°C)	60.6	

Table 34 Viscoelastic Test Results after RTFO with Fly Ash (Class F)

	Fly Ash (Class F)	
	RTFO	
Temperature (°C)	58 °C	64 °C
G*(kPa)	2.5795	1.2709
delta	84.5	85.7
G*/sin(delta), kPa	2.5913	1.2749
PGAC (°C)	60.7	

Table 35 Viscoelastic Test Results after RTFO with Blast Furnace Slag

	Slag	
	RTFO	
Temperature (°C)	58 °C	64 °C
G*(kPa)	2.4493	1.1375
delta	84.7	86.1
G*/sin(delta), kPa	2.4599	1.1401
PGAC (°C)	60.1	

Table 36 Viscoelastic Test Results after RTFO with Portland Cement

	Portland Cement	
	RTFO	
Temperature (°C)	58 °C	64 °C
G*(kPa)	2.4565	1.1824
delta	84.7	86.3
G*/sin(delta), kPa	2.4669	1.1848
PGAC (°C)	60.2	

4.10.4.1 Discussion

It is interesting to note that with an increase of aging time (after short-term aging), the complex modulus (G*) increases and the phase angle decreases respectively. Similar

effects are found associated with temperature, where the complex modulus increases as temperature decreases, and the phase angle decreases as the temperature (Huang, 2007).

4.10.5 Dynamic Shear Test Analysis after Long Term Aging

The "G*" multiplied by sine "δ" (G*sin (δ)) value is used to evaluate fatigue cracking properties after the pressure aging process for 20 hours (simulation of 20 years of aging) by the pressure aging vessel (PAV). The test result is acceptable when the test limit is less than 5000 kPa at an intermediate temperature of 19°C. Asphalt samples with G*sin(δ) results greater then 5000 kPa have a greater tendency to suffer from fatigue cracking. All mixes showed the tendency to improve fatigue cracking compared to the control binder sample shown by the reduction of G*sin (δ) values. Class C fly ash having the greatest performance of all since it has the lowest G*sin (δ) value to provide greater flexibility to against fatigue cracking. All test results are shown in Table 37.

Table 37 Dynamic Shear Test (after PAV) Test Results

PAV Aging Temp Dynamic Shear	Temperature (°C)	Control (PG 58-28)	Fly Ash "C"	Fly Ash "F"	Portland Cement	Slag
G* (kPa)	19	3816	3360	3470	3672	3722
Phase Angle (delta)	19	48.8	47.2	48.1	47.1	47.2
G* sin(delta), kPa	19	2871	2465	2583	2690	2731

The results obtained in this section correlate to the findings in Huang and Zeng's (2006) study. They concluded that there is a reduction of stiffness after long term aging when adding mineral filler to asphalt binder. The G* value and G*sin(δ) decreases in this

case, as presented in Table 37.

4.10.6 Low Temperature Testing with BBR

4.10.6.1 Creep Stiffness (S) Analysis

All asphalt samples with filler have the tendency to increase creep stiffness at -18 °C. They also all meet the specification requirement of not exceeding 300 MPa, as listed in Figure 36. Figure 36 shows the excessively high stiffness values obtained by the Blast Furnace Slag filler sample, which means it has the greatest tendency to crack at low temperatures out of all samples tested. Asphalt samples with a higher S value close to the limit (300 MPa) are usually too stiff to provide flexibility to the pavement structures at low temperatures. The control asphalt and Class F fly ash, however, may perform better in terms of creep stiffness and provide more flexibility to the pavement when compared to other tested fillers.

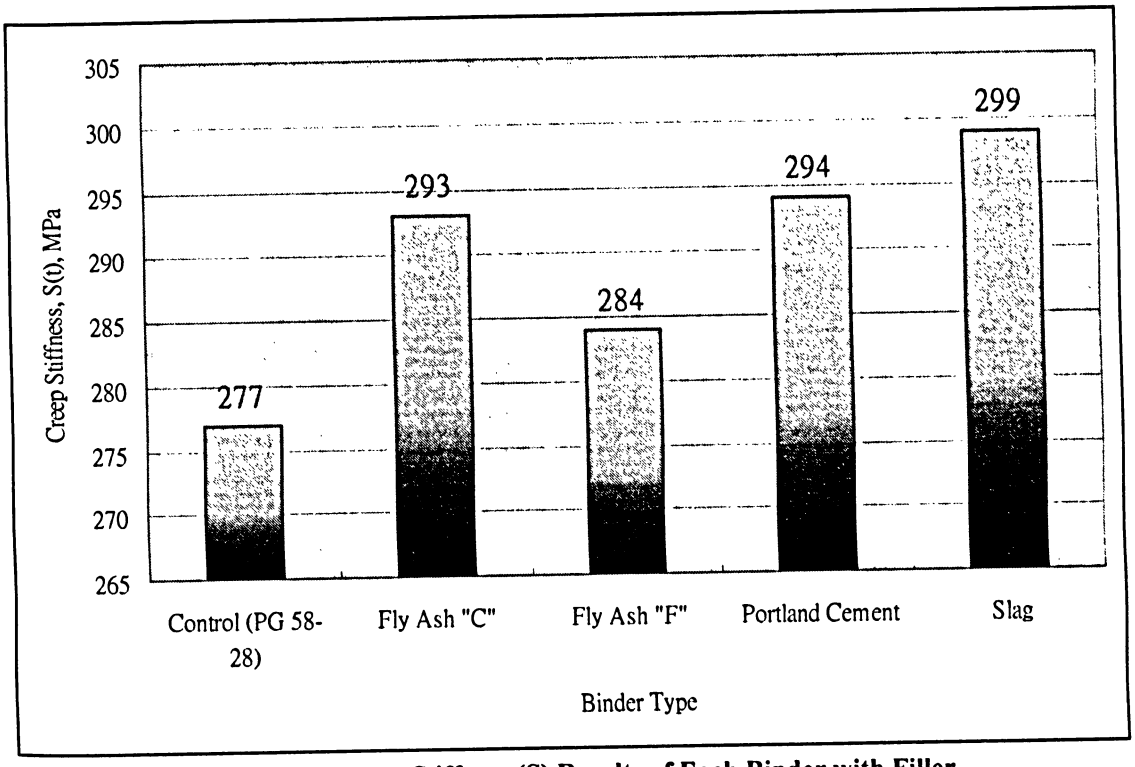

Figure 36 Creep Stiffness (S) Results of Each Binder with Filler

4.6.10.2 m – value analysis

The m-value represents the rate of change of binder stiffness over time. A higher m-value is more favourable because pavement contraction occurs at cold temperatures and the asphalt binder behaves less stiff as m-value increases. Figure 37 shows all filler binder samples obtained higher results than the control sample. It is clear that the Blast Furnace Slag filler has the highest results. This allows the binder to "relax" the applied load, which causes less tensile stresses in the binder and reduces susceptibility to low temperatures and fatigue cracking. Asphalt with a lower m-value (e.g. control sample) have internal stress exceeding the tensile strength of the asphalt binder, which causes cracking as a result. Binder samples with Class C Fly ash and Portland cement show significant improvements as well.

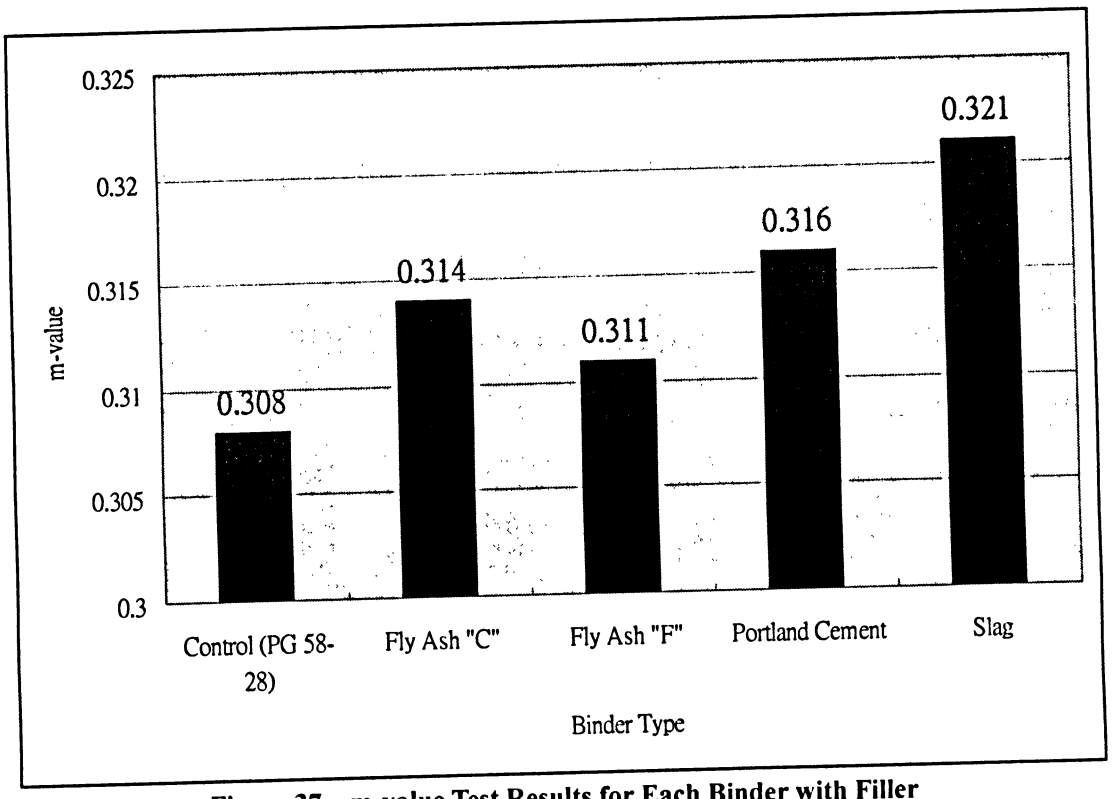

Figure 37 m-value Test Results for Each Binder with Filler

4.10.6.3 Discussion

Although the Blast Furnace Slag filler has the best performance in m-value, its creep stiffness result is marginal when compared to all of tested samples, which means that it may not provide the necessary flexibility in the pavement structure. As a compromise between the results, Class C Fly ash and Portland cement filler are recommended. They provide lower creep stiffness (S) results, while allowing some flexibility in the pavement structure and letting the binder "relax" with a desirable m-value to prevent fatigue cracking at low temperatures.

CHAPTER 5

CONCLUSIONS

Based on the investigations conducted in this study, the conclusions are summarized as follows:

1. Fly ash (Class C) and fly ash (Class F) reduces moisture sensitivity. It enhances asphalt and aggregate bonding, which improves stripping.
2. Fly Ash (Class C) can generate the most economical mix compared to the other fillers tested. The optimum asphalt content was reduced by 0.3% in this experiment. Mixtures with blast furnace slag contained the same asphalt content as the control and Portland cement has a 0.2% increment compared to the control which increase the production cost of hot mixes.
3. Mixes with fly ash fillers showed the best TSR values, which indicate it provides excellent resistance to stripping. Similar TSR value was obtained from Blast furnace slag therefore similar stripping performance is expected.
4. Mixtures with 4% fly ash replacement meet all Marshall design properties, including stability, flow, VMA, and VFA.
5. Samples with fly ash (Class C) and fly ash (Class F) have the best compaction characteristics compared to all other mixtures tested. Less compaction effort is needed to achieve air void and compaction with a much denser matrix.
6. Binder with fly ash (Class C) filler had the highest elastic values compared to other filler sources tested at 58°C. It has the greatest improvement on G*/Sin (delta) value at 58°C and 64°C. This means binder with Class C fly ash has the

highest rutting resistance at high temperatures.

7. A slight increase of G*/Sin (delta) was observed with Class C fly ash filler (2% weight of asphalt binder) added to the asphalt binder at 58°C and 64°C after short term aging (RTFO). Mixes with fly ash (Class C) also have greater tendency to improve rutting compared to all fillers tested.
8. Asphalt binder with fly ash (Class C) filler performed the best in dynamic shear test at 19°C (intermediate testing temperature) after long-term aging. It therefore has the greatest tendency to improve fatigue cracking when compared to all of the tested fillers.
9. Asphalt samples with fly ash (Class C) and Portland cement filler have more favourable performance in terms of creep stiffness and m-value properties to provide some flexibility, while still providing the capability for the binder to "relax" at low temperatures.

In general, asphalt mixes with fly ash (Class C) have improved the overall binder performance and mix properties. At the same time, it is the most economical mix tested with a 0.3% reduction of the asphalt binder content compared to the control mix. Fly ash fillers have many positive effects on stripping, rutting, and fatigue resistance in hot mix asphalt.

CHAPTER 6

RECOMMENDATIONS

Although, fly ash has the best overall hot mix performances, blast furnace slag is also an alternative mineral filler in asphalt hot mixes. Blast furnace slag fillers have similar tensile strength ratio (TSR) as that of fly ash and it has the highest indirect tensile strength (ITS). This provides excellent resistance to stripping. The blast furnace slag binder sample behaves more elastic than fly ash (Class C) at 64°C, which tends to recover more from traffic loads and provide better rutting resistance. It also has the capability to improve fatigue cracking by given more flexibility to the binder. However, it has a high creep stiffness (S) value, which means it has the greatest tendency to crack at low temperatures (-18 °C) out of all samples tested. Even blast furnace slag filler may not performe as well as fly ash at low temperatures in hot mix, more field tests and studies should be conducted to evaluate their rutting and fatigue behaviour.

In addition, the performance graded asphalt cement test may not statistically significant, since only one asphalt binder sample was tested. The best approach from a statistical point of view is to test more samples to assess the significance of the results. There is a possibility that the variations in obtained test values of binder with different fillers are within the reputability of the test methods and not due to differences in the properties of the samples.

REFERENCES

1. Aljassar A.H., and Metwali S. "Effect of Filler Types on Marshall Stability and Retained Strength of Asphalt Concrete" International Journal of Pavement Engineering, Volume 5, Number 1, pp. 47-51(5), March 2004.

2. Anderson, D.A, Bahia, H.U. and Dongre. R, "Rheological Properties of Mineral Filler-Asphalt Mastics and it Importance to Pavement Performance", American Society for Testing and Materials, Philadelphia, pp. 131-153, 1992.

3. Anderson, D.A., H. U. Bahia, J. J. Button, "Binder characterization and evaluation": Report SHRP-A-369, The Strategic Highway Research Program, National Research Council, Washington, D. C., Volume 3, 1994.

4. Asphalt Institute, "Performance Graded Asphalt Binder Specification and Testing", Superpave Series No. 1 (SP-1), 1995.

5. Asphalt Institute, "Construction of Hot Mix Asphalt Pavements", Manual Series No. 22, Second Edition, Lexignton, Kentucky.

6. Bayomy, F.M., "Development and Analysis of Cement-Coated Aggregate for Asphalt Mixture," American Society for Testing and Materials, Philadelphia, 1992.

7. Branthaver, J.F. Petersen, J.C., Robertson, R.E. Duvall, "Binder Characterization and Evaluation.", National Reseach Council, Washington, SC, Report No. SHRP-A-369, pp 475, Volume 2, 1993.

8. Campen, W. H. and Nebraska "The Effects of Traffic on the Density of Bituminous Paving Mixtures," Proc. AAPT, Vol. 30, 1993.

9. Carpenter, Carl A, "Fillers in Asphaltic Concrete," Public Roads, Volume 27, No. 5, December 1982.

10. Collins, R.J., and Emery, J. J. "Kiln dust-fly ash systems for highway bases and subbases." Rep. FHWA/RD-82/167, Federal Highway Administartion, Washington, D.C. September, 1983.

11. Dallas N. Little & Jon A. Epps, "The Benefits of Hydrated Lime in Hot Mix Asphalt", National Lime Association, pp 1-48, 2001.

12. Dukatz, E., and Anderson. D. "The Effect of Various Fillers on the Mechanical Behavior of Asphalt and Asphaltic Concrete". Association of Asphalt Paving Technologists, pp 39-70, Volume 49. 1980.

13. El, Mohamed, "Stripping of Asphalt Concrete Surfaces" Department of Civil and Environmental Engineering, Carleton University, Ottawa, Canada, 1991.

14. Epps, J. A., (1992) "Hydrated Lime in Hot Mix", Presentation Manual, FHWA, AASHTO, NLA.

15. Gallagher, K.P, Bahia H.U., Guerra, J.D., and Keating, J. "The Influence of Air-blowing on the Performance Related Properties of Paving Asphalt", Transportation Research Board, January, 1996.

16. Galloway, B.M., "A Review of the Use of Mineral Filler in Asphalt-Aggregate Mixtures," Proceeding of the Fly Ash Application in 1980 Conference, Texas, 1980.

17. Gubler, R.,Liu Y, Anderson D.A., and Partl M.N., "Investigation of the System Filler and Asphalt Binders by Rheological Means" Association of Asphalt Paving Technologists, Vol. 68, pp. 284-304, 1999.

18. Hartman A.M. and Gilchrist M.D "Effect of Mixture Compaction on Indirect Tensile Stiffness and Fatigue" Journal of Transportation Engineering, pp370-378, Vol. 127, 2001.

19. Hills, J.F. and D. Brien, "The Fracture of Bitumens and Asphalt mixes by Temperature Induced Stresses." Proceedings, Association of Asphalt Paving Technologist, pp92-309, Vol. 35. 1996.

20. Huang S.C., and Zeng M. "Characterization of aging effect on rheological properties of asphalt-filler systems" The Hunan University, Changsha, Hunan, China, International Journal of Pavement Engineering, pp 213-223, Volume 8, Issue 3 September 2007.

21. Hunt, L and Boyle, G.E, "Steel Slag in Hot Mix Asphalt Conrete," State Research Project No. 511, Department of Transportation, Salem, Oregon, 2000.

22. Jiang, R.B, Lin, J. D. and Lin D. F. "Rheology of Asphaltic Binders and Their Effects on Asphalt Concrete" Transportation Research Record 1535, National Research Council,Washington, D.C., pp. 74-81, 1996.

23. J.J. Lingle, Discussion in Proc. AAPT, Vol. 25, 1986, P.103.

24. Johannson, L., (1998) "Bitumen Aging and Hydrated Lime," Dissertation, Kungl Tekniska Hogkolan, Royal Institute of Technology.

25. Jones, G.M., "The Effect of Hydrated Lime on Asphalt in Bituminous Pavements," Utah DOT, May, 1997.

26. Kallas, B.F. and Puzinauskas, V.P, "A study of mineral fillers in asphalt paving mixtures. Asphalt Paving Technology. pp. 493-528, Volume 30, 1961.

27. Kandhal, P. S. and Mallick, R. B. "Effect of Mix Gradation on Rutting Potential of Dense-Graded Asphalt Mixtures", Transportation Research Record 1767, Washington, D.C., 2001.

28. Kandhal, P. S., and Mallick R. B. "Evaluation of Asphalt Pavement Analyzer for HMA Mix Design", Report No. 99-4, National Center for Asphalt Technology, Auburn University, Alabama, 1999.

29. King, G.N., and King, H.W., "Influence of asphalt grade and polymers concentration on low temperature performance of polymer modified asphalt" Assoc. of Asphalt Paving Techonologists, vol.62, 1-22, (1993).

30. Kraszowski, L., and Emery, J. J.. "Use of cement kiln dust as filler in asphalt mixes." Proc., OFR/CANMET Symposium on Mineral Fillers, Ontario Research Foundation, Toronto, 19810.

31. Kumar, A., and Goetz, W.H. "Asphalt hardening as affected by film thickness, voids, and permeability in asphaltic pvements." Assoc. of Asphalt Paving Technologist, Vol. 46, 571-605, 1997.

32. Lackner R., Spiegl, M, Blab R., and Eberhardsteiner J, "Is Low-Temperature Creep of Asphalt Mastic Independent of Filler Shape and Mineralogy?" Journal of Materials in Civil Engineering, pg, 485-491, September 2005.

33. Lesueur, Didier & Dallas N. Little, "Effect of Hydrated Lime on Rheology, Fracture and Aging of Bitumen," Transportation Research Report 1661, 1999.

34. Lesueur et al. & Little D.N., "The Effect of Hydrated Lime on the Rheology, Fracture and Aging of Bitumen and Asphalt Mixtures, "Lhoist HMA Symposium, Dusseldorf, Germany, 1998.

35. Lesueur, D. and Little, D., "Hydrated Lime as an Active Filler in Bitumen," Washington, D.C., 1999.

36. Little, D.N.. "The benefits of hydrated lime in hot mix asphalt", National Lime Association, 2001.

37. Little, D. N., "Performance Assessment of Binder-Rich Polyethylene Modified Asphalt Concrete Mixture", Transportation Research Board, Washington, D.C. (1991)

38. Little, D.N and Petersen J.C. "Unique Effects of Hydrated Lime Filler on the Performance Related Properties of Asphalt Cements: Physical and Chemical

Interactions Revisited" Journal of Materials in Civil Engineering, April 2005.

39. Nahass, N. C. Jaques, B"Polymer Modified Asphalts for High Performance Hot Mix Pavement Binders", J. Assoc. of Asphalt Paving Technolo., 59, 509-525. 1990.

40. Petersen, J.C., H. Plancher and P.M. Hamsbergen, "Lime Treatment of Asphalt to Reduce Age Hardening and Improve Flow Properties", AAPT Vol. 56, 1987.

41. Pioro L.S., and Pioro I.L., "Reprocessing of Metallurgical Slag into Materials for the Building Industtry", Waste Management, Volume 24, Issue 4, Page 371-379, 2004.

42. Ramswamy, S.D. and Aziz, M.A, "Effect of Filler Type and Shape of Aggregates on the Stability of Bituminous Mixes", Road Engineering Association of Asia and Australasia 3, 171-177, Jakarta, Indonesia, 1983.

43. Ramzi Taha, Amer Al-Rawas, "Use of Cement Bypass Dust as Filler in Asphalt Concrete Mixtures" Journal of Materials in Civil Engineering, July/August, 2002.

44. Rodriguez, T and Mershon, E, Construction Project Narrative, Oregon Department of Transportation, August 24, 1995.

45. Rosener, John C., James G. Ghehovits and Gene R. Morris, "Fly Ash as a Mineral Filler and Anti-Stripping Agent for Asphalt Concrete", Proceeding of the Sixth International Ash Utilization Symposium. Volume 1, Washington, DC, 1982.

46. Suheibani, A.R.S, "The use of Fly Ash as an Asphalt Extender,", Univ. of Michigan, 1986.

47. Suhaibani, A.A, Mudaiheem J.A. "Effect of Filler Type and Content on Properties of Asphalt Concrete Mixes" American Society for Testing and Material, Philadelphia, 1992.

48. Tons, E. et. Al. (1983), "Fly Ash as an Asphalt Reducer in Bituminous base Courses." University of Michigan.

49. Wu. S., Xue. Y., and Chen, Y., (2006) "Utilization of Steel Slag as Aggregates for Stone Mastic Asphalt (SMA) Mixtures", Elsevier Ltd.

50. Zimmer, Frank V. (1970) "Fly Ash as Bituminous Filler", Proceeding of the Second Ash Utilization Symposium, No. 8488, Pittsburgh, Pennsylvania.

APPENDIX 1

Volumetric Property

Worksheets

Control Mix with 3.5% A.C.

Superpave Bituminious Laboratory Worksheet					
	PARAMETER	Briquette Number			
		1	2	3	Average
A1	Mass of Compacted Specimen in Air	4885.2	4882.6	4882.9	
A2	Surface Dry Mass of Specimen in Air	4906.8	4905.4	4905.3	
B1	Mass of Compacted Specimen in Water	2935.4	2932.6	2939.6	
B2	Volume = A2-B1	1971.4	1972.8	1965.7	
C	Bulk Relative Density = A1/B2	2.478	2.475	2.484	2.479
C1	Flask Number	D	E		
D	Mass of Flask and Mixture in Air	2572.3	2521.5		
E	Mass of Flask in Air	653.1	633.8		
F	Mass of Mixture in Air = D-E	1919.2	1887.7		
F1	Surface Dry Mass of Mixture in Air				
G	Mass of Flask and Mixture in Water	1751.2	1715.6		
H	Mass of Flask in Water	571.2	553.7		
I1	Mass of Mixture in Water = G-H	1180	1161.9		
I2	Volume = F-I1	739.2	725.8		
I3	S.D. Volume = F1-I1				
J	Maximum Relative Density = F/I2	2.596	2.601		2.599
J1	S.D. Maximum Relative Density = F/I2				
K	Percent Voids in Mixture = J-C/J*100	4.6			
K1	Binder Content (%)	3.5			
L	Gb =	2.773			
M	VMA = 100-[(100-A.C.)*Avg.C/L]	13.7			
N	VFA = 100*(M-K)/M	66.4			

Control Mix with 4.0% A.C.

Superpave Bituminious Laboratory Worksheet					
	PARAMETER	Briquette Number			
		1	2	3	Average
A1	Mass of Compacted Specimen in Air	4881.2	4836.5	4836.7	
A2	Surface Dry Mass of Specimen in Air	4899.7	4852.3	4850.4	
B1	Mass of Compacted Specimen in Water	2931.6	2908.3	2902.3	
B2	Volume = A2-B1	1968.1	1944	1948.1	
C	Bulk Relative Density = A1/B2	2.480	2.488	2.483	2.484
C1	Flask Number	D	E		
D	Mass of Flask and Mixture in Air	2581.3	2525.5		
E	Mass of Flask in Air	653.1	633.8		
F	Mass of Mixture in Air = D-E	1928.2	1891.7		
F1	Surface Dry Mass of Mixture in Air				
G	Mass of Flask and Mixture in Water	1757.2	1714.2		
H	Mass of Flask in Water	571.2	553.7		
I1	Mass of Mixture in Water = G-H	1186	1160.5		
I2	Volume = F-I1	742.2	731.2		
I3	S.D. Volume = F1-I1				
J	Maximum Relative Density = F/I2	2.598	2.587		2.593
J1	S.D. Maximum Relative Density = F/I2				
K	Percent Voids in Mixture = J-C/J*100	4.2			
K1	Binder Content (%)	4.0			
L	Gb =	2.773			
M	VMA = 100-[(100-A.C.)*Avg.C/L]	14.0			
N	VFA = 100*(M-K)/M	70.0			

Control Mix with 4.5% A.C.

Superpave Bituminious Laboratory Worksheet					
	PARAMETER	Briquette Number			
		1	2	3	Average
A1	Mass of Compacted Specimen in Air	4888.4	4882.7	4882.4	
A2	Surface Dry Mass of Specimen in Air	4892.5	4897.3	4889.2	
B1	Mass of Compacted Specimen in Water	2933.2	2937.8	2930.6	
B2	Volume = A2-B1	1959.3	1959.5	1958.6	
C	Bulk Relative Density = A1/B2	2.495	2.492	2.493	2.493
C1	Flask Number	D	E		
D	Mass of Flask and Mixture in Air	2588.2	2584.1		
E	Mass of Flask in Air	653.1	633.8		
F	Mass of Mixture in Air = D-E	1935.1	1950.3		
F1	Surface Dry Mass of Mixture in Air				
G	Mass of Flask and Mixture in Water	1756.2	1751.3		
H	Mass of Flask in Water	571.2	553.7		
I1	Mass of Mixture in Water = G-H	1185	1197.6		
I2	Volume = F-I1	750.1	752.7		
I3	S.D. Volume = F1-I1				
J	Maximum Relative Density = F/I2	2.580	2.591		2.585
J1	S.D. Maximum Relative Density = F/I2				
K	Percent Voids in Mixture = J-C/J*100	3.6			
K1	Binder Content (%)	4.5			
L	Gb =	2.773			
M	VMA = 100-[(100-A.C.)*Avg.C/L]	14.1			
N	VFA = 100*(M-K)/M	74.8			

Control Mix with 5.0% A.C.

Superpave Bituminious Laboratory Worksheet					
	PARAMETER	Briquette Number			
		1	2	3	Average
A1	Mass of Compacted Specimen in Air	4883.4	4882.9	4875.2	
A2	Surface Dry Mass of Specimen in Air	4890.7	4892.8	4880.1	
B1	Mass of Compacted Specimen in Water	2934.5	2935.2	2931.9	
B2	Volume = A2-B1	1956.2	1957.6	1948.2	
C	Bulk Relative Density = A1/B2	2.496	2.494	2.502	2.498
C1	Flask Number	D	E		
D	Mass of Flask and Mixture in Air	2591.2	2598.5		
E	Mass of Flask in Air	653.1	633.8		
F	Mass of Mixture in Air = D-E	1938.1	1964.7		
F1	Surface Dry Mass of Mixture in Air				
G	Mass of Flask and Mixture in Water	1757.1	1753.7		
H	Mass of Flask in Water	571.2	553.7		
I1	Mass of Mixture in Water = G-H	1185.9	1200		
I2	Volume = F-I1	752.2	764.7		
I3	S.D. Volume = F1-I1				
J	Maximum Relative Density = F/I2	2.577	2.569		2.573
J1	S.D. Maximum Relative Density = F/I2				
K	Percent Voids in Mixture = J-C/J*100	2.9			
K1	Binder Content (%)	5.0			
L	Gb =	2.773			
M	VMA = 100-[(100-A.C.)*Avg.C/L]	14.4			
N	VFA = 100*(M-K)/M	79.8			

Control Mix with 5.5% A.C.

Superpave Bituminious Laboratory Worksheet					
	PARAMETER	Briquette Number			
		1	2	3	Average
A1	Mass of Compacted Specimen in Air	4893.1	4894.6	4888.2	
A2	Surface Dry Mass of Specimen in Air	4899.7	4898.8	4898.9	
B1	Mass of Compacted Specimen in Water	2947.8	2937.9	2942.1	
B2	Volume = A2-B1	1951.9	1960.9	1956.8	
C	Bulk Relative Density = A1/B2	2.507	2.496	2.498	2.500
C1	Flask Number	D	E		
D	Mass of Flask and Mixture in Air	2588.2	2537.5		
E	Mass of Flask in Air	653.1	633.8		
F	Mass of Mixture in Air = D-E	1935.1	1903.7		
F1	Surface Dry Mass of Mixture in Air				
G	Mass of Flask and Mixture in Water	1749.6	1718.1		
H	Mass of Flask in Water	571.2	553.7		
I1	Mass of Mixture in Water = G-H	1178.4	1164.4		
I2	Volume = F-I1	756.7	739.3		
I3	S.D. Volume = F1-I1				
J	Maximum Relative Density = F/I2	2.557	2.575		2.566
J1	S.D. Maximum Relative Density = F/I2				
K	Percent Voids in Mixture = J-C/J*100	2.6			
K1	Binder Content (%)	5.5			
L	Gb =	2.773			
M	VMA = 100-[(100-A.C.)*Avg.C/L]	14.8			
N	VFA = 100*(M-K)/M	82.6			

Fly Ash (Class C) mix with 3.5% A.C.

Superpave Bituminious Laboratory Worksheet					
	PARAMETER	Briquette Number			
		1	2	3	Average
A1	Mass of Compacted Specimen in Air	4949.6	4955.8	4942.2	
A2	Surface Dry Mass of Specimen in Air	4965.3	4969.2	4963.8	
B1	Mass of Compacted Specimen in Water	2973.8	2977.1	2971.8	
B2	Volume = A2-B1	1991.5	1992.1	1992	
C	Bulk Relative Density = A1/B2	2.485	2.488	2.481	2.485
C1	Flask Number	G	H		
D	Mass of Flask and Mixture in Air	2596.6	2561.4		
E	Mass of Flask in Air	632.7	634.2		
F	Mass of Mixture in Air = D-E	1963.9	1927.2		
F1	Surface Dry Mass of Mixture in Air				
G	Mass of Flask and Mixture in Water	1763.4	1743.6		
H	Mass of Flask in Water	553.1	554.2		
I1	Mass of Mixture in Water = G-H	1210.3	1189.4		
I2	Volume = F-I1	753.6	737.8		
I3	S.D. Volume = F1-I1				
J	Maximum Relative Density = F/I2	2.606	2.612		2.609
J1	S.D. Maximum Relative Density = F/I2				
K	Percent Voids in Mixture = J-C/J*100	4.8			
K1	Binder Content (%)	3.5			
L	Gb =	2.776			
M	VMA = 100-[(100-A.C.)*Avg.C/L]	13.6			
N	VFA = 100*(M-K)/M	65.1			

Fly Ash (Class C) mix with 4.0% A.C.

Superpave Bituminious Laboratory Worksheet					
	PARAMETER	Briquette Number			
		1	2	3	Average
A1	Mass of Compacted Specimen in Air	4948.6	4949.8	4944.5	
A2	Surface Dry Mass of Specimen in Air	4962.8	4964.1	4966.2	
B1	Mass of Compacted Specimen in Water	2979.2	2983.6	2980.8	
B2	Volume = A2-B1	1983.6	1980.5	1985.4	
C	Bulk Relative Density = A1/B2	2.495	2.499	2.490	2.495
C1	Flask Number	G	H		
D	Mass of Flask and Mixture in Air	2612.3	2591.1		
E	Mass of Flask in Air	632.7	634.2		
F	Mass of Mixture in Air = D-E	1979.6	1956.9		
F1	Surface Dry Mass of Mixture in Air				
G	Mass of Flask and Mixture in Water	1770.1	1760.4		
H	Mass of Flask in Water	553.1	554.2		
I1	Mass of Mixture in Water = G-H	1217	1206.2		
I2	Volume = F-I1	762.6	750.7		
I3	S.D. Volume = F1-I1				
J	Maximum Relative Density = F/I2	2.596	2.607		2.601
J1	S.D. Maximum Relative Density = F/I2				
K	Percent Voids in Mixture = J-C/J*100	4.1			
K1	Binder Content (%)	4.0			
L	Gb =	2.776			
M	VMA = 100-[(100-A.C.)*Avg.C/L]	13.7			
N	VFA = 100*(M-K)/M	70.3			

Fly Ash (Class C) mix with 4.5% A.C.

Superpave Bituminious Laboratory Worksheet					
	PARAMETER	Briquette Number			
		1	2	3	Average
A1	Mass of Compacted Specimen in Air	4894.2	4894.5	4880.2	
A2	Surface Dry Mass of Specimen in Air	4906.7	4908.2	4899.3	
B1	Mass of Compacted Specimen in Water	2953.9	2956.1	2955.9	
B2	Volume = A2-B1	1952.8	1952.1	1943.4	
C	Bulk Relative Density = A1/B2	2.506	2.507	2.511	2.508
C1	Flask Number	G	H		
D	Mass of Flask and Mixture in Air	2576.3	2591.1		
E	Mass of Flask in Air	632.7	634.2		
F	Mass of Mixture in Air = D-E	1943.6	1956.9		
F1	Surface Dry Mass of Mixture in Air				
G	Mass of Flask and Mixture in Water	1747.7	1755.4		
H	Mass of Flask in Water	553.1	554.2		
I1	Mass of Mixture in Water = G-H	1194.6	1201.2		
I2	Volume = F-I1	749	755.7		
I3	S.D. Volume = F1-I1				
J	Maximum Relative Density = F/I2	2.595	2.590		2.592
J1	S.D. Maximum Relative Density = F/I2				
K	Percent Voids in Mixture = J-C/J*100	3.2			
K1	Binder Content (%)	4.5			
L	Gb =	2.776			
M	VMA = 100-[(100-A.C.)*Avg.C/L]	13.7			
N	VFA = 100*(M-K)/M	76.4			

Fly Ash (Class C) mix with 5.0% A.C.

Superpave Bituminious Laboratory Worksheet					
	PARAMETER	Briquette Number			
		1	2	3	Average
A1	Mass of Compacted Specimen in Air	4884.6	4886.1	4888.9	
A2	Surface Dry Mass of Specimen in Air	4892.4	4895.8	4894.4	
B1	Mass of Compacted Specimen in Water	2943.5	2949.2	2953.1	
B2	Volume = A2-B1	1948.9	1946.6	1941.3	
C	Bulk Relative Density = A1/B2	2.506	2.510	2.518	2.512
C1	Flask Number	G	H		
D	Mass of Flask and Mixture in Air	2578.4	2584.6		
E	Mass of Flask in Air	632.7	634.2		
F	Mass of Mixture in Air = D-E	1945.7	1950.4		
F1	Surface Dry Mass of Mixture in Air				
G	Mass of Flask and Mixture in Water	1746.3	1750.9		
H	Mass of Flask in Water	553.1	554.2		
I1	Mass of Mixture in Water = G-H	1193.2	1196.7		
I2	Volume = F-I1	752.5	753.7		
I3	S.D. Volume = F1-I1				
J	Maximum Relative Density = F/I2	2.586	2.588		2.587
J1	S.D. Maximum Relative Density = F/I2				
K	Percent Voids in Mixture = J-C/J*100	2.9			
K1	Binder Content (%)	5.0			
L	Gb =	2.776			
M	VMA = 100-[(100-A.C.)*Avg.C/L]	14.0			
N	VFA = 100*(M-K)/M	79.3			

Fly Ash (Class C) mix with 5.5% A.C.

Superpave Bituminious Laboratory Worksheet					
	PARAMETER	Briquette Number			
		1	2	3	Average
A1	Mass of Compacted Specimen in Air	4892.7	4894.2	4889.4	
A2	Surface Dry Mass of Specimen in Air	4904.5	4906.8	4908.9	
B1	Mass of Compacted Specimen in Water	2964.4	2961.7	2968.5	
B2	Volume = A2-B1	1940.1	1945.1	1940.4	
C	Bulk Relative Density = A1/B2	2.522	2.516	2.520	2.519
C1	Flask Number	G	H		
D	Mass of Flask and Mixture in Air	2534.8	2528.6		
E	Mass of Flask in Air	632.7	634.2		
F	Mass of Mixture in Air = D-E	1902.1	1894.4		
F1	Surface Dry Mass of Mixture in Air				
G	Mass of Flask and Mixture in Water	1715.8	1713.2		
H	Mass of Flask in Water	553.1	554.2		
I1	Mass of Mixture in Water = G-H	1162.7	1159		
I2	Volume = F-I1	739.4	735.4		
I3	S.D. Volume = F1-I1				
J	Maximum Relative Density = F/I2	2.572	2.576		2.574
J1	S.D. Maximum Relative Density = F/I2				
K	Percent Voids in Mixture = J-C/J*100	2.1			
K1	Binder Content (%)	5.5			
L	Gb =	2.776			
M	VMA = 100-[(100-A.C.)*Avg.C/L]	14.2			
N	VFA = 100*(M-K)/M	85.0			

Fly Ash (Class F) mix with 3.5% A.C.

Superpave Bituminious Laboratory Worksheet					
	PARAMETER	Briquette Number 1	2	3	Average
A1	Mass of Compacted Specimen in Air	4950.3	4954.2	4955.5	
A2	Surface Dry Mass of Specimen in Air	4968.5	4973.5	4974.8	
B1	Mass of Compacted Specimen in Water	2967.8	2972.4	2971.2	
B2	Volume = A2-B1	2000.7	2001.1	2003.6	
C	Bulk Relative Density = A1/B2	2.474	2.476	2.473	2.474
C1	Flask Number		D		
D	Mass of Flask and Mixture in Air	3056.6	3041.5		
E	Mass of Flask in Air	649.8	635.1		
F	Mass of Mixture in Air = D-E	2406.8	2406.4		
F1	Surface Dry Mass of Mixture in Air				
G	Mass of Flask and Mixture in Water	2051.5	2038.2		
H	Mass of Flask in Water	567.4	556.7		
I1	Mass of Mixture in Water = G-H	1484.1	1481.5		
I2	Volume = F-I1	922.7	924.9		
I3	S.D. Volume = F1-I1				
J	Maximum Relative Density = F/I2	2.608	2.602		2.605
J1	S.D. Maximum Relative Density = F/I2				
K	Percent Voids in Mixture = J-C/J*100	5.0			
K1	Binder Content (%)	3.5			
L	Gb =	2.767			
M	VMA = 100-[(100-A.C.)*Avg.C/L]	13.7			
N	VFA = 100*(M-K)/M	63.4			

Fly Ash (Class F) mix with 4.0% A.C.

Superpave Bituminious Laboratory Worksheet					
	PARAMETER	Briquette Number			
		1	2	3	Average
A1	Mass of Compacted Specimen in Air	4947.8	4955.2	4946.0	
A2	Surface Dry Mass of Specimen in Air	4968.6	4977.4	4966.6	
B1	Mass of Compacted Specimen in Water	2983.8	2981.9	2980.4	
B2	Volume = A2-B1	1984.8	1995.5	1986.2	
C	Bulk Relative Density = A1/B2	2.493	2.483	2.490	2.489
C1	Flask Number	C	D		
D	Mass of Flask and Mixture in Air	3311.4	2789.2		
E	Mass of Flask in Air	649.8	635.1		
F	Mass of Mixture in Air = D-E	2661.6	2154.1		
F1	Surface Dry Mass of Mixture in Air				
G	Mass of Flask and Mixture in Water	2201.3	1879.8		
H	Mass of Flask in Water	567.4	556.7		
I1	Mass of Mixture in Water = G-H	1633.9	1323.1		
I2	Volume = F-I1	1027.7	831		
I3	S.D. Volume = F1-I1				
J	Maximum Relative Density = F/I2	2.590	2.592		2.591
J1	S.D. Maximum Relative Density = F/I2				
K	Percent Voids in Mixture = J-C/J*100	3.9			
K1	Binder Content (%)	4.0			
L	Gb =	2.767			
M	VMA = 100-[(100-A.C.)*Avg.C/L]	13.7			
N	VFA = 100*(M-K)/M	71.2			

Fly Ash (Class F) mix with 4.5% A.C.

Superpave Bituminious Laboratory Worksheet					
	PARAMETER	Briquette Number			
		1	2	3	Average
A1	Mass of Compacted Specimen in Air	4938.8	4942.5	4948.5	
A2	Surface Dry Mass of Specimen in Air	4954.1	4966.4	4964.8	
B1	Mass of Compacted Specimen in Water	2983.5	2990.5	2997.4	
B2	Volume = A2-B1	1970.6	1975.9	1967.4	
C	Bulk Relative Density = A1/B2	2.506	2.501	2.515	2.508
C1	Flask Number	C	D		
D	Mass of Flask and Mixture in Air	3192.4	3208.6		
E	Mass of Flask in Air	649.8	635.1		
F	Mass of Mixture in Air = D-E	2542.6	2573.5		
F1	Surface Dry Mass of Mixture in Air				
G	Mass of Flask and Mixture in Water	2126.1	2133.5		
H	Mass of Flask in Water	567.4	556.7		
I1	Mass of Mixture in Water = G-H	1558.7	1576.8		
I2	Volume = F-I1	983.9	996.7		
I3	S.D. Volume = F1-I1				
J	Maximum Relative Density = F/I2	2.584	2.582		2.583
J1	S.D. Maximum Relative Density = F/I2				
K	Percent Voids in Mixture = J-C/J*100	2.9			
K1	Binder Content (%)	4.5			
L	Gb =	2.767			
M	VMA = 100-[(100-A.C.)*Avg.C/L]	13.5			
N	VFA = 100*(M-K)/M	78.4			

Fly Ash (Class F) mix with 5.0% A.C.

Superpave Bituminious Laboratory Worksheet					
	PARAMETER	Briquette Number			
		1	2	3	Average
A1	Mass of Compacted Specimen in Air	4972.0	4976.1	4968.9	
A2	Surface Dry Mass of Specimen in Air	4986.8	4995.8	4984.4	
B1	Mass of Compacted Specimen in Water	3004.8	3017.2	3014.5	
B2	Volume = A2-B1	1982	1978.6	1969.9	
C	Bulk Relative Density = A1/B2	2.509	2.515	2.522	2.515
C1	Flask Number	G	H		
D	Mass of Flask and Mixture in Air	2575.3	2580.0		
E	Mass of Flask in Air	632.7	634.2		
F	Mass of Mixture in Air = D-E	1942.6	1945.8		
F1	Surface Dry Mass of Mixture in Air				
G	Mass of Flask and Mixture in Water	1740.6	1745.4		
H	Mass of Flask in Water	553.1	554.2		
I1	Mass of Mixture in Water = G-H	1187.5	1191.2		
I2	Volume = F-I1	755.1	754.6		
I3	S.D. Volume = F1-I1				
J	Maximum Relative Density = F/I2	2.573	2.579		2.576
J1	S.D. Maximum Relative Density = F/I2				
K	Percent Voids in Mixture = J-C/J*100	2.3			
K1	Binder Content (%)	5.0			
L	Gb =	2.767			
M	VMA = 100-[(100-A.C.)*Avg.C/L]	13.7			
N	VFA = 100*(M-K)/M	82.7			

Fly Ash (Class F) mix with 5.5% A.C.

Superpave Bituminious Laboratory Worksheet					
	PARAMETER	Briquette Number			
		1	2	3	Average
A1	Mass of Compacted Specimen in Air	4867.9	4863.4	4856.2	
A2	Surface Dry Mass of Specimen in Air	4879.2	4877.6	4869.6	
B1	Mass of Compacted Specimen in Water	2945.5	2942.3	2944.5	
B2	Volume = A2-B1	1933.7	1935.3	1925.1	
C	Bulk Relative Density = A1/B2	2.517	2.513	2.523	2.518
C1	Flask Number	G	H		
D	Mass of Flask and Mixture in Air	2577.8	2552.6		
E	Mass of Flask in Air	632.7	634.2		
F	Mass of Mixture in Air = D-E	1945.1	1918.4		
F1	Surface Dry Mass of Mixture in Air				
G	Mass of Flask and Mixture in Water	1742.4	1727.9		
H	Mass of Flask in Water	553.1	554.2		
I1	Mass of Mixture in Water = G-H	1189.3	1173.7		
I2	Volume = F-I1	755.8	744.7		
I3	S.D. Volume = F1-I1				
J	Maximum Relative Density = F/I2	2.574	2.576		2.575
J1	S.D. Maximum Relative Density = F/I2				
K	Percent Voids in Mixture = J-C/J*100	2.2			
K1	Binder Content (%)	5.5			
L	Gb =	2.767			
M	VMA = 100-[(100-A.C.)*Avg.C/L]	14.0			
N	VFA = 100*(M-K)/M	84.2			

Slag mix with 3.5% A.C.

Superpave Bituminious Laboratory Worksheet					
	PARAMETER	Briquette Number			
		1	2	3	Average
A1	Mass of Compacted Specimen in Air	4953.6	4954.9	4957.1	
A2	Surface Dry Mass of Specimen in Air	4974.5	4975.7	4978.5	
B1	Mass of Compacted Specimen in Water	2979.8	2983	2988.6	
B2	Volume = A2-B1	1994.7	1992.7	1989.9	
C	Bulk Relative Density = A1/B2	2.483	2.487	2.491	2.487
C1	Flask Number	E	F		
D	Mass of Flask and Mixture in Air	2722.3	2548.5		
E	Mass of Flask in Air	633.8	635.8		
F	Mass of Mixture in Air = D-E	2088.5	1912.7		
F1	Surface Dry Mass of Mixture in Air				
G	Mass of Flask and Mixture in Water	1843.3	1734.3		
H	Mass of Flask in Water	553.7	555.1		
I1	Mass of Mixture in Water = G-H	1289.6	1179.2		
I2	Volume = F-I1	798.9	733.5		
I3	S.D. Volume = F1-I1				
J	Maximum Relative Density = F/I2	2.614	2.608		2.611
J1	S.D. Maximum Relative Density = F/I2				
K	Percent Voids in Mixture = J-C/J*100	4.7			
K1	Binder Content (%)	3.5			
L	Gb =	2.778			
M	VMA = 100-[(100-A.C.)*Avg.C/L]	13.6			
N	VFA = 100*(M-K)/M	65.1			

Slag mix with 4.0% A.C.

Superpave Bituminious Laboratory Worksheet					
	PARAMETER	Briquette Number			
		1	2	3	Average
A1	Mass of Compacted Specimen in Air	4958.7	4955.6	4956.7	
A2	Surface Dry Mass of Specimen in Air	4975.4	4972	4976.4	
B1	Mass of Compacted Specimen in Water	2985.2	2988.4	2988.9	
B2	Volume = A2-B1	1990.2	1983.6	1987.5	
C	Bulk Relative Density = A1/B2	2.492	2.498	2.494	2.495
C1	Flask Number	E	F		
D	Mass of Flask and Mixture in Air	2753.4	2555.1		
E	Mass of Flask in Air	633.8	635.8		
F	Mass of Mixture in Air = D-E	2119.6	1919.3		
F1	Surface Dry Mass of Mixture in Air				
G	Mass of Flask and Mixture in Water	1860.3	1736.6		
H	Mass of Flask in Water	553.7	555.1		
I1	Mass of Mixture in Water = G-H	1306.6	1181.5		
I2	Volume = F-I1	813	737.8		
I3	S.D. Volume = F1-I1				
J	Maximum Relative Density = F/I2	2.607	2.601		2.604
J1	S.D. Maximum Relative Density = F/I2				
K	Percent Voids in Mixture = J-C/J*100	4.2			
K1	Binder Content (%)	4.0			
L	Gb =	2.778			
M	VMA = 100-[(100-A.C.)*Avg.C/L]	13.8			
N	VFA = 100*(M-K)/M	69.6			

Slag mix with 4.5% A.C.

Superpave Bituminious Laboratory Worksheet					
	PARAMETER	Briquette Number 1	2	3	Average
A1	Mass of Compacted Specimen in Air	4949.4	4956.2	4962.1	
A2	Surface Dry Mass of Specimen in Air	4965.2	4974.2	4979.4	
B1	Mass of Compacted Specimen in Water	2986.3	2996.7	2998.6	
B2	Volume = A2-B1	1978.9	1977.5	1980.8	
C	Bulk Relative Density = A1/B2	2.501	2.506	2.505	2.504
C1	Flask Number	E	F		
D	Mass of Flask and Mixture in Air	2764.2	2528.5		
E	Mass of Flask in Air	633.8	635.8		
F	Mass of Mixture in Air = D-E	2130.4	1892.7		
F1	Surface Dry Mass of Mixture in Air				
G	Mass of Flask and Mixture in Water	1866.4	1716.7		
H	Mass of Flask in Water	553.7	555.1		
I1	Mass of Mixture in Water = G-H	1312.7	1161.6		
I2	Volume = F-I1	817.7	731.1		
I3	S.D. Volume = F1-I1				
J	Maximum Relative Density = F/I2	2.605	2.589		2.597
J1	S.D. Maximum Relative Density = F/I2				
K	Percent Voids in Mixture = J-C/J*100	3.6			
K1	Binder Content (%)	4.5			
L	Gb =	2.778			
M	VMA = 100-[(100-A.C.)*Avg.C/L]	13.9			
N	VFA = 100*(M-K)/M	74.3			

Slag mix with 5.0% A.C.

Superpave Bituminious Laboratory Worksheet					
	PARAMETER	Briquette Number			
		1	2	3	Average
A1	Mass of Compacted Specimen in Air	4952.8	4955.1	4957.9	
A2	Surface Dry Mass of Specimen in Air	4962.3	4963.8	4971.8	
B1	Mass of Compacted Specimen in Water	2988.5	2992.4	2998.7	
B2	Volume = A2-B1	1973.8	1971.4	1973.1	
C	Bulk Relative Density = A1/B2	2.509	2.513	2.513	2.512
C1	Flask Number	E	F		
D	Mass of Flask and Mixture in Air	2567.3	2573.4		
E	Mass of Flask in Air	633.8	635.8		
F	Mass of Mixture in Air = D-E	1933.5	1937.6		
F1	Surface Dry Mass of Mixture in Air				
G	Mass of Flask and Mixture in Water	1740.7	1742.3		
H	Mass of Flask in Water	553.7	555.1		
I1	Mass of Mixture in Water = G-H	1187	1187.2		
I2	Volume = F-I1	746.5	750.4		
I3	S.D. Volume = F1-I1				
J	Maximum Relative Density = F/I2	2.590	2.582		2.586
J1	S.D. Maximum Relative Density = F/I2				
K	Percent Voids in Mixture = J-C/J*100	2.9			
K1	Binder Content (%)	5.0			
L	Gb =	2.778			
M	VMA = 100-[(100-A.C.)*Avg.C/L]	14.1			
N	VFA = 100*(M-K)/M	79.7			

Slag mix with 5.5% A.C.

Superpave Bituminious Laboratory Worksheet					
	PARAMETER	Briquette Number			
		1	2	3	Average
A1	Mass of Compacted Specimen in Air	4963.8	4966.2	4959.4	
A2	Surface Dry Mass of Specimen in Air	4971.3	4973.5	4970.7	
B1	Mass of Compacted Specimen in Water	2997.8	2999.4	3001.7	
B2	Volume = A2-B1	1973.5	1974.1	1969	
C	Bulk Relative Density = A1/B2	2.515	2.516	2.519	2.517
C1	Flask Number	E	F		
D	Mass of Flask and Mixture in Air	2567.2	2557.1		
E	Mass of Flask in Air	633.8	635.8		
F	Mass of Mixture in Air = D-E	1933.4	1921.3		
F1	Surface Dry Mass of Mixture in Air				
G	Mass of Flask and Mixture in Water	1738.6	1729.2		
H	Mass of Flask in Water	553.7	555.1		
I1	Mass of Mixture in Water = G-H	1184.9	1174.1		
I2	Volume = F-I1	748.5	747.2		
I3	S.D. Volume = F1-I1				
J	Maximum Relative Density = F/I2	2.583	2.571		2.577
J1	S.D. Maximum Relative Density = F/I2				
K	Percent Voids in Mixture = J-C/J*100	2.4			
K1	Binder Content (%)	5.5			
L	Gb =	2.778			
M	VMA = 100-[(100-A.C.)*Avg.C/L]	14.4			
N	VFA = 100*(M-K)/M	83.8			

Portland Cement mix with 3.5% A.C.

Superpave Bituminious Laboratory Worksheet					
	PARAMETER	Briquette Number			
		1	2	3	Average
A1	Mass of Compacted Specimen in Air	4967.3	4966.2	4967.5	
A2	Surface Dry Mass of Specimen in Air	4982.4	4984.5	4986.3	
B1	Mass of Compacted Specimen in Water	2958.4	2964.3	2969.6	
B2	Volume = A2-B1	2024	2020.2	2016.7	
C	Bulk Relative Density = A1/B2	2.454	2.458	2.463	2.459
C1	Flask Number	C	D		
D	Mass of Flask and Mixture in Air	2755.2	2746.6		
E	Mass of Flask in Air	649.8	635.1		
F	Mass of Mixture in Air = D-E	2105.4	2111.5		
F1	Surface Dry Mass of Mixture in Air				
G	Mass of Flask and Mixture in Water	1874.3	1865.4		
H	Mass of Flask in Water	567.4	556.7		
I1	Mass of Mixture in Water = G-H	1306.9	1308.7		
I2	Volume = F-I1	798.5	802.8		
I3	S.D. Volume = F1-I1				
J	Maximum Relative Density = F/I2	2.637	2.630		2.633
J1	S.D. Maximum Relative Density = F/I2				
K	Percent Voids in Mixture = J-C/J*100	6.6			
K1	Binder Content (%)	3.5			
L	Gb =	2.781			
M	VMA = 100-[(100-A.C.)*Avg.C/L]	14.7			
N	VFA = 100*(M-K)/M	55.0			

Portland Cemen mix with 4.0% A.C.

Superpave Bituminious Laboratory Worksheet					
	PARAMETER	Briquette Number			
		1	2	3	Average
A1	Mass of Compacted Specimen in Air	4926.3	4929.5	4933.8	
A2	Surface Dry Mass of Specimen in Air	4938.4	4943.8	4944.1	
B1	Mass of Compacted Specimen in Water	2945.2	2951	2957.3	
B2	Volume = A2-B1	1993.2	1992.8	1986.8	
C	Bulk Relative Density = A1/B2	2.472	2.474	2.483	2.476
C1	Flask Number	C	D		
D	Mass of Flask and Mixture in Air	2736.2	2757.2		
E	Mass of Flask in Air	649.8	635.1		
F	Mass of Mixture in Air = D-E	2086.4	2122.1		
F1	Surface Dry Mass of Mixture in Air				
G	Mass of Flask and Mixture in Water	1858.4	1869.2		
H	Mass of Flask in Water	567.4	556.7		
I1	Mass of Mixture in Water = G-H	1291	1312.5		
I2	Volume = F-I1	795.4	809.6		
I3	S.D. Volume = F1-I1				
J	Maximum Relative Density = F/I2	2.623	2.621		2.622
J1	S.D. Maximum Relative Density = F/I2				
K	Percent Voids in Mixture = J-C/J*100	5.6			
K1	Binder Content (%)	4.0			
L	Gb =	2.781			
M	VMA = 100-[(100-A.C.)*Avg.C/L]	14.5			
N	VFA = 100*(M-K)/M	61.7			

Portland Cemen mix with 4.5% A.C.

Superpave Bituminious Laboratory Worksheet					
	PARAMETER	Briquette Number			
		1	2	3	Average
A1	Mass of Compacted Specimen in Air	4945.4	4944.7	4941.5	
A2	Surface Dry Mass of Specimen in Air	4956.2	4953.5	4951.6	
B1	Mass of Compacted Specimen in Water	2972.6	2976.5	2973.2	
B2	Volume = A2-B1	1983.6	1977	1978.4	
C	Bulk Relative Density = A1/B2	2.493	2.501	2.498	2.497
C1	Flask Number	C	D		
D	Mass of Flask and Mixture in Air	2750.8	2755.8		
E	Mass of Flask in Air	649.8	635.1		
F	Mass of Mixture in Air = D-E	2101	2120.7		
F1	Surface Dry Mass of Mixture in Air				
G	Mass of Flask and Mixture in Water	1859.3	1862.4		
H	Mass of Flask in Water	567.4	556.7		
I1	Mass of Mixture in Water = G-H	1291.9	1305.7		
I2	Volume = F-I1	809.1	815		
I3	S.D. Volume = F1-I1				
J	Maximum Relative Density = F/I2	2.597	2.602		2.599
J1	S.D. Maximum Relative Density = F/I2				
K	Percent Voids in Mixture = J-C/J*100	3.9			
K1	Binder Content (%)	4.5			
L	Gb =	2.781			
M	VMA = 100-[(100-A.C.)*Avg.C/L]	14.3			
N	VFA = 100*(M-K)/M	72.5			

Portland Cemen mix with 5.0% A.C.

Superpave Bituminious Laboratory Worksheet					
	PARAMETER	Briquette Number			
		1	2	3	Average
A1	Mass of Compacted Specimen in Air	4955.8	4955.4	4957.1	
A2	Surface Dry Mass of Specimen in Air	4967.2	4968.5	4970.5	
B1	Mass of Compacted Specimen in Water	2985.4	2991.5	2990.1	
B2	Volume = A2-B1	1981.8	1977	1980.4	
C	Bulk Relative Density = A1/B2	2.501	2.507	2.503	2.503
C1	Flask Number	C	D		
D	Mass of Flask and Mixture in Air	2757.1	2748		
E	Mass of Flask in Air	649.8	635.1		
F	Mass of Mixture in Air = D-E	2107.3	2112.9		
F1	Surface Dry Mass of Mixture in Air				
G	Mass of Flask and Mixture in Water	1860.3	1852.9		
H	Mass of Flask in Water	567.4	556.7		
I1	Mass of Mixture in Water = G-H	1292.9	1296.2		
I2	Volume = F-I1	814.4	816.7		
I3	S.D. Volume = F1-I1				
J	Maximum Relative Density = F/I2	2.588	2.587		2.587
J1	S.D. Maximum Relative Density = F/I2				
K	Percent Voids in Mixture = J-C/J*100	3.2			
K1	Binder Content (%)	5.0			
L	Gb =	2.781			
M	VMA = 100-[(100-A.C.)*Avg.C/L]	14.5			--
N	VFA = 100*(M-K)/M	77.6			

Portland Cemen mix with 5.5% A.C.

Superpave Bituminious Laboratory Worksheet					
	PARAMETER	Briquette Number 1	2	3	Average
A1	Mass of Compacted Specimen in Air	4959.9	4969.2	4963.9	
A2	Surface Dry Mass of Specimen in Air	4969.1	4971.5	4970.3	
B1	Mass of Compacted Specimen in Water	3000.3	2999.1	2996.2	
B2	Volume = A2-B1	1974.1	1972.4	1968.8	
C	Bulk Relative Density = A1/B2	2.515	2.519	2.519	2.518
C1	Flask Number	C	D		
D	Mass of Flask and Mixture in Air	3100.2	2787.4		
E	Mass of Flask in Air	649.8	635.1		
F	Mass of Mixture in Air = D-E	2450.4	2152.3		
F1	Surface Dry Mass of Mixture in Air				
G	Mass of Flask and Mixture in Water	2064.5	1872.6		
H	Mass of Flask in Water	567.4	556.7		
I1	Mass of Mixture in Water = G-H	1497.1	1315.9		
I2	Volume = F-I1	953.3	836.4		
I3	S.D. Volume = F1-I1				
J	Maximum Relative Density = F/I2	2.570	2.573		2.572
J1	S.D. Maximum Relative Density = F/I2				
K	Percent Voids in Mixture = J-C/J*100	2.1			
K1	Binder Content (%)	5.5			
L	Gb =	2.781			
M	VMA = 100-[(100-A.C.)*Avg.C/L]	14.5			
N	VFA = 100*(M-K)/M	85.5			

APPENDIX 2

Volumetric Properties

@ Optimum Asphalt

Content

Control Mix with 4.3% A.C.

Superpave Bituminious Laboratory Worksheet								
PARAMETER		Briquette Number						
		N_{design}				N_{max}		
		1	2		Average	1	2	Average
A1	Mass of Compacted Specimen in Air	4938.5	4944.1	4943.7		4942.5	4943.4	
A2	Surface Dry Mass of Specimen in Air	4951.6	4966.8	4966.4		4951.7	4953.4	
B1	Mass of Compacted Specimen in Water	2967.8	2977.2	2977.6		2985.8	2984.5	
B2	Volume = A2-B1	1983.8	1989.6	1988.8		1965.9	1968.9	
C	Bulk Relative Density = A1/B2	2.489	2.485	2.486	2.487	2.514	2.511	2.512
C1	Flask Number	D	E					
D	Mass of Flask and Mixture in Air	2553.1	2547.1					
E	Mass of Flask in Air	653.1	633.8					
F	Mass of Mixture in Air = D-E	1900	1913.3					
F1	Surface Dry Mass of Mixture in Air							
G	Mass of Flask and Mixture in Water	1737.4	1726.7					
H	Mass of Flask in Water	571.2	553.7					
I1	Mass of Mixture in Water = G-H	1166.2	1173					
I2	Volume = F-I1	733.8	740.3					
I3	S.D. Volume = F1-I1							
J	Maximum Relative Density = F/I2	2.589	2.584		2.587			
J1	S.D. Maximum Relative Density = F/I2							
K	Percent Voids in Mixture = J-C/J*100	3.9				2.9		
K1	Binder Content (%)	4.3				4.3		
L	Gb =	2.773				2.773		
M	VMA = 100-[(100-A.C.)*Avg.C/L]	14.2				13.3		
N	VFA = 100*(M-K)/M	72.7				78.4		

Fly Ash (Class C) Mix with 4.0% A.C.

Superpave Bituminious Laboratory Worksheet								
PARAMETER		Briquette Number						
		N_{design}				N_{max}		
		1	2		Average	1	2	Average
A1	Mass of Compacted Specimen in Air	4948.6	4949.8	4944.5		4941.4	4947.9	
A2	Surface Dry Mass of Specimen in Air	4962.8	4964.1	4966.2		4950.0	4956.2	
B1	Mass of Compacted Specimen in Water	2979.2	2983.6	2980.8		2997.2	2998.8	
B2	Volume = A2-B1	1983.6	1980.5	1985.4		1952.8	1957.4	
C	Bulk Relative Density = A1/B2	2.495	2.499	2.490	2.495	2.530	2.528	2.529
C1	Flask Number	G	H					
D	Mass of Flask and Mixture in Air	2612.3	2591.1					
E	Mass of Flask in Air	632.7	634.2					
F	Mass of Mixture in Air = D-E	1979.6	1956.9					
F1	Surface Dry Mass of Mixture in Air							
G	Mass of Flask and Mixture in Water	1770.1	1760.4					
H	Mass of Flask in Water	553.1	554.2					
I1	Mass of Mixture in Water = G-H	1217	1206.2					
I2	Volume = F-I1	762.6	750.7					
I3	S.D. Volume = F1-I1							
J	Maximum Relative Density = F/I2	2.596	2.607		2.601			
J1	S.D. Maximum Relative Density = F/I2							
K	Percent Voids in Mixture = J-C/J*100	4.1				2.8		
K1	Binder Content (%)	4.0				4.0		
L	Gb =	2.776				2.776		
M	VMA = 100-[(100-A.C.)*Avg.C/L]	13.7				12.5		
N	VFA = 100*(M-K)/M	70.2				77.9		

Fly Ash (Class F) Mix with 4.0% A.C.

Superpave Bituminious Laboratory Worksheet								
PARAMETER		Briquette Number						
		N_{design}				N_{max}		
		1	2		Average	1	2	Average
A1	Mass of Compacted Specimen in Air	4947.8	4955.2	4946		4943.2	4948.5	
A2	Surface Dry Mass of Specimen in Air	4968.6	4977.4	4966.6		4952.4	4959.7	
B1	Mass of Compacted Specimen in Water	2983.8	2981.9	2980.4		2994.6	2996.8	
B2	Volume = A2-B1	1984.8	1995.5	1986.2		1957.8	1962.9	
C	Bulk Relative Density = A1/B2	2.493	2.483	2.490	2.489	2.525	2.521	2.523
C1	Flask Number	C	D					
D	Mass of Flask and Mixture in Air	3311.4	2789.2					
E	Mass of Flask in Air	649.8	635.1					
F	Mass of Mixture in Air = D-E	2661.6	2154.1					
F1	Surface Dry Mass of Mixture in Air							
G	Mass of Flask and Mixture in Water	2201.3	1879.8					
H	Mass of Flask in Water	567.4	556.7					
I1	Mass of Mixture in Water = G-H	1633.9	1323.1					
I2	Volume = F-I1	1027.7	831					
I3	S.D. Volume = F1-I1							
J	Maximum Relative Density = F/I2	2.590	2.592		2.591			
J1	S.D. Maximum Relative Density = F/I2							
K	Percent Voids in Mixture = J-C/J*100	3.9				2.6		
K1	Binder Content (%)	4.0				4.0		
L	Gb =	2.767				2.767		
M	VMA = 100-[(100-A.C.)*Avg.C/L]	13.7				12.5		
N	VFA = 100*(M-K)/M	71.1				78.9		

Slag Mix with 4.3% A.C.

Superpave Bituminious Laboratory Worksheet								
PARAMETER		Briquette Number						
		N_{design}				N_{max}		
		1	2		Average	1	2	Average
A1	Mass of Compacted Specimen in Air	4944.8	4942.2	4946.5		4945.9	4943.6	
A2	Surface Dry Mass of Specimen in Air	4959.1	4954.5	4958.3		4952.5	4950.2	
B1	Mass of Compacted Specimen in Water	2978.2	2975.5	2980.5		2991.7	2989.3	
B2	Volume = A2-B1	1980.9	1979	1977.8		1960.8	1960.9	
C	Bulk Relative Density = A1/B2	2.496	2.497	2.501	2.498	2.522	2.521	2.522
C1	Flask Number	E	F					
D	Mass of Flask and Mixture in Air	2537.5	2543.8					
E	Mass of Flask in Air	633.8	635.8					
F	Mass of Mixture in Air = D-E	1903.7	1908					
F1	Surface Dry Mass of Mixture in Air							
G	Mass of Flask and Mixture in Water	1724.7	1730.8					
H	Mass of Flask in Water	553.7	555.1					
I1	Mass of Mixture in Water = G-H	1171	1175.7					
I2	Volume = F-I1	732.7	732.3					
I3	S.D. Volume = F1-I1							
J	Maximum Relative Density = F/I2	2.598	2.605		2.602			
J1	S.D. Maximum Relative Density = F/I2							
K	Percent Voids in Mixture = J-C/J*100	4.0				3.1		
K1	Binder Content (%)	4.3				4.3		
L	Gb =	2.778				2.778		
M	VMA = 100-[(100-A.C.)*Avg.C/L]	13.9				13.1		
N	VFA = 100*(M-K)/M	71.4				76.5		

Portland Cement Mix with 4.5% A.C.

Superpave Bituminious Laboratory Worksheet								
PARAMETER		Briquette Number						
		N_{design}				N_{max}		
		1	2		Average	1	2	Average
A1	Mass of Compacted Specimen in Air	4945.4	4944.7	4941.5		4947.7	4946.3	
A2	Surface Dry Mass of Specimen in Air	4956.2	4953.5	4951.6		4955.4	4954.6	
B1	Mass of Compacted Specimen in Water	2972.6	2976.5	2973.2		2995.7	2996.3	
B2	Volume = A2-B1	1983.6	1977	1978.4		1959.7	1958.3	
C	Bulk Relative Density = A1/B2	2.493	2.501	2.498	2.497	2.525	2.526	2.525
C1	Flask Number	C	D					
D	Mass of Flask and Mixture in Air	2750.8	2755.8					
E	Mass of Flask in Air	649.8	635.1					
F	Mass of Mixture in Air = D-E	2101	2120.7					
F1	Surface Dry Mass of Mixture in Air							
G	Mass of Flask and Mixture in Water	1859.3	1862.4					
H	Mass of Flask in Water	567.4	556.7					
I1	Mass of Mixture in Water = G-H	1291.9	1305.7					
I2	Volume = F-I1	809.1	815					
I3	S.D. Volume = F1-I1							
J	Maximum Relative Density = F/I2	2.597	2.602		2.599			
J1	S.D. Maximum Relative Density = F/I2							
K	Percent Voids in Mixture = J-C/J*100	3.9				2.9		
K1	Binder Content (%)	4.5				4.5		
L	Gb =	2.781				2.781		
M	VMA = 100-[(100-A.C.)*Avg.C/L]	14.2				13.3		
N	VFA = 100*(M-K)/M	72.4				78.5		

APPENDIX 3

Test Result Work

Sheets at N_{design} & N_{max}

Filename	Control Mix with 4% Limestone Dust	Date	09/08/07

% AC =	4.3%
Rice (Gmm) =	2.587

Mix Design	19mm SP

Gsb =	2.773
% Passing No. 200 Sieve =	4.0%

Specimen 1

	Height	Gmb-Corr	% Gmm
Nini	125.1	2.276	88.0%
Ndes	114.6	2.485	96.1%

Gmb	2.485

Specimen 2

	Height	Gmb-Corr	% Gmm
Nini	125.8	2.285	88.3%
Ndes	115.5	2.489	96.2%

Gmb	2.489

Specimen 3

	Height	Gmb-Corr	% Gmm
Nini	125.7	2.282	88.2%
Ndes	115.4	2.486	96.1%

Gmb	2.486

Specimen 4

	Height	Gmb-Corr	% Gmm
Nini			
Ndes			

Gmb	

Specimen 5

	Height	Gmb-Corr	% Gmm
Nini			
Ndes			

Gmb	

Specimen 6

	Height	Gmb-Corr	% Gmm
Nini			
Ndes			

Gmb	

	Avg Gmb	% Gmm	VTM
Nini	2.281	88.2%	11.82 %

	Avg Gmb	% Gmm	VTM
Ndes	2.487	96.1%	3.88%

	VMA	VFA	DP
Ndes	14.2 %	72.7%	0.94

User must input data into yellow cells only.

Filename	Control Mix with 4% Limestone Dust	Date	09/08/07

% AC =	4.3%
Rice (Gmm) =	2.587

Mix Design	19mm SP

Gsb =	2.773
% Passing No. 200 Sieve =	4.0%

Specimen 1

	Height	Gmb-Corr	% Gmm
Nini	125.8	2.274	87.9%
Ndes	115.4	2.479	95.8%
Nmax	113.8	2.514	97.2%

Gmb	2.514

Specimen 2

	Height	Gmb-Corr	% Gmm
Nini	125.7	2.267	87.6%
Ndes	115.2	2.474	95.6%
Nmax	113.5	2.511	97.1%

Gmb	2.511

Specimen 3

	Height	Gmb-Corr	% Gmm
Nini			
Ndes			
Nmax			

Gmb	

Specimen 4

	Height	Gmb-Corr	% Gmm
Nini			
Ndes			
Nmax			

Gmb	

Specimen 5

	Height	Gmb-Corr	% Gmm
Nini			
Ndes			
Nmax			

Gmb	

Specimen 6

	Height	Gmb-Corr	% Gmm
Nini			
Ndes			
Nmax			

Gmb	

	Avg Gmb	% Gmm	VTM
Nini	2.271	87.8%	12.22 %
Nmax	2.513	97.1%	2.88%

	Avg Gmb	% Gmm	VTM
Ndes	2.477	95.7%	4.27%

	VMA	VFA	DP
Ndes	14.5%	70.6%	0.94

User must input data into yellow cells only.

Filename	4.0% Fly Ash (Class C)	Date	09/08/07

% AC =	4.0%
Rice (Gmm) =	2.601

Mix Design	SP 19mm

Gsb =	2.776
% Passing No. 200 Sieve =	4.0%

Specimen 1

	Height	Gmb-Corr	% Gmm
Nini	123.4	2.311	88.9%
Ndes	114.3	2.495	95.9%

Gmb	2.495

Specimen 2

	Height	Gmb-Corr	% Gmm
Nini	124.8	2.315	89.0%
Ndes	115.6	2.499	96.1%

Gmb	2.499

Specimen 3

	Height	Gmb-Corr	% Gmm
Nini	122.7	2.315	89.0%
Ndes	114.1	2.490	95.7%

Gmb	2.490

Specimen 4

	Height	Gmb-Corr	% Gmm
Nini			
Ndes			

Gmb	

Specimen 5

	Height	Gmb-Corr	% Gmm
Nini			
Ndes			

Gmb	

Specimen 6

	Height	Gmb-Corr	% Gmm
Nini			
Ndes			

Gmb	

	Avg Gmb	% Gmm	VTM
Nini	2.314	89.0%	11.04 %

	Avg Gmb	% Gmm	VTM
Ndes	2.495	95.9%	4.09%

	VMA	VFA	DP
Ndes	13.7 %	70.2%	1.00

User must input data into yellow cells only.

Filename	4.0% Fly Ash (Class C)	Date	09/08/07

% AC =	4.0%
Rice (Gmm) =	2.601

Mix Design	19mm SP

Gsb =	2.776
% Passing No. 200 Sieve =	4.0%

Specimen 1

	Height	Gmb-Corr	% Gmm
Nini	122.4	2.311	88.8%
Ndes	113.5	2.492	95.8%
Nmax	111.8	2.530	97.3%
Gmb	2.53		

Specimen 2

	Height	Gmb-Corr	% Gmm
Nini	123.5	2.311	88.9%
Ndes	114.7	2.488	95.7%
Nmax	112.9	2.528	97.2%
Gmb	2.528		

Specimen 3

	Height	Gmb-Corr	% Gmm
Nini			
Ndes			
Nmax			
Gmb			

Specimen 4

	Height	Gmb-Corr	% Gmm
Nini			
Ndes			
Nmax			
Gmb			

Specimen 5

	Height	Gmb-Corr	% Gmm
Nini			
Ndes			
Nmax			
Gmb			

Specimen 6

	Height	Gmb-Corr	% Gmm
Nini			
Ndes			
Nmax			
Gmb			

	Avg Gmb	% Gmm	VTM
Nini	2.311	88.8%	11.15 %
Nmax	2.529	97.2%	2.77%
Ndes	2.490	95.7%	4.26%

	VMA	VFA	DP
Ndes	13.9%	69.3%	1.00

User must input data into yellow cells only.

Filename	4.0% Fly Ash (Class F)	Date	09/08/07

% AC =	4.0%
Rice (Gmm) =	2.591

Mix Design	SP 19mm

Gsb =	2.767
% Passing No. 200 Sieve =	4.0%

Specimen 1

	Height	Gmb-Corr	% Gmm
Nini	123.8	2.288	88.3%
Ndes	113.6	2.493	96.2%
Gmb	2.493		

Specimen 2

	Height	Gmb-Corr	% Gmm
Nini	124.7	2.292	88.5%
Ndes	115.1	2.483	95.8%
Gmb	2.483		

Specimen 3

	Height	Gmb-Corr	% Gmm
Nini	123.6	2.285	88.2%
Ndes	113.4	2.490	96.1%
Gmb	2.490		

Specimen 4

	Height	Gmb-Corr	% Gmm
Nini			
Ndes			
Gmb			

Specimen 5

	Height	Gmb-Corr	% Gmm
Nini			
Ndes			
Gmb			

Specimen 6

	Height	Gmb-Corr	% Gmm
Nini			
Ndes			
Gmb			

	Avg Gmb	% Gmm	VTM
Nini	2.288	88.3%	11.69 %

	Avg Gmb	% Gmm	VTM
Ndes	2.489	96.1%	3.95%

	VMA	VFA	DP
Ndes	13.7 %	71.1%	1.00

User must input data into yellow cells only.

Filename	4.0% Fly Ash (Class F)	Date	09/08/07

% AC =	4.0%
Rice (Gmm) =	2.591

Mix Design	19mm SP

Gsb =	2.776
% Passing No. 200 Sieve =	4.0%

Specimen 1

	Height	Gmb-Corr	% Gmm
Nini	123.3	2.296	88.6%
Ndes	113.8	2.487	96.0%
Nmax	112.1	2.525	97.5%
Gmb	2.525		

Specimen 2

	Height	Gmb-Corr	% Gmm
Nini	124.5	2.294	88.5%
Ndes	114.7	2.490	96.1%
Nmax	113.2	2.523	97.4%
Gmb	2.523		

Specimen 3

	Height	Gmb-Corr	% Gmm
Nini			
Ndes			
Nmax			
Gmb			

Specimen 4

	Height	Gmb-Corr	% Gmm
Nini			
Ndes			
Nmax			
Gmb			

Specimen 5

	Height	Gmb-Corr	% Gmm
Nini			
Ndes			
Nmax			
Gmb			

Specimen 6

	Height	Gmb-Corr	% Gmm
Nini			
Ndes			
Nmax			
Gmb			

	Avg Gmb	% Gmm	VTM
Nini	2.295	88.6%	11.43 %
Nmax	2.524	97.4%	2.59%

	Avg Gmb	% Gmm	VTM
Ndes	2.489	96.0%	3.95%

	VMA	VFA	DP
Ndes	13.9%	71.7%	0.97

User must input data into yellow cells only.

Filename	4.0% Slag	Date	09/08/07

% AC =	4.3%
Rice (Gmm) =	2.602

Mix Design	SP 19mm

Gsb =	2.778
% Passing No. 200 Sieve =	4.0%

Specimen 1

	Height	Gmb-Corr	% Gmm
Nini	123.7	2.284	87.8%
Ndes	113.2	2.496	95.9%

Gmb	2.496

Specimen 2

	Height	Gmb-Corr	% Gmm
Nini	123.6	2.289	88.0%
Ndes	113.3	2.497	96.0%

Gmb	2.497

Specimen 3

	Height	Gmb-Corr	% Gmm
Nini	124.4	2.288	87.9%
Ndes	113.8	2.501	96.1%

Gmb	2.501

Specimen 4

	Height	Gmb-Corr	% Gmm
Nini			
Ndes			

Gmb	

Specimen 5

	Height	Gmb-Corr	% Gmm
Nini			
Ndes			

Gmb	

Specimen 6

	Height	Gmb-Corr	% Gmm
Nini			
Ndes			

Gmb	

	Avg Gmb	% Gmm	VTM
Nini	2.287	87.9%	12.11 %

	Avg Gmb	% Gmm	VTM
Ndes	2.498	96.0%	4.00%

	VMA	VFA	DP
Ndes	13.9 %	71.3%	0.98

User must input data into yellow cells only.

Filename	4.0% Slag

Date	09/08/07

% AC =	4.3%
Rice (Gmm) =	2.602

Mix Design	19mm SP

Gsb =	2.778
% Passing No. 200 Sieve =	4.0%

Specimen 1

	Height	Gmb-Corr	% Gmm
Nini	124.2	2.276	87.5%
Ndes	113.7	2.487	95.6%
Nmax	112.1	2.522	96.9%

Gmb	2.522

Specimen 2

	Height	Gmb-Corr	% Gmm
Nini	124.0	2.273	87.4%
Ndes	113.4	2.485	95.5%
Nmax	111.8	2.521	96.9%

Gmb	2.521

Specimen 3

	Height	Gmb-Corr	% Gmm
Nini			
Ndes			
Nmax			

Gmb	

Specimen 4

	Height	Gmb-Corr	% Gmm
Nini			
Ndes			
Nmax			

Gmb	

Specimen 5

	Height	Gmb-Corr	% Gmm
Nini			
Ndes			
Nmax			

Gmb	

Specimen 6

	Height	Gmb-Corr	% Gmm
Nini			
Ndes			
Nmax			

Gmb	

	Avg Gmb	% Gmm	VTM
Nini	2.275	87.4%	12.58 %

	Avg Gmb	% Gmm	VTM
Ndes	2.486	95.5%	4.46%

	Avg Gmb	% Gmm	VTM
Nmax	2.522	96.9%	3.09%

	VMA	VFA	DP
Ndes	14.4%	68.9%	0.98

User must input data into yellow cells only.

Filename	4% Portland Cement	Date	09/08/07

% AC =	4.5%
Rice (Gmm) =	2.599

Mix Design	SP 19mm

Gsb =	2.781
% Passing No. 200 Sieve =	4.0%

Specimen 1

	Height	Gmb-Corr	% Gmm
Nini	124.4	2.281	87.7%
Ndes	113.8	2.493	95.9%
Gmb	2.493		

Specimen 2

	Height	Gmb-Corr	% Gmm
Nini	124.3	2.288	88.0%
Ndes	113.7	2.501	96.2%
Gmb	2.501		

Specimen 3

	Height	Gmb-Corr	% Gmm
Nini	124.0	2.284	87.9%
Ndes	113.4	2.498	96.1%
Gmb	2.498		

Specimen 4

	Height	Gmb-Corr	% Gmm
Nini			
Ndes			
Gmb			

Specimen 5

	Height	Gmb-Corr	% Gmm
Nini			
Ndes			
Gmb			

Specimen 6

	Height	Gmb-Corr	% Gmm
Nini			
Ndes			
Gmb			

	Avg Gmb	% Gmm	VTM
Nini	2.284	87.9%	12.11 %

	Avg Gmb	% Gmm	VTM
Ndes	2.497	96.1%	3.91%

	VMA	VFA	DP
Ndes	14.2 %	72.5%	0.94

User must input data into yellow cells only.

Filename	4% Portland Cement	Date	09/08/07

% AC =	4.5%
Rice (Gmm) =	2.599

Mix Design	19mm SP

Gsb =	2.781
% Passing No. 200 Sieve =	4.0%

Specimen 1

	Height	Gmb-Corr	% Gmm
Nini	124.0	2.275	87.5%
Ndes	113.4	2.487	95.7%
Nmax	111.7	2.525	97.2%
Gmb	2.525		

Specimen 2

	Height	Gmb-Corr	% Gmm
Nini	124.2	2.276	87.6%
Ndes	113.5	2.490	95.8%
Nmax	111.9	2.526	97.2%
Gmb	2.526		

Specimen 3

	Height	Gmb-Corr	% Gmm
Nini			
Ndes			
Nmax			
Gmb			

Specimen 4

	Height	Gmb-Corr	% Gmm
Nini			
Ndes			
Nmax			
Gmb			

Specimen 5

	Height	Gmb-Corr	% Gmm
Nini			
Ndes			
Nmax			
Gmb			

Specimen 6

	Height	Gmb-Corr	% Gmm
Nini			
Ndes			
Nmax			
Gmb			

	Avg Gmb	% Gmm	VTM
Nini	2.275	87.5%	12.46 %

	Avg Gmb	% Gmm	VTM
Ndes	2.489	95.8%	4.24%

	Avg Gmb	% Gmm	VTM
Nmax	2.526	97.2%	2.83%

	VMA	VFA	DP
Ndes	14.5%	70.8%	0.94

User must input data into yellow cells only.

APPENDIX 4

Performance Graded Asphalt Cement (PGAC) Test

Sample Name: Control Sample

Date Tested: 22-Jun-07

PGAC Grade: PG 58-28

	Test	AASHTO MP 1	Test Temp (oC)	Test Results	Unit	Pass/Fail
Original Binder	Brookfield Viscosity	≤ 3.00 Pa*s	135	0.317	Pa*s	Pass
			160		Pa*s	Fail
	Dynamic Shear G*/sin(delta)	≥ 1.00 kPa @ 10 rad/sec	58	1.3497	kPa	Pass
			64	0.6492	kPa	Fail
RTFO Residue	Dynamic Shear G*/sin(delta)	≥ 2.00 kPa @ 10 rad/sec	58	2.535	kPa	Pass
			64	1.1887	kPa	Fail
PAV Residue	PAV Aging Temp.		100		-	
	Dynamic Shear G*sin(delta)	≤ 5000 kPa @ 10 rad/sec	19	2871	kPa	Pass
	Bending Beam Creep Stiffness s @ 60 sec	≤ 300 Mpa	-18	277	Mpa	Pass
	Slope m @ 60 sec	≥ 0.300	-18	0.308	-	Pass

Sample Name:	2% Fly Ash (Class C)
Date Tested:	22-Jun-07
PGAC Grade:	PG 58-28

	Test	AASHTO MP 1	Test Temp (oC)	Test Results	Unit	Pass/Fail
Original Binder	Brookfield Viscosity	≤ 3.00 Pa*s	135		Pa*s	Pass
			160		Pa*s	Fail
	Dynamic Shear		58	1.4269	kPa	Pass
	G*/sin(delta)	≥ 1.00 kPa @ 10 rad/sec	64	0.68651	kPa	Fail
RTFO Residue	Dynamic Shear		58	2.6335	kPa	Pass
	G*/sin(delta)	≥ 2.00 kPa @ 10 rad/sec	64	1.1892	kPa	Fail
PAV Residue	PAV Aging Temp.		100		-	
	Dynamic Shear G*sin(delta)	≤ 5000 kPa @ 10 rad/sec	19	2465	kPa	Pass
	Bending Beam Creep Stiffness s @ 60 sec	≤ 300 Mpa	-18	293	Mpa	Pass
	Slope m @ 60 sec	≥ 0.300	-18	0.314	-	Pass

Sample Name:	2% Fly Ash (Class F)
Date Tested:	22-Jun-07
PGAC Grade:	PG 58-28

	Test	AASHTO MP 1	Test Temp (oC)	Test Results	Unit	Pass/Fail
Original Binder	Brookfield Viscosity	≤ 3.00 Pa*s	135		Pa*s	Pass
			160		Pa*s	Fail
	Dynamic Shear G*/sin(delta)	≥ 1.00 kPa @ 10 rad/sec	58	1.3774	kPa	Pass
			64	0.64561	kPa	Fail
RTFO Residue	Dynamic Shear G*/sin(delta)	≥ 2.00 kPa @ 10 rad/sec	58	2.5913	kPa	Pass
			64	1.2749	kPa	Fail
PAV Residue	PAV Aging Temp.		100		-	
	Dynamic Shear G*sin(delta)	≤ 5000 kPa @ 10 rad/sec	19	2583	kPa	Pass
	Bending Beam Creep Stiffness s @ 60 sec	≤ 300 Mpa	-18	284	Mpa	Pass
	Slope m @ 60 sec	≥ 0.300	-18	0.311	-	Pass

Sample Name: 2% Blast Furnace Slag

Date Tested: 22-Jun-07

PGAC Grade: PG 58-28

	Test	AASHTO MP 1	Test Temp (oC)	Test Results	Unit	Pass/Fail
Original Binder	Brookfield Viscosity	≤ 3.00 Pa*s	135		Pa*s	Pass
			160		Pa*s	Fail
	Dynamic Shear G*/sin(delta)	≥ 1.00 kPa @ 10 rad/sec	58	1.3958	kPa	Pass
			64	0.67824	kPa	Fail
RTFO Residue	Dynamic Shear G*/sin(delta)	≥ 2.00 kPa @ 10 rad/sec	58	2.4599	kPa	Pass
			64	1.1401	kPa	Fail
PAV Residue	PAV Aging Temp.		100		-	
	Dynamic Shear G*sin(delta)	≤ 5000 kPa @ 10 rad/sec	19	2731	kPa	Pass
	Bending Beam Creep Stiffness s @ 60 sec	≤ 300 Mpa	-18	299	Mpa	Pass
	Slope m @ 60 sec	≥ 0.300	-18	0.321	-	Pass

Sample Name:	2% Portland Cement
Date Tested:	22-Jun-07
PGAC Grade:	PG 58-28

	Test	AASHTO MP 1	Test Temp (oC)	Test Results	Unit	Pass/Fail
Original Binder	Brookfield Viscosity	≤ 3.00 Pa*s	135		Pa*s	Pass
			160		Pa*s	Fail
	Dynamic Shear		58	1.3755	kPa	Pass
	G*/sin(delta)	≥ 1.00 kPa @ 10 rad/sec	64	0.6766	kPa	Fail
RTFO Residue	Dynamic Shear		58	2.4669	kPa	Pass
	G*/sin(delta)	≥ 2.00 kPa @ 10 rad/sec	64	1.1846	kPa	Fail
PAV Residue	PAV Aging Temp.		100		-	
	Dynamic Shear G*sin(delta)	≤ 5000 kPa @ 10 rad/sec	19	2690	kPa	Pass
	Bending Beam Creep Stiffness s @ 60 sec	≤ 300 Mpa	-18	294	Mpa	Pass
	Slope m @ 60 sec	≥ 0.300	-18	0.316	-	Pass